BOEM 2023-017

Mississippi Offshore Sediment Resources Inventory: Late Quaternary Stratigraphic Evolution of the Mississippi-Alabama Shelf

US Department of the Interior
Bureau of Ocean Energy Management
New Orleans Office

BOEM
Bureau of Ocean Energy Management

BOEM 2023-017

Mississippi Offshore Sediment Resources Inventory: Late Quaternary Stratigraphic Evolution of the Mississippi-Alabama Shelf

Authors

Davin J. Wallace

February 2023

Prepared under BOEM Cooperative Agreement M16AC00012
by
University of Southern Mississippi
1020 Balch Blvd.
Stennis Space Center, MS 39529

Published by

US Department of the Interior
Bureau of Ocean Energy Management
New Orleans Office

DISCLAIMER

Study collaboration and funding were provided by the US Department of the Interior, Bureau of Ocean Energy Management (BOEM), Marine Minerals Program, New Orleans, LA, under Agreement Number M16AC00012 with the University of Southern Mississippi (USM). This report has been technically reviewed by BOEM, and it has been approved for publication. The views and conclusions contained in this document are those of the authors and should not be interpreted as representing the opinions or policies of BOEM, nor does mention of trade names or commercial products constitute endorsement or recommendation for use.

REPORT AVAILABILITY

To download a PDF file of this report, go to the US Department of the Interior, Bureau of Ocean Energy Management Marine Minerals Program Marine Minerals Resource Evaluation Research webpage (https://www.boem.gov/marine-minerals/marine-mineral-research-studies/marine-mineral-resource-evaluation-research) and use the Browse Library tools to search report title, region (state), or year.

CITATION

Wallace, DJ (University of Southern Mississippi, Stennis Space Center, MS). 2023. Mississippi offshore sediment resources inventory: Late Quaternary stratigraphic evolution of the Mississippi-Alabama Shelf. New Orleans (LA): US Department of the Interior, Bureau of Ocean Energy Management. 75 p. Obligation No.: M16AC00012. Report No.: BOEM 2023-017.

ACKNOWLEDGMENTS

The authors gratefully acknowledge the participation of current and former BOEM colleagues in the work supported by this cooperative agreement, including Mike Miner, Jessica Mallindine, Ana Rice, Tershara Matthews, Jennifer Steele, Nicholas Ferina, Barton Rogers, Brian Cameron, Lora Turner, Ariel Kay, and Kerby Dobbs. This study benefited greatly from numerous scientists across a wide range of agencies including James Flocks (US Geological Survey St. Petersburg Coastal and Marine Science Center) and George Ramseur (Mississippi Department of Environmental Quality). Many former and current USM graduate students made huge contributions to this study, including Clayton Dike, Nina Gal, Shara Gremillion, Rob Hollis, Erin Culver-Miller, Carrie Miller, and Sarah Monica.

Portions and text excerpts of this report (Table of Contents, sections 6.3, 6.4, 6.5, 7.1, 7.2, and 7.3) were published in Hollis RJ, Wallace DJ, Miner MD, Gal NS, Dike C, Flocks JG. (2019). Late Quaternary evolution and stratigraphic framework influence on coastal systems along the North-Central Gulf of Mexico, USA. Quaternary Science Reviews, 223.

Contents

List of Figures

List of Tables

List of Abbreviations and Acronyms

Short form	Long form
µm	micrometer
BOEM	Bureau of Ocean Energy Management
Co-Op	Cooperative Agreement
Gulf	Gulf of Mexico
ka	kilo annum (thousand years)
kyr	kilo year (thousand years)
LiDAR	Light Detection and Ranging
MsCIP	Mississippi Coastal Improvements Program
MIS	marine isotope stage
mm	millimeter
MMP	Marine Minerals Program
MSL	mean sea level
MMIS	Marine Minerals Information System
Northern Gulf	Northern Gulf of Mexico
NEPA	National Environmental Protection Act
OCS	Outer Continental Shelf
OSL	optically stimulated luminescence
RSL	relative sea level
R/V	Research Vessel
USM	University of Southern Mississippi

1 Summary

The Northern Gulf of Mexico (Northern Gulf) is among the most vulnerable sections of coastline in the United States due to the combined vulnerability to sea-level rise, frequent hurricane impacts, subsidence, oil spills, and natural and/or anthropogenic reductions of sediment supply. These barrier islands, marshes, and bay environments comprising the coasts are important tourism destinations, support critical infrastructure, and provide protection from the previously mentioned coastal hazards. State and Federal agencies rely on known Outer Continental Shelf (OCS) sediment resources to develop coastal restoration projects. The state of Mississippi has had a long history of these nourishment projects and has the fourth largest total nourishment volume in the US normalized by length of shoreline over the last century.

Understanding the availability, nourishment quality, and location of sediment resources is imperative to develop restoration projects that maintain the sustainability and coastal resilience of the Northern Gulf of Mexico coast. Due to this need, the Bureau of Ocean Energy Management (BOEM) funded a cooperative agreement (Co-Op) with the University of Southern Mississippi (USM) entitled “Mississippi offshore sediment resources inventory: Late Quaternary stratigraphic evolution of the inner shelf: M16AC00012” from 2016 to 2022 (MS Co-Op1). The goal of this research directly was to address past coastal system response to coastal change mechanisms, improving our predictive capabilities for future sediment searches. The overall goal of this study is to understand the geologic evolution of Late Quaternary deposits offshore Mississippi and to delineate and develop volumetric reserve estimates of restoration quality sediment resources located on the OCS.

The findings provide a reconnaissance-level assessment of available sediment resources and improve our understanding of barrier stability, shoreline response to accelerated relative sea-level (RSL) rise, backbarrier-sedimentation dynamics, and fluvial deltaic geomorphology by examining the evolution of Late Quaternary geologic systems deposited and preserved on the Northern Gulf shelf. These findings have also led to an assessment of data gaps that could be investigated in the future.

2 Relevance to BOEM Issues and the State of Mississippi

Numerous coastal municipalities provide billions of dollars to the economy of the Mississippi coastal zone, mostly through fishing, industry, and tourism. However, this coastal system along the Northern Gulf is among the most vulnerable sections of the US (Figure 1) due to climate change (Pendleton et al. 2010), primarily because of sensitivity to increases in the rate of RSL rise (Oppenheimer et al. 2019), natural and anthropogenic reduced sediment delivery (Blum and Roberts 2009, Wallace et al. 2009, Anderson et al. 2010, Hein et al. 2011, Anderson et al. 2014 and 2016), and the changing frequency and intensity of storms (Emanuel 2005 and 2021, Webster et al. 2005, Elsner et al. 2008, McCarthy 2009). In 2020 alone, unprecedented hurricane activity in the Atlantic Basin produced thirty named storms, the highest number on record, with seven named storms impacting within 200 miles of the Mississippi Coast (NOAA 2021). These storms are stark recent reminders that understanding the availability and quality of sediment resources for restoration and resiliency in the region is paramount. These sediment resources include clay (0.00006 millimeters [mm] to 0.0039 mm), silt (0.0039 mm to 0.0625 mm), sand (0.0625 mm to 2.0 mm), and gravel (2.0 mm to 4096 mm) (Wentworth, 1922). Sand sizes are often targeted for barrier islands and shoreline restoration projects. However, other grain sizes and/or mixed sediment packages are important to examine because of the wide distribution of potential applicabilities, including marsh restoration projects. The region has a long history of restoration and nourishment projects, targeting such environments as barrier islands, beaches, and marshes. The most recent example, the Mississippi Coastal Improvements Program (MsCIP) restoration project, was the second largest restoration project in the history of the National Park Service (Hrvacevic 2020). Nearly 18 million cubic yards of sand, at a cost of $300 million, were used to fill in Camille Cut, formed after Hurricane Camille in 1969 (Hrvacevic 2020). Including this massive project, Mississippi is the fourth highest state in the US for total nourishment volume normalized by length of shoreline from 1921 to 2020 (Elko et al. 2021). In 2018 alone, Mississippi's 22 million cubic yards of nourished sediment accounted for more than 30% of the annual total beach nourishment volume for the entire US (Elko et al. 2021).

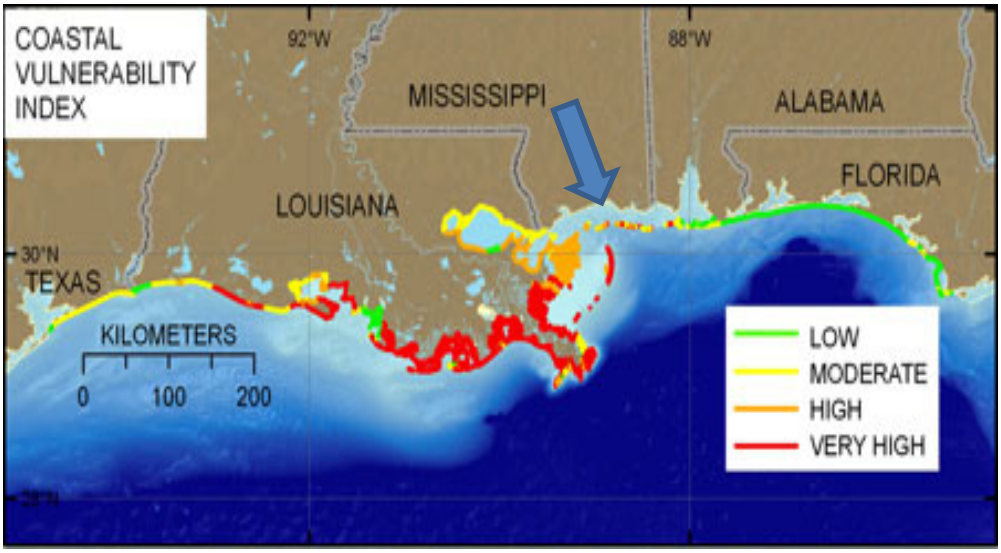

Figure 1. Coastal vulnerability index for the Northern Gulf of Mexico.
Note the generally high to very high vulnerability of the Mississippi Coast (blue arrow for location). Figure modified from Pendleton et al. 2010.

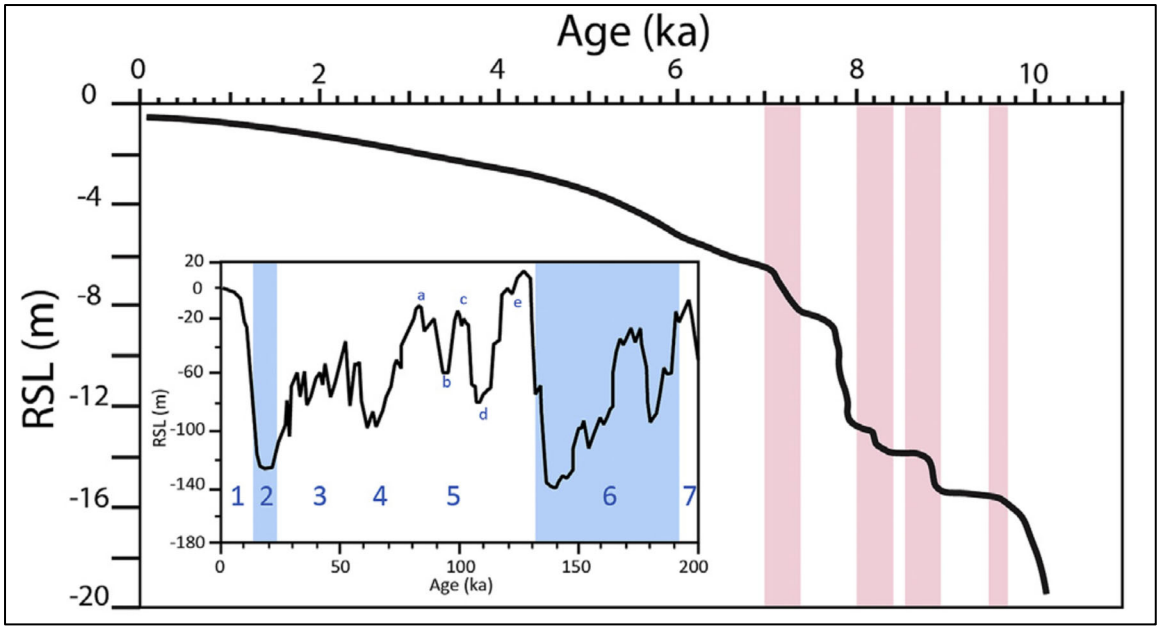

Figure 2. Sea-level curves for the Gulf of Mexico.
Figure from Hollis et al. 2019.
Holocene curve shown with pink bars pink bars representing rapid sea-level rise rates. Inset shows sea-level history for last 200 ka with blue bars representing the previous two lowstands (MIS2 and MIS6).

This study directly addresses the fundamental goals of BOEM through the Marine Minerals Program (MMP) and the State of Mississippi. An offshore OCS sediment budget for the Northern Gulf allows for a better assessment of sediment resources that could be used for future coastal restoration efforts that will aide in coastal resiliency. Understanding the distribution of sediment resources on the OCS would also allow for informed planning of future pipeline infrastructure and oil gas, and/or renewable energy leases. Furthermore, understanding past coastal evolution in the geologic record can help us better predict the fate of similar systems in the future (Anderson et al. 2014).

3 Background

A series of basic geologic principles governs the methodology of the study (MS Co-Op1). The last 125,000 years is a time where climate, sea level, and sediment supply variations for the Northern Gulf are relatively well constrained. Two prominent sea-level lowstands defined by global glacial periods occurred at ~125 ka (Marine Isotope Stage (MIS) 6) and ~20 ka (MIS 2). Sea level was ~135 m and ~120 m lower than present for MIS 6 and MIS 2, respectively (Figure 2).

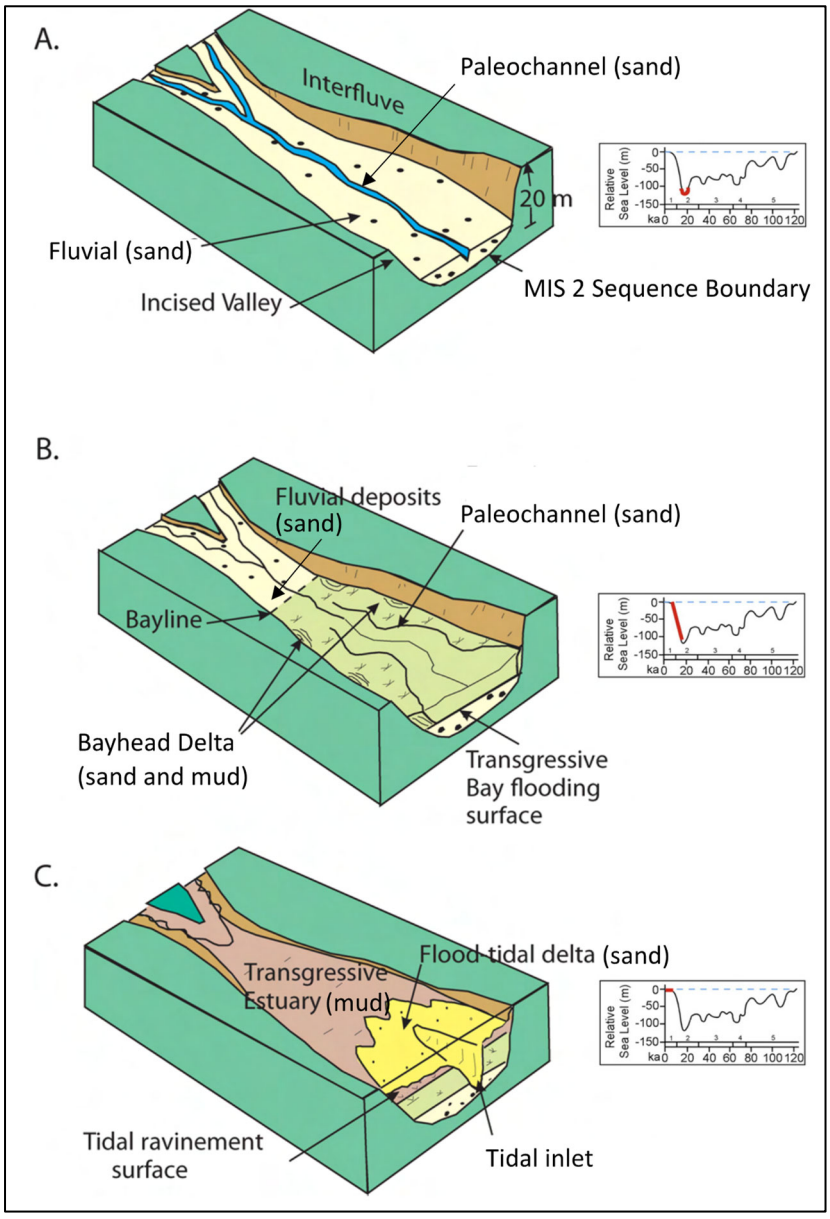

Figure 3. Generalized evolution of incised valleys.
Modified from Allen and Posamentier 1993; Nordfjord et al. 2006.
Systems tracts depicted include lowstand (A), transgression (B), and highstand (C), with time period highlighted in red from Figure 2.

During these lower sea level positions, fluvial systems incised across the shelf environment to build falling stage and lowstand deltas with associated slope fans in the Gulf of Mexico (Gulf) (Figure 2).

Erosion and transport thus occurred from the inner to outer shelf. Coastal features deposited during the lowstand are fairly large in spatial extent, and represent sizeable sediment resources today. During the transgression of sea level (~20 ka [kilo annum] to present), sea level rose ~120 m in 20 kilo years [kyr] (Figure 2). High-resolution Holocene sea level records (Figure 2) from the Northern Gulf demonstrate that the rate of relative sea level rise was ~4.2 mm/yr from 10 to 7 kyr, ~1.4 mm/yr from 7 to 4 kyr, and ~0.5 mm/yr for the last 4 kyr (Anderson et al. 2014 and references therein). During this time period in the Gulf previously deposited lowstand features were ravined and coastal systems rapidly backstepped landward across the shallow gradient shelf (Figure 2) (Anderson et al. 2016). This ravinement, therefore, produced a significant amount of sediment through decapitation and reworking of coastal features, supplying transgressive coastal systems with sand. This process has been previously identified as a main contributor of sand to Holocene coastal systems in the Gulf, because they transgressed across the shelf to reach the near modern-day positions (Anderson et al. 2004, 2014, and 2016, Gal et al. 2021, Hollis et al. 2019). Transgressive ravinement is an efficient process, with the exception of incised valleys, where the MIS 2 surface is the deepest (Figure 3). Here, the preservation of Holocene sandy sediment resources is highest within the incised valleys (Figure 3), because the sediments subside more quickly and they are deposited at deeper depths (Anderson et al. 2004, 2014, and 2016, Gal et al. 2021, Hollis et al. 2019). Incised valleys generally consist of basal fluvial sands, backstepping bayhead deltas and tidal deltas, and sandy mud estuarine deposits (Figure 3). These facies represent the most viable sediment resources because 1) they are Holocene and are generally easier to dredge 2) they are genetically related to the same erosional systems that need renourishment.

4 Study Area

The modern-day Mississippi Gulf Coast consists of a barrier island chain (from west to east: Cat, Ship, Horn, and Petit Bois islands), coastal marshes, three moderate size fluvial systems (Pearl, Biloxi, Pascagoula-Escatawpa Rivers), and several estuaries (St. Louis Bay, Biloxi Bay, Pascagoula Bay, and Mississippi Sound) (Figure. 4). Landward of the Mississippi Sound, the shoreline is composed of mostly low-lying marshes. The coast has a microtidal range (< 1 m). The shoreline typically is influenced by fair-weather nearshore waves ranging in height between 30 and 60 cm and periods between 2 and 6 seconds. The Chandeleur Islands (Louisiana) bound the western part of the study area, and the Alabama barrier islands (Dauphin, Fort Morgan) bound the east (Figure 4 and Figure 5).

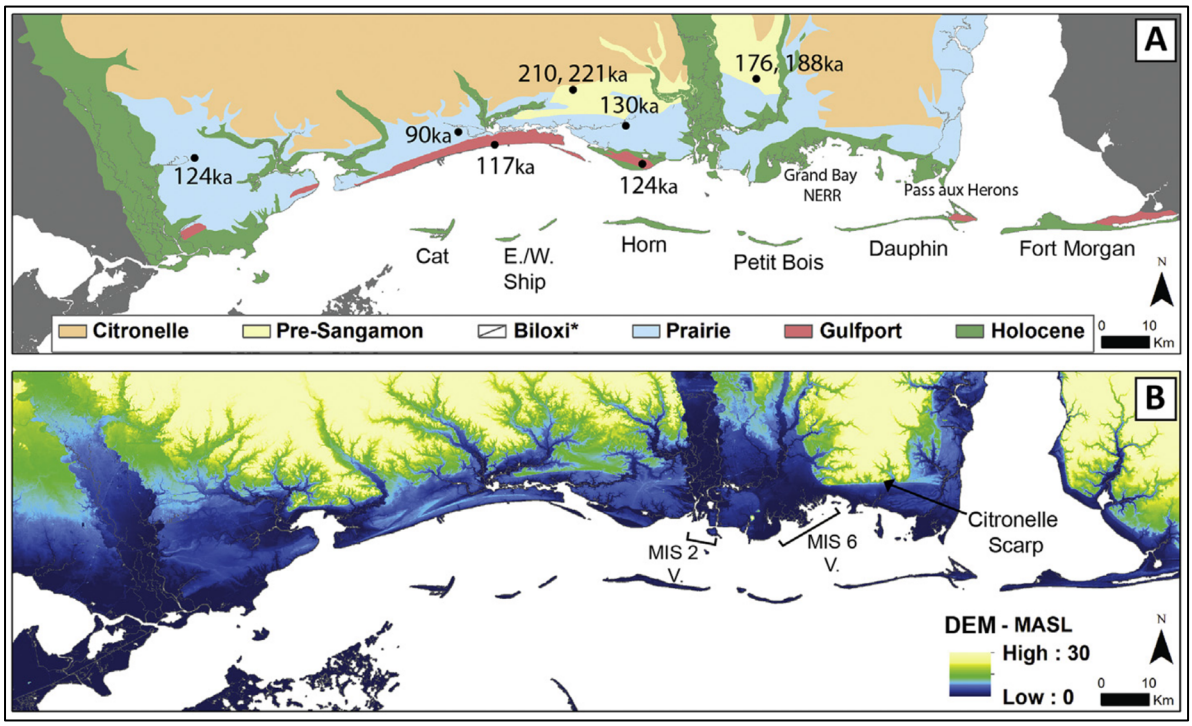

Figure 4. Geology of the Mississippi Gulf Coast.
Figure from Hollis et al. 2019.
A) OSL ages (in ka) with formation ages. B) Digital elevation model based on Light Detection and Ranging (LiDAR) data.

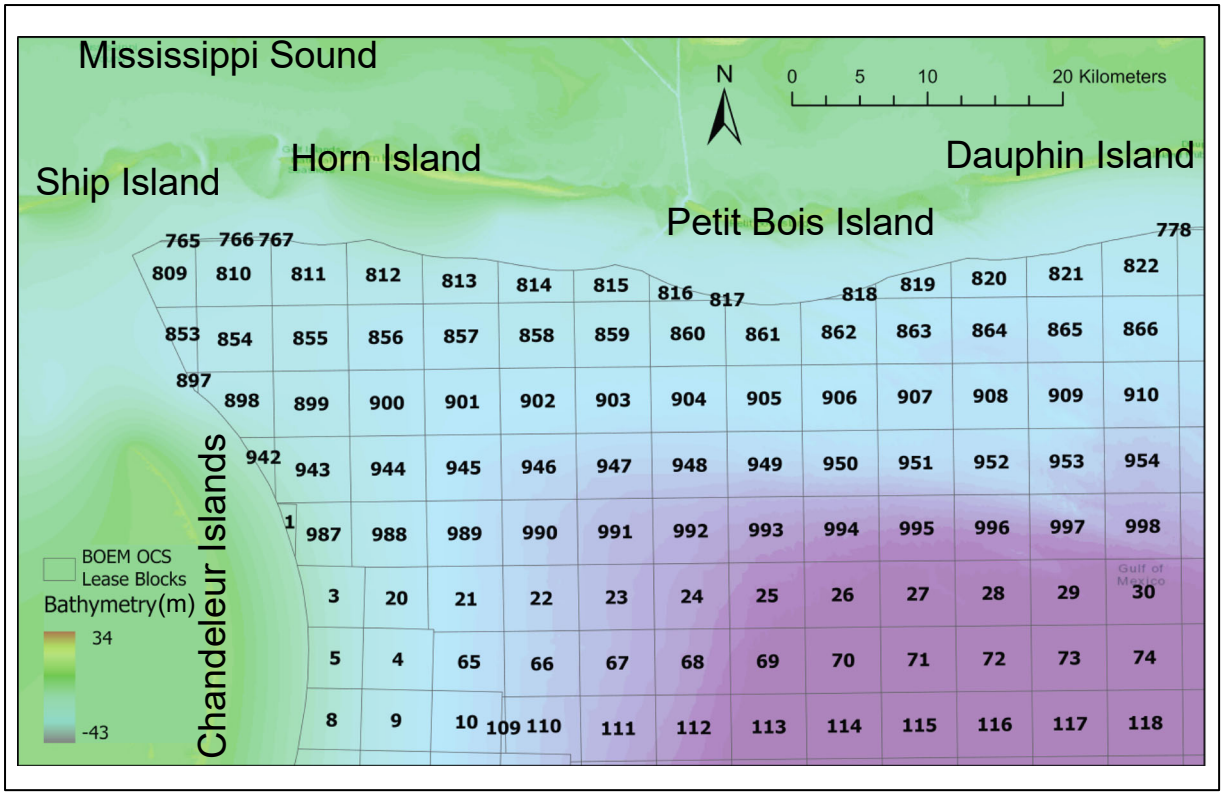

Figure 5. Northern Gulf of Mexico BOEM lease blocks.
Inner and/or outer shelf environment bathymetry and geographic features shown. Study area includes OCS blocks (Protraction number NH16-04) 897-908, 942-952, 987-996.

A vast inner-outer shelf environment exists seaward of the barrier islands (Figure 5). The Mississippi Bight extends from the Chandeleur Islands east towards Florida, where there are a series of shoreface attached storm sand ridges offshore Fort Morgan Peninsula and Petit Bois Island at the ~20 m isobath (Figure 5). In general, the area has a fairly low gradient. When the Loop Current is in extended mode, it abuts the shelf break and occasionally has cyclonic rings spin off which impact the Northern Gulf (McGowen et al. 1977). Since 1852, 129 total storms (14 were Category 3 and above) have passed within 100 miles of the Mississippi Coast (NOAA 2021). Based on National Oceanic and Atmospheric Administration (NOAA) tide gauge 8747437 in Bay St. Louis, Mississippi (NOAA 2020), the current rate of relative sea-level rise is 4.81 ± 0.79 mm/yr from 1978 to 2019.

5 Objective and Hypothesis

The overall goal of this study is to develop an understanding of the geologic evolution of Late Quaternary deposits offshore Mississippi and to delineate and develop volumetric reserve estimates of restoration quality sediment resources located on the OCS**.**

The main hypothesis for this proposed work is that extensive lowstand systems for different river systems exist on the outer Northern Gulf shelf, and each transitioned to back-stepping transgressive systems during the early to Late Holocene. By examining their evolution in detail, these systems will also provide important analogues for expected future change along the Northern Gulf coast. These incised valleys from the MIS 2 lowstand consist of the most viable and valuable sediment resources along the Northern Gulf OCS (OCS Blocks Protraction number NH16-04 898-908, 942-952, and 987-996) (Figure 5).

6 Methods and Analyses

A number of seminal studies (e.g. Saucier 1968, Frazier 1967, Otvos 1978, 1981, Anderson et al. 2004, Roberts et al. 2004, Greene et al. 2007) have been done on the inner and outer Mississippi shelf for decades. However, much of the data remain fragmentary and discrete and have yet to be holistically synthesized.

Single and multi-beam, geophysical data, and sediment cores have been collected on the Mississippi inner shelf (DeWitt et al. 2012, Flocks et al. 2011, 2014, and 2015, Forde et al. 2011) and offshore the Mississippi barrier islands (Kelso and Flocks, 2015, Pendleton et al. 2010, Pfeiffer et al. 2011, Twichell et al. 2011). A number of unpublished coastal geology datasets have been collected by the State of Mississippi (Mississippi Department of Environmental Quality 2016). Light Detection and Ranging (LiDAR) data has been collected for the barriers (Smith et al. 2016a, 2016b) and coastal marshes (Nayegandhi 2016a, 2016b). Though the Pearl River incised valley geometry and depth has been mapped in detail (Frazier 1974), no age constraints currently exist. Given the wealth of data that exists for this study area, a comprehensive synthesis and compilation of existing geologic and geophysical data, as well as new data collection, was necessary to understand the system in a source to sink framework. To undertake this, this project undertook a series of tasks leading to deliverables presented in this report.

6.1 Major Tasks

1. Collect existing geophysical and geological data (digital and analog forms from various sources including USM, BOEM, Mississippi Department of Marine Resources, Mississippi Department of Transportation, Mississippi Department of Environmental Quality, US Army Corps of Engineers, US Geological Survey, etc.) for the study area and compile into a spatial geodatabase using BOEM-specified formatting (including compliant metadata). This included:

    A. Digitization of analog data
    B. Georectification of data for projection in GIS
    C. Integrating navigation data with geophysical profiles.
    D. Other data specific subtasks necessary to bring data into GIS and other analytical software (e.g., SonarWiz)

2. Literature review and synthesis and compilation of a reference database of relevant literature. The literature review focused on lowstand, transgression, and highstand fluvial deltaic system evolution for the NGOM and nearly 150 publications were considered relevant. Any spatially relevant products were included in the spatial database complied under Task 1 (e.g. data points; interpreted locations or isopachs of sand bodies, valley fills, channel fills, etc.). The compilation focused on the Mississippi Sound near the barrier islands extending to the OCS.
3. Perform quality assurance and quality control (QA/QC), reprocess if necessary, and analyze existing data assembled under Task 1 to interpret stratigraphic framework and evolution of late Quaternary coastal and/or shelf deposits Mississippi. This included:

    A. Compilation of data into software suitable for seismic and/or core analysis, integration of core and seismic data, volume calculations, etc.
    B. Reprocessing digital geophysical data to provide improved resolution for seismic stratigraphic interpretations
    C. Analysis of core logs, photographs, samples, etc.

4. Develop, in coordination with BOEM, a stratigraphic-based nomenclature and organization scheme for sand-rich lithofacies types identified in the study area.
5. Delineate (interpret) sand-rich lithofacies in plan form (Esri™ polygon shapefiles for GIS) and provide information on sediment textural properties, volumes of deposit, type of deposit, overburden thickness, percent sand, and other criteria agreed upon between BOEM and USM.
6. Identify data gaps or areas where further sampling (geophysical or geologic) is needed.
7. Collect and analyze new geological and geophysical data (and incorporate into MMIS database) to improve geologic interpretations and estimate restoration-quality sand reserves. Vibracores (using a USM system) were collected using USM vessels. We collected appropriate data using a boomer system (1.5 kHz).
8. Collect, prepare, and analyze samples for absolute dating (radiocarbon) and incorporated results to inform chronostratigraphic interpretations.
9. Develop a conceptual stratigraphic evolutionary model for Late Quaternary to recent deposits offshore Mississippi, including but not limited to lowstand shelf fluvial deposits, transgressive shelf deposits, and the modern shelf-coastal system.
10. Integrate all newly acquired and/or analyzed data, and other relevant products into a final spatial database (MMIS).

6.2 Sand Environmental Assessment

In 2019, *Sand Survey Activities for BOEM's Marine Minerals Program Atlantic and Gulf of Mexico Final Environmental Assessment* (Sand Survey EA; BOEM 2019) was prepared to describe and evaluate the potential environmental impacts related to shallow geological and very high-resolution geophysical survey activities that support identification, delineation, monitoring, and scientific investigation of sand resources on the Atlantic and Gulf OCS. This National Environmental Protection Act (NEPA) process has been integrated to achieve compliance with other environmental regulations to reflect relevant environmental concerns, avoid delays, and address potential conflicts or challenges. A rigorous mitigation strategy to minimize environmental effects, outlined in Appendix B, is included as a component of activities funded in whole or in part by BOEM that fall within the scope of the Sand Survey EA. Through the publication of the Sand Survey EA, BOEM agreed to incorporate certain mitigation measures to minimize or eliminate impacts to environmental resources. BOEM-funded research using Geology and Geophysics are required to satisfy the agreed-upon mitigation measures and incorporate them into work plans for the funded activities.

6.3 Geophysical

This project compiled ~2050 km and ~7252 km of archived chirp (Forde et al. 2011a, 2011b, and 2015, Greene et al. 2007) and boomer and/or minisparker seismic data (Bosse et al. 2017a and 2017b, Sanford et al. 2016a, 2016b, and 2016c) (Figure 6 and Figure 7), respectively. Chirp data collected using Edgetech SB-512i offered the greatest penetration and detail in shallow, sandier areas. The Edgetech SB-216s or SB-424 provided sufficient detail in muddier areas of the Mississippi Sound. Dataset line spacing, vertical resolution and horizontal accuracy varied greatly. This required weighted quality control between datasets and subsequent interpretation. Recently collected chirp data was weighted higher overall due to greater vertical resolution (<20 cm) and spatial accuracy (<2 m) from GPS relative to archive seismic data collected with LORAN-C (<1 m, < 0.4 km). Geophysical data were classified based on the amount of ringing and/or noise present. Seismic profiles were used where chirp data were spatially absent and to delineate deeper stratigraphic boundaries.

New geophysical data was collected where data gaps existed during this study (Figure 9B) using a single-channel Applied Acoustics boomer with a CSP1000 power supply and Hypack data acquisition software (Miller et al. 2021 and 2022, Culver-Miller et al. 2021 and 2022). Analog geophysical trace information was converted to a digital signal through a National Instruments conversion system. The boomer had a source level of 212 dB re 1µPa [microPascal] @1m, output frequency of 1.5 kHz, operational level of 350 J [Joules], and was set to 5594 shots/mile, and both the source and receiver were towed at the sea surface. Navigation was provided by a WAAS enabled Trimble DPGS enabling a horizontal spatial accuracy of ~± 3 m. During the surveys, the speed of the boat was 4 knots. Seafloor reflectors from legacy and new geophysical data were adjusted to a common bathymetric datum using hydrographic survey data (NOAA 2009 2007), which was corrected to mean sea level (MSL) using the Dauphin Island tide gauge (NOAA 2019a, Station 8735180).

Chirp and seismic produced SEGY data were analyzed and interpreted using SonarWiz 6 (Chesapeake Technologies 2018) and were ground-truthed sediment cores. Sound velocities of 1500m/s were used and yielded good correlation between reflectors and changes in lithology in sediment cores. Both seismic and lithologic facies were constructed based on stratigraphic relationships following facies models described by Zaitlin et al. (1994), Mitchum et al. (1977), Allen and Possamentier (1993) and Cattaneo and Steel (2003). Characterized reflector picks were all exported as xyz data and subsequently gridded using the kriging function in Golden Software Surfer 15. Separate surfaces using nodal points spaced both at 75 m and 200 m resolution were created and merged due to variable chirp and legacy seismic data coverage. A smoothing function was made to remove gridding artifacts. All interpolated surfaces were incorporated into MMIS as rasters.

6.4 Sediment Cores

This study integrated over 1,175 previously collected sediment cores (Figure 8; Table 1). This included vibracores, rotary drill cores, and platform borings from numerous sources. This information was used to ground-truth geophysical information and to create stratigraphic geometries. The type of information available ranged from geotechnical core description logs with some photographs to archived physical cores that were available for sampling. Photos and descriptions were primarily used to ground truth the subaerial exposure surface in geophysics, indicating the Holocene-Pleistocene contact and/or lowstand sequence boundary. Physical archived sediment cores provided more detailed sedimentary structure descriptions and were used to distinguish lithofacies.

We also collected 35 new cores, aboard the R/V *Apalachee*, using a Rossfelder (Figure 9B). These cores were each 3.5-inch diameter, and were up to 20 feet in length. Once retrieved from the field, cores were split, sectioned into 1.5-m sections, and housed at 4ºC in the USM core storage facility. Cores collected for this study were photographed, described visually for general grain size, sedimentary structure, shell content, contact relationships and radiocarbon sample type. Select cores were also analyzed for microfossil analysis in a separate Cooperative Agreement between University of Alabama and BOEM (Microfossil Assemblage Analysis in Support of the Mississippi Offshore Sediment Resources Inventory [M21AC00000]). This work supports MS-CoOp1 by examining the geologic sediment sources, reconstructing paleoenvironments, and providing additional material for radiocarbon dating.

Particle size analysis was also run on 3,000 discrete samples using a Malvern Mastersizer 3000 housed at USM. Grain size samples were based on representative facies to determine sediment volumes of a given size. The laser particle size analyzer produces highly precise and reproduceable results between 0.01µm to 3,500 µm.

6.5 Radiocarbon Dating

Thirty-eight radiocarbon dates were synthesized from the literature (Table 3). These dates were recalibrated using the Marine13 and IntCal13 curves for marine and terrestrial samples, respectively (Reimer et al. 2013). A global 400-year marine reservoir was applied with no additional local reservoir corrections.

New radiocarbon ages were obtained from either legacy physical cores or newly acquired cores (Tables 2 and 4). Fifty-three new radiocarbon dates were obtained using the continuous flow gas bench accelerator mass spectrometer method at the National Ocean Sciences Accelerator Mass Spectrometry (NOSAMS) of the Woods Hole Oceanographic Institution. These ages were calibrated using the Marine13 curve (Reimer et al. 2013) with the global 400 year-marine reservoir.

All ages (recalibrated and new) are reported in calendar years before present (BP, where "present" refers to the year 1950 CE by convention), using median probability with associated two-sigma ranges.

6.6 Short-lived Isotopic Dating

Modern ages were analyzed in house using a Canberra Germanium detectors (well-type) by measuring the short-lived isotopes 210-Pb [Lead] and 137-Cs [Cesium]. Peak fitting, data reduction and analysis was performed in house with PC workstations, and a variety of laptop computers.

6.7 Sand-rich Deposit Volume Calculations

Based on the literature review, geophysical data, sediment cores, and radiometric dating techniques, we estimate locations and volumes of sand-rich deposits. This consisted of quantifying areas and thicknesses of sand-rich facies, and multiplying these corresponding volumes by percent sand. When available, we report the total deposit volume, and an estimate for total sand volume. Our estimates are provided in MMIS.

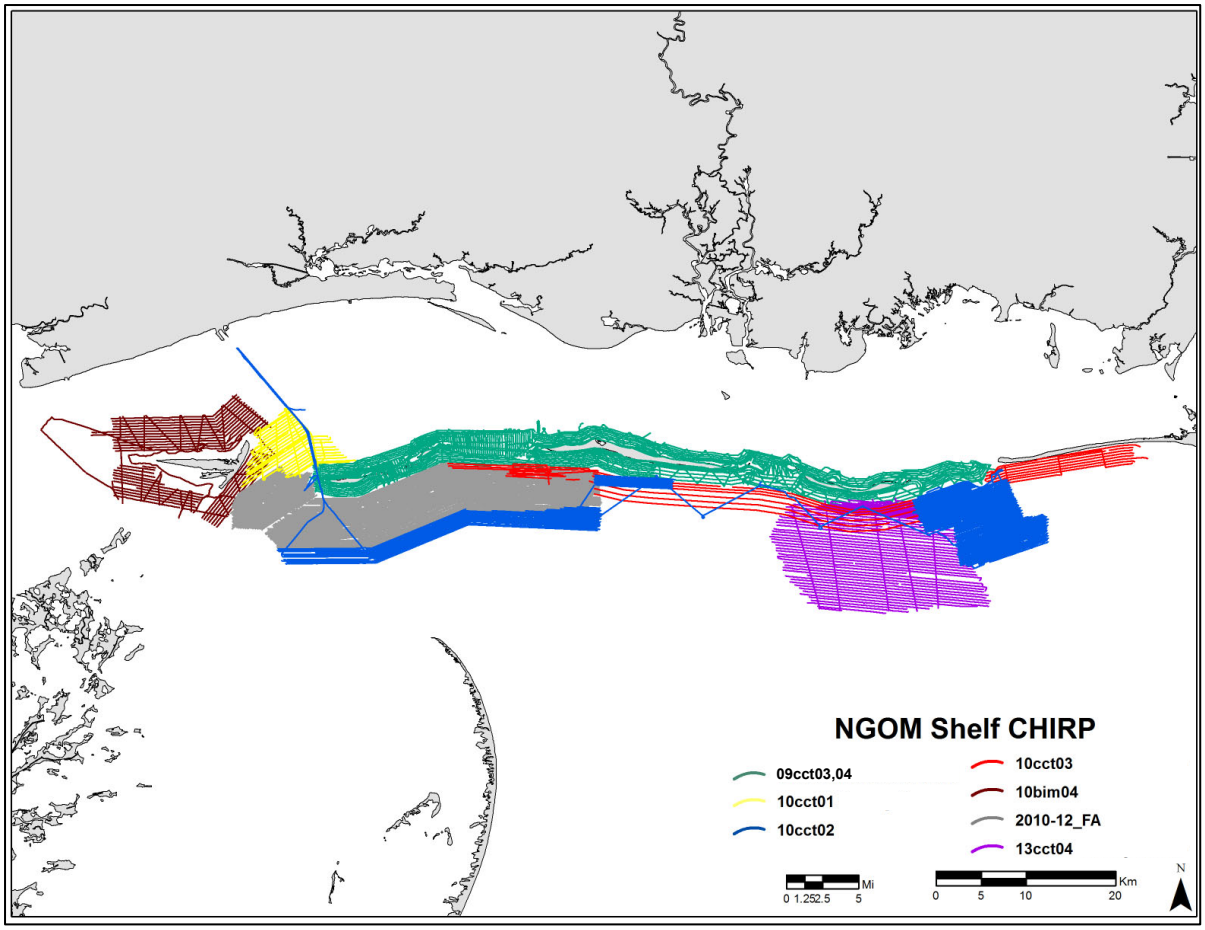

Figure 6. Northern Gulf legacy CHIRP data compiled in the USM database.
Data were QA/QC and will be added to MMIS.

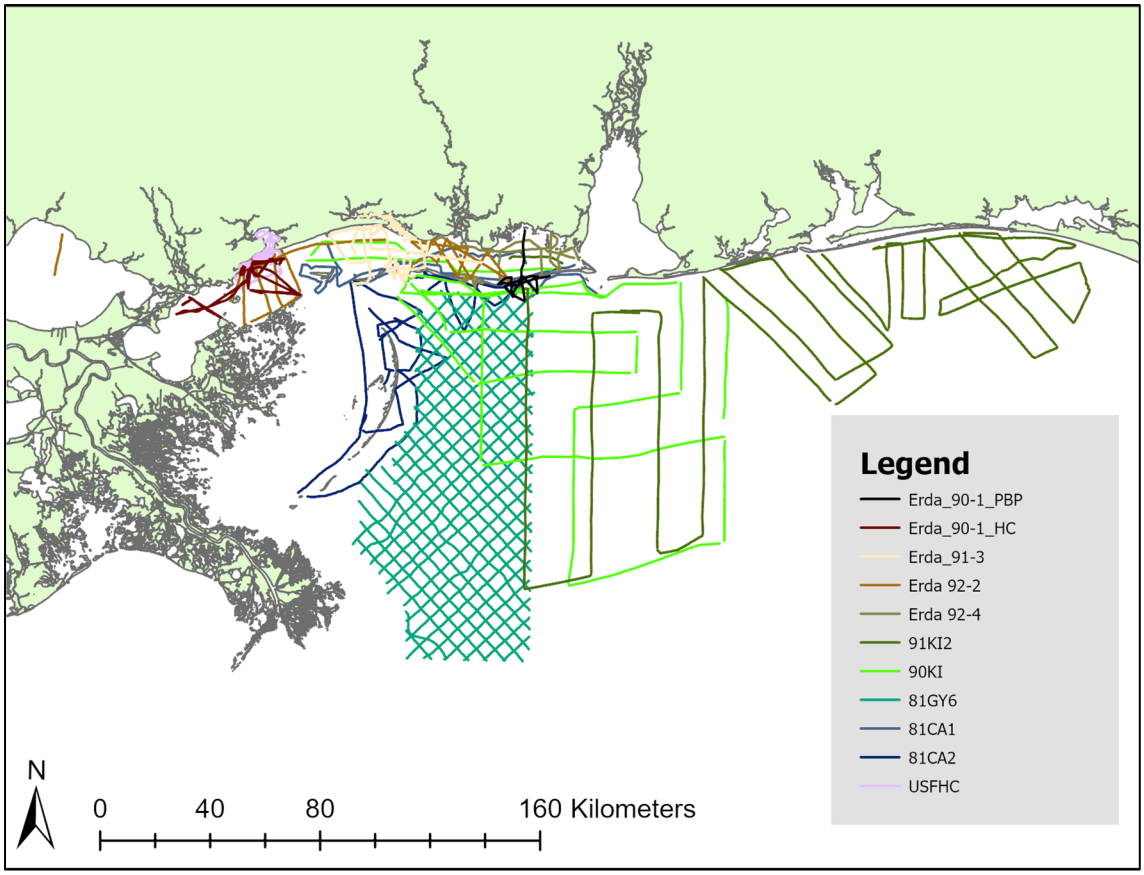

Figure 7. Northern Gulf legacy seismic data compiled in the USM database.
From Dike, 2022.
Data were QA/QC and will be added to MMIS.

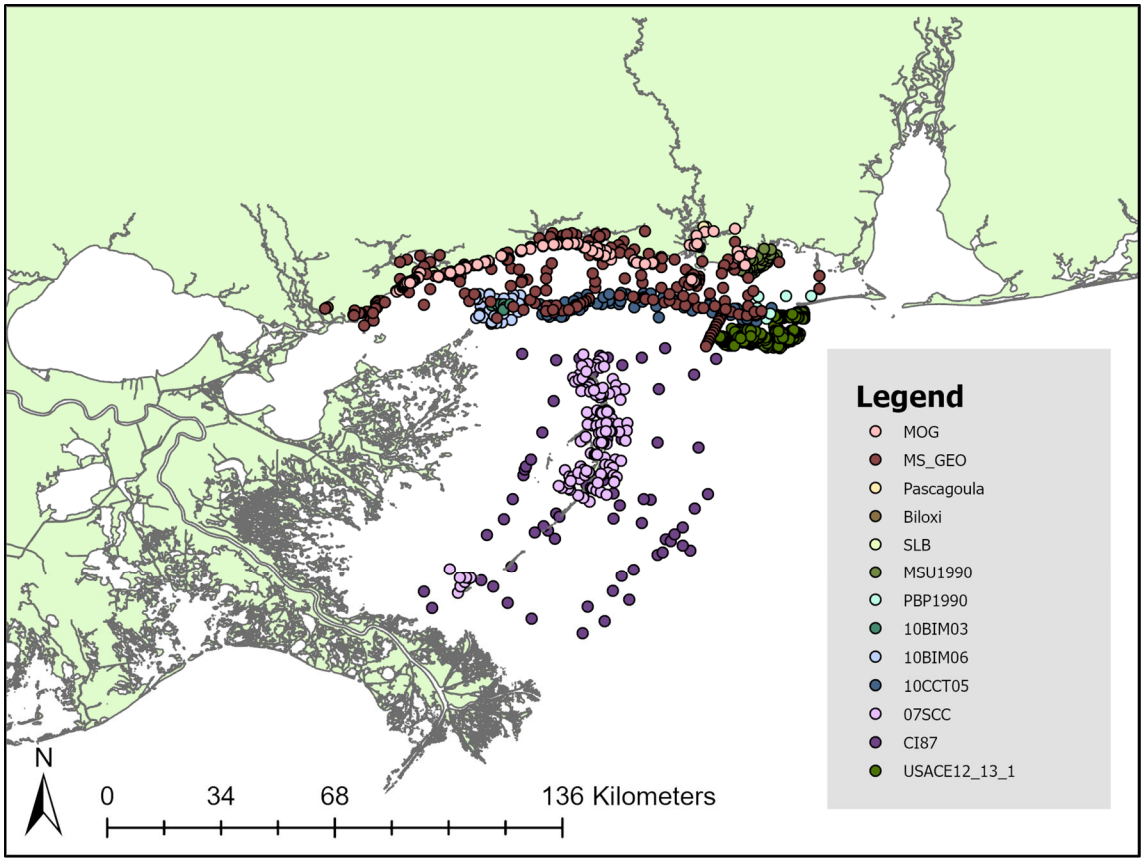

Figure 8. Northern Gulf legacy core data compiled in the USM database.
From Dike 2022.
Data were QA/QC and will be added to MMIS.

Table 1. Legacy core and geophysical data collected in USM database.

Modified from Dike 2022.

Data Name	Location	Type	Dates	Associated Publications	Citation
MOG	Hancock County, Deer Island, Harrison County, Belle Fontaine and Round Island, Grand Bay NERR	vibracores, auger-cores, and hand-cores	1999–2003		(Gulf Coast Research Lab 2004)
MS_GEO	Barrier islands, Gulf inner shelf, Hancock County, Harrison County, Jackson County, major bays (Bay St. Louis, Biloxi Back Bay), Mississippi Sound	vibracores and rotary cores	1980–2003	(Otvos and Giardino 2004, Otvos 2001)	(Gulf Coast Research Lab 2021)
Pascagoula	Pascagoula River	rotary wash	2016		(Burns, Cooley, Dennis Inc. 2009)
Biloxi	Biloxi River	rotary wash	2005–2006		(Burns, Cooley, Dennis Inc. 2009)
SLB	Bay St. Louis		2005–2006		(Burns, Cooley, Dennis Inc. 2009)
MSU1990	Grand Bay National Estuary Research Reserve	Vibracores	1990		(Kramer 1990)
PBP1990	Petit Bois Island	Vibracores	1990	(McBride et al. 1991)	(McBride et al. 1991)
10BIM03	Cat Island	Vibracores	2010	(Kindinger et al. 2014, Miselis et al. 2014)	(Buster et al. 2014)
10BIM03	Cat Island	Vibracores	2010	(Kindinger et al. 2014, Miselis et al. 2014)	(Buster et al. 2014)
10CCT05	Ship, Horn, and Petit Bois Islands	Vibracores	2010		(Kelso and Flocks 2015)
07SCC	Chandeleur and Breton Islands	Vibracores	2007		(Dreher et al. 2010)
CI87	Chandeleur Islands	Vibracores	1987	(Brooks et al. 1995, Kindinger et al. 1989)	(Dreher et al. 2010)
USACE12_13	Mississippi Sound and Mississippi-Alabama Barrier Islands	Vibracores	2010–2013	(Flocks et al. 2015, Flocks et al. 2014)	
Erda_90-1_PBP	Petit Bois Pass	Boomer	1990	(McBride et al. 1991)	(Bosse et al. 2017a)
Erda_90-1_HC	Lake Borgne and Mississippi Sound	boomer	1990		(Bosse et al. 2017a)

Data Name	Location	Type	Dates	Associated Publications	Citation
Erda_91-3	Mississippi Sound	boomer	1991	(Gal et al. 2021)	(Bosse et al. 2017a)
Erda 92-2	Grand, Cat, and Horn Islands	boomer	1992	(Hollis et al. 2019, Gal et al. 2021)	(Bosse et al. 2018a)
Erda 92-4	Horn and Petit Bois Islands	boomer	1992	(Hollis et al. 2019, Gal et al. 2021)	(Bosse et al. 2018a)
91KI2	Mississippi-Alabama-Florida Shelf	boomer	1991	(Kindinger et al. 1994)	(Bosse et al. 2018b)
90KI	Mississippi-Alabama Shelf	boomer	1990	(Kindinger et al. 1994)	(Bosse et al. 2018b)
81GY6	Mississippi-Alabama-Louisiana Shelf	minisparker	1981	(Greene et al. 2007, Kindinger 1988, Kindinger et al. 1994, Roberts et al. 2004)	(Bosse et al. 2018b)
81CA1	Mississippi-Alabama-Louisiana Shelf	boomer	1981	(Penland et al. 1985)	(Bosse et al. 2018b)
81CA2	Mississippi-Alabama-Louisiana Shelf	boomer	1981	(Penland et al. 1985)	(Bosse et al. 2018b)
USFHC	Bay St. Louis and Mississippi Sound	boomer	1989		(Bosse et al. 2018c)
09cct03,04	Horn and Petit Bois islands	CHIRP	2009	(Hollis et al. 2019, Gal et al. 2021)	(Forde et al. 2011a)
10cct01	Cat Island	CHIRP	2010		(Forde et al. 2011b)
10cct02	Ship and Horn islands	CHIRP	2010	(Hollis et al. 2019, Gal et al. 2021)	(Forde et al. 2011b)
10cct03	Horn, Petit Bois and Dauphin islands	CHIRP	2010	(Hollis et al. 2019, Gal et al. 2021)	(Forde et al. 2011b)
10bim04	Cat Island	CHIRP	2010		(Forde et al. 2012)
2010-12 FA	Ship and Horn islands	CHIRP	2010	(Gal et al. 2021)	(Pendleton et al. 2011)
13cct04	Petit Bois Island	CHIRP	2013	(Hollis et al. 2019)	(Forde et al. 2015)

7 Results

From our detailed legacy data compilation with new data collection based on data gaps (Tasks 1-3, 5, 6, 7, 8), we developed a stratigraphic-based nomenclature and organization scheme for sand-rich lithofacies types identified in the study area (Task 4 and Task 9). As an important component of this task, we developed a conceptual stratigraphic evolutionary model for Late Quaternary to recent deposits offshore Mississippi including lowstand shelf fluvial deposits, transgressive shelf deposits and the modern shelf-coastal system. The following results section is framed in this context.

7.1 Quaternary Chronostratigraphic Framework

Both seismic and lithofacies units were created for this project and are based largely on previous work assembled for this Mississippi Co-Op1and reinterpreted holistically (Flocks et al. 2015, Hummel and Parker 1995, Kramer 1990, McBride et al. 1991, Otvos 1986, 1985, 1981, 1979, Twichell et al. 2011). These units characterize the stratigraphic record and constrain the Quaternary evolution of the area and geologic framework.

Fourteen facies, two sequence boundaries, and numerous bounding ravinement surfaces were identified from geophysical and sediment core data. The two sequence boundaries are associated with subsequent lowstands (MIS 6 and MIS 2). Both formed as subaerial exposure surfaces and exhibit varying fluvial incisional geometries (Figure 10 and Figure11). Legacy and newly collected radiocarbon ages constrain the evolutionary timing of these facies (Tables 2-4). Additionally, grain size data are used to characterize several facies where available (Gal et al. 2021).

Table 2. New radiocarbon ages for this study.

From Hollis et al. 2019.

Core	El. (msl)	Material Dated	^{14}C Age	Median ± Cal. 2σ Age (yrs BP)	Cal. 2σ Age Range (yrs BP)	Facies
10cct05-02	−11.59	*Mulinia lateralis*	2210 ± 120	1808 ± 289	1526–2104	U Shoreface
10cct05-02	−12.61	*Mulinia lateralis*	2840 ± 160	2570 ± 393	2162–2947	L Shoreface
10cct05-02	−13.61	*Raeta plicatella*	6500 ± 120	7001 ± 274	6712–7260	U Shoreface
10cct05-03	−14.11	*Rangia flexuosa*	6420 ± 120	6912 ± 283	6629–7195	Estuarine
10cct05-03	−15.80	*Crassostrea virginica* *	>38,900	–	–	Estuarine
10cct05-03	−15.8	*Noetia ponderosa* *	>40,900	–	–	Estuarine
10cct05-03	−15.91	*Mercenaria campechiensis* *	>41,000	–	–	Marine
10cct05-06	−5.14	*Cyclinella tenuis*	930 ± 100	537 ± 229	334–681	Flood Tidal Delta
10cct05-06	−5.64	*Strombus alatus*	2610 ± 110	2295 ± 313	2019–2644	Flood Tidal Delta
10cct05-07	−5.79	*Abra aequalis*	>Modern	–	–	Estuarine
10cct05-07	−6.10	*Mulinia lateralis*	>Modern	–	–	Estuarine
10cct05-07	−6.11	*Mulinia lateralis*	115 ± 100	–	–	Estuarine
10cct05-08	−5.37	*Abra aequalis*	920 ± 100	529 ± 171	329–671	Estuarine
PBO17-2	−11.11	*Abra aequalis*	2480 ± 110	2123 ± 268	1855–2390	Estuarine
MS-1	−3.55	Shell frag[a]	2940 ± 110	2702 ± 280	2376–2953	Flood Tidal Delta
MS-1	−4.53	Shell frag[a]	4070 ± 140	4070 ± 381	3725–4486	Flood Tidal Delta
MS-5	−3.04	*Cyclinella tenuis*	1650 ± 110	1199 ± 232	949 - 1412	Estuarine
MS-5	−3.69	*Trachycardium* sp.[a]	2720 ± 110	2450 ± 274	2166–2714	Estuarine
MS-5	−4.07	Shell frag[a]	3680 ± 110	3600 ± 296	3319–3911	Estuarine
MS-9	−3.93	*Mulinia lateralis*	Modern	–	–	Estuarine
MS-9	−3.98	*Mercenaria mercenaria*	Modern	–	–	Marine/Flood Tidal Delta
MS-9	−4.88	*Abra aequalis*	400 ± 100	–	–	Barrier (overwash)
MS-9	−5.85	*Cyrtopleura costata*	2150 ± 110	1740 ± 265	1475–2005	Estuarine
MS-9b	−5.85	*Cyrtopleura costata*	2120 ± 110	1703 ± 265	1433–1962	Estuarine

Note: [a] notes single intact valve or reworked samples and * notes samples near and/or beyond the radiocarbon detection limit.

Table 3. Legacy radiocarbon ages for this study.

From Hollis et al. 2019.

Core	El. (msl)	Material	^{14}C Age	Median ± Cal. 2σ Age (yrs BP)	Cal. 2σ Age Range (yrs BP)	Facies	Citation
DI-1	−12.30	Peat [b]	23,500 ± 3825	27,434 ± 8168	18,875–35,211	Estuarine	Otvos (1979)
DI-2	−11.40	Wood [b]	25,840 ± 1330	29,887 ± 2606	27,433–32,645	Estuarine	Otvos (1979)
DI-2	−11.90	Wood [b]	36,290 ± 2060	40,434 ± 3957	36,103–44,018	Estuarine	Otvos (1979)
DI-2	−13.20	Wood [b]	30,400 ± 2185	34,506 ± 4579	30,254–39,412	Estuarine	Otvos (1979)
DI-3	−2.90	Mollusk	6670 ± 165	7175 ± 348	6795–7490	Inlet Fill/Spit	Otvos (1979)
DI-6	−2.57	Oyster Shell [a]	1215 ± 80	798 ± 145	654–943	Flood Tidal Delta	Otvos (1986)
DI-8	−0.20	Humate	7700 ± 820	8665 ± 1874	6848–10,596	Salt Marsh	Otvos (1979)
P-3	−13.63	Wood	7815 ± 80	8613 ± 187	8420–8793	Estuarine	Otvos (1979)
P-4	−18.00	*Strombus alatus* [a]	38,960 ± 3125	42,430 ± 6029	36,162–48,219	Marine Mud	Otvos (1979)
R-1	−11.89	Wood	7315 ± 85	8127 ± 174	7975–8323	Estuarine	Otvos (1979)
R-3	−8.40	Dispersed plant	6765 ± 270	7635 ± 511	7155–8176	Estuarine	Otvos (1979)
R-3	−15.40	Wood	7825 ± 160	8678 ± 346	8342–9034	Estuarine	Otvos (1979)
H-1	−11.10	*Cardium* sp.	4615 ± 215	4839 ± 567	4284–5418	Barrier	Otvos (1979)
H-2	−16.20	Peat	8010 ± 85	8865 ± 244	8604–9092	Freshwater Marsh	Otvos (1979)
H-7	−18.60	Wood	34,935 ± 1820	39,202 ± 3526	35,400–42,451	Estuarine	Otvos (1979)
SS-4	−15.59	*Strombus alatus*	6315 ± 80	6779 ± 156	6582–6894	Marine Mud	Otvos (1985)
SS-4	−16.50	Oyster shell [a]	21,640 ± 4690	24,827 ± 10,440	13,722–34,602	Estuarine	Otvos (1985)
SS-8	−15.44	Mollusk	4160 ± 305	4223 ± 793	3438–5023	Marine Mud	Otvos (1985)
SS-8	−18.17	*Strombus alatus*	4735 ± 115	5004 ± 299	4704–5302	Marine Mud	Otvos (1985)
SS-10	−18.47	*Cyrtopleura costata*	4865 ± 175	5153 ± 407	4768–5581	Estuarine?	Otvos (1985)
SS-11	−21.20	Wood	8800 ± 80	9849 ± 282	9595–10,158	Estuarine	Otvos (1985)
SS-12	−19.68	*Mercenaria m. texana*	6560 ± 95	7070 ± 210	6847–7266	Sand Sheet	Otvos (1985)
SS-12	−21.20	*Mercenaria campechiensis* [a]	6400 ± 75	6879 ± 203	6686–7092	Flood Tidal Delta	Otvos (1985)
MS-9	−7.12	Peat	6590 ± 60	7491 ± 80	7420–7580	Salt Marsh	Hummel and Parker (1995)

Core	El. (msl)	Material	^{14}C Age	Median ± Cal. 2σ Age (yrs BP)	Cal. 2σ Age Range (yrs BP)	Facies	Citation
MS-11	−7.57	Organic sediment	6040 ± 150	6905 ± 359	6544–7261	Salt Marsh	Hummel and Parker (1995)
MS-13	−4.54	Wood (root)	6860 ± 100	7710 ± 157	7565–7878	Estuarine/Delta	Hummel and Parker (1995)
MS-14	−6.06	Peat	6190 ± 80	7086 ± 191	6887–7269	Salt Marsh	Hummel and Parker (1995)
MS-15	−3.85	Oyster shell	3700 ± 60	3618 ± 169	3460–3798	Oyster Biostrome	Hummel and Parker (1995)
MS-24	−4.15	Oyster shell	3570 ± 70	3465 ± 172	3301–3644	Oyster Biostrome	Hummel and Parker (1995)
MS-25	−3.82	Oyster shell	2690 ± 60	2401 ± 193	2262–2648	Oyster Biostrome	Hummel and Parker (1995)
MS-27	−2.48	Wood	4020 ± 110	4512 ± 300	4230–4830	Estuarine	Hummel and Parker (1995)
MS-28	−1.64	Oyster shell	710 ± 60	359 ± 108	257–473	Oyster Biostrome	Hummel and Parker (1995)
MS-28	−4.27	Wood	19,540 ± 220	23,531 ± 539	22,972–24,049	Alluvial	Hummel and Parker (1995)
MS-29	−5.03	Oyster shell	3900 ± 80	3877 ± 225	3644–4093	Oyster Biostrome	Hummel and Parker (1995)
MS04-1	−7.76	*Probythenella lousianae*	4030 ± 30	4046 ± 112	3935–4159	Estuarine	Greene et al. (2007)
MS04-1	−8.66	Wood*	>48,000	–	–	Alluvial/Estuarine	Greene et al. (2007)
MS04-1	−10.52	Wood*	>48,000	–	–	Alluvial/Estuarine	Greene et al. (2007)
MS04-4	−5.91	Peat	5470 ± 50	6272 ± 106	6184–6396	Marsh	Greene et al. (2007)
MS04-5	−12.58	Wood*	38,400 ± 330	–	–	Alluvial/Estuarine	Greene et al. (2007)

Note: [a] notes previously reported reworked samples, [b] notes previously reported contaminated age samples, and * notes samples near and/or beyond radiocarbon detection limit.

Table 4. New radiocarbon ages for this study.

From Gal et al. 2021.

Core	Depth relative to core (cm)	Uncalibrated ^{14}C Age	Error	Calibrated median age BP	Calibrated median age BP (2 sigma)	Accession number	Taxa	Environment (from Andrews 1981)
10CCT05–48	354	5900	220	6320	5844-6836	OS-140807	*Raeta plicatella**	Lives on sandy bottom of outer surf zone; epifauna
10CCT05–13	106	810	150	423	113-671	OS-140808	Cirripedia: Balanomorpha (Barnacle)	N/A
10CCT05–9	164–169	7250	230	7730	7300-8177	OS-140802	*Strombus alatus*	Intertidal to nearshore; epifauna
10CCT05–9	260	6700	230	7191	6678-7623	OS-140806	*Mulinia lateralis**	Clayey sediments; infauna
10CCT05-14B	57	1660	160	1209	887–1552	OS-140809	*Eurytellina alternata**	Tidal inlet environment
10CCT05–40	363–369	3010	210	2788	2294-3324	OS-140803	*Raeta plicatella**	Lives on sandy bottom of outer surf zone; epifauna
10CCT05–40	393	3470	210	3340	2814-3852	OS-140805	*Mulinia lateralis**	Clayey sediments; infauna
10CCT05–40	460	3720	220	3660	3097-4248	OS-140804	*Parvilucina crenella**	Offshore and inlet-influenced areas; infauna
10CCT05–41	345	1590	160	1138	800–1471	OS-140810	Gastropod	N/A
10CCT05–42	489–490	4190	120	4270	3922-4599	OS-139808	*Foveamysia soror**	Inlet-influenced areas; infauna
10CCT05–42	505	4070	110	4110	3819-4410	OS-139802	*Americoliva sayana*	Inlets and offshore; infauna
10CCT05–42	510	4340	110	4482	4186-4796	OS-139806	*Phlyctiderma semiaspera***	Open-bay centers, jetties, inlet-influenced areas; infauna
10CCT05–42	510	4950	180	5256	4817-5651	OS-139807	*Phlyctiderma semiaspera*	Open-bay centers, jetties,

Core	Depth relative to core (cm)	Uncalibrated ^{14}C Age	Error	Calibrated median age BP	Calibrated median age BP (2 sigma)	Accession number	Taxa	Environment (from Andrews 1981)
								inlet-influenced areas; infauna
10CCT05–43	80	3530	110	3419	3137-3692	OS-139805	*Americoliva sayana*	Inlets and offshore; infauna
10CCT05–43	145	4740	110	5009	4722-5302	OS-139804	*Strombus alatus*	Intertidal to nearshore; epifauna
10CCT05–43	276	4410	110	4576	4276-4836	OS-139803	*Americoliva sayana*	Inlets and offshore; infauna
10CCT05–43	283	5400	130	5775	5505–6088	OS-139800	*Phlyctiderma* cf. *soror***	Inlet-influenced areas; infauna
10CCT05–43	283	4780	110	5059	4789-5328	OS-139801	*Phlyctiderma* cf. *soror* **	Inlet-influenced areas; infauna

Note: Taxa designated with a * indicate they were articulated when extracted from the core. Taxa designated with a ** indicate a likely reworked sample.

7.1.1 Marine Isotope Stage 6 Lowstand Sequence Boundary

The marine isotope stage 6 sequence boundary (MIS 6 SB) is defined by a medium to high amplitude, semi to highly continuous reflector, ranging in depth between 10 and 45 m below sea level (mbsl) (4–25 m below seafloor (mbsf)). This surface is characterized by channel geometries truncating underlying reflectors below with onlapping reflectors above. This surface represents the oldest surface found in the dataset. These large, wide MIS 6 SB valleys (Figure 10) are truncated by a younger, shallower sequence boundary (MIS 2 SB) south of Horn Island. On the OCS, four dated samples from the MIS 6 valley fill in seaward areas dated between MIS 3 and 5, confirming the valley is MIS 6.

Previous publications on the area reported a similar interpretation to the Pre-MIS 2 sequence boundary (Gonzalez et al. 2017, Greene et al. 2007). The shelf edge Lagniappe Delta is dated to be MIS 6 or 8 age (Roberts et al. 2004). A Lagniappe Delta feeder valley on the mid-shelf trending towards the Pascagoula River was investigated by (Bartek et al. 2004). In an eastern section of the valley, the fill is older than MIS 2 (Gonzalez et al. 2017), dated to be MIS 3–4 (Reese et al. 2018). We associate this Lagniappe feeder valley as the downdip contemporaneous pre-MIS 2 surface in our study site associated MIS 6, and it will be referred to as MIS 6 SB for the remainder of this report for simplicity. The timing is constrained to between MIS 3 to MIS 6.

7.1.2 Marine Isotope Stage 2 Lowstand Sequence Boundary

The marine isotope stage 2 sequence boundary (MIS 2 SB) is defined by a low to high amplitude, semi to highly continuous reflector, ranging in depth between 3 and 30 meters below sea level (mbsl) (0–15 m mbsf). The MIS 2 SB had previously been interpreted to truncate a deeper sequence boundary (Flocks et al. 2015), supporting our interpretation. This time-transgressive subaerial surface formed during the Last Glacial Maximum (MIS 2 SB) (Figures 10 and 11). Radio- carbon ages directly overlying the MIS 2 SB are Holocene (Table 3), confirming it is amalgamated with a transgressive surface.

7.1.3 Surfaces

This section describes five surfaces observed in geophysics and sediment cores: transgressive, wave ravinement, tidal ravinement, bay ravinement, sand ridge ravinement surfaces.

7.1.3.1 Unconformity 1: Transgressive Surface (TS)

This erosional boundary represents the unconformable separation of lowstand fluvial deposits from estuarine and/or marine deposits above (Figure 12 through Figure 19). It is a continuous surface throughout the study area and is often amalgamated with other surfaces in interfluvial areas. It is interpreted as the transgressive surface (TS) (Cattaneo and Steel 2003).

7.1.3.2 Unconformity 2: Wave Ravinement Surface (wRs)

This erosional boundary separates estuarine, alluvial, and marine sediments (Figure 12 through Figure 19). It is generally manifest as a high amplitude continuous reflector and composed of a coarse shell lag layer (Figure 20) in most cases (with the exception of capping paleovalleys). It is often be amalgamated with the other ravinement surfaces (Figures 12 through 19). It is interpreted as the wave ravinement surface (wRs) (Cattaneo and Steel 2003), similar a shoreface ravinement surface observed along the Texas coast (Rodriguez et al. 2001). Its depth varies widely within the study area generally between 7 and 10 mbsl. The surface is found to be thick shell hash, marine muds and/or shelly inner shelf sand deposits which onlap shoreface deposits. Some areas show a hiatus with no preserved Holocene deposits

representing a minimum ravinement depth. The wRs defines the seaward extent of active barrier island sediment transport.

7.1.3.3 Unconformity 3: Tidal Ravinement Surface (tRs)

This erosional boundary represents the separation of alluvial and estuarine deposits (lower) from tidal deposits (higher) (Figure 14 through Figure 17). It is found throughout paleovalleys, within Mississippi Sound and beneath all barrier islands. It is observed in some cases lower than the wave ravinement surface (Figure 16B) or amalgamated with the TS (Figure 16B). It is composed of an erosional base as a coarser-grained shell lag layer and is found associated with other tidal deposits (i.e., inlets, tidal deltas). It is interpreted as the tidal ravinement surface (tRs) (Cattaneo and Steel 2003).

7.1.3.4 Unconformity 4: Bay Ravinement Surface (bRs)

Bay ravinement is an erosional process related with the lower energy wave base of open marine Gulf conditions. It results in shallower erosion due to more protection from wind. Within estuarine deposits in the study area, an observed erosional boundary separates alluvial from estuarine deposits. This boundary is identified as the bay ravinement surface (bRs) (Cattaneo and Steel 2003).

The bRs is found between 1 and 4 mbsl and is composed of slightly coarser material in certain Mississippi Sound cores (Hummel and Parker 1995).

A)

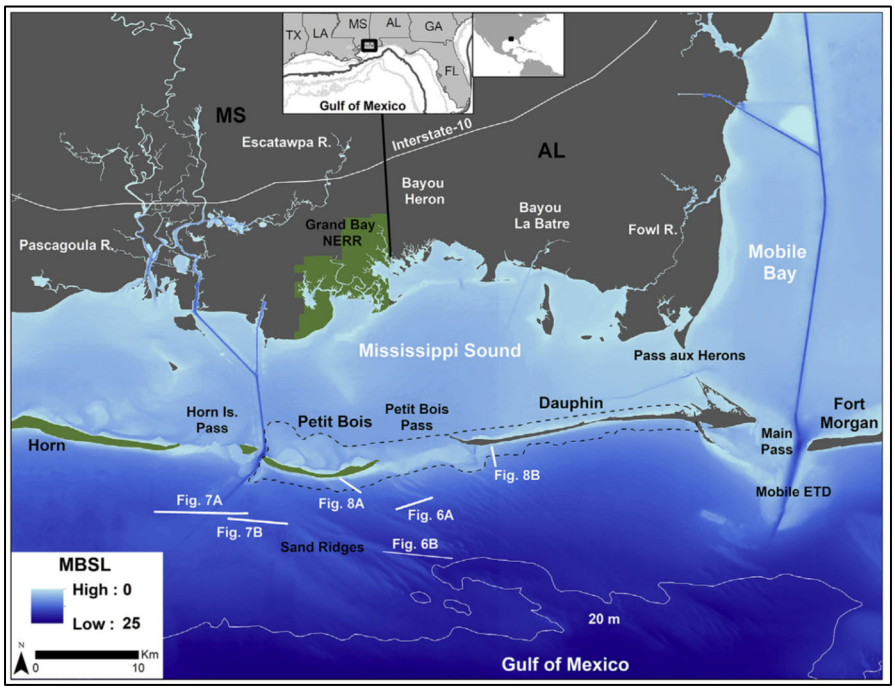

B)

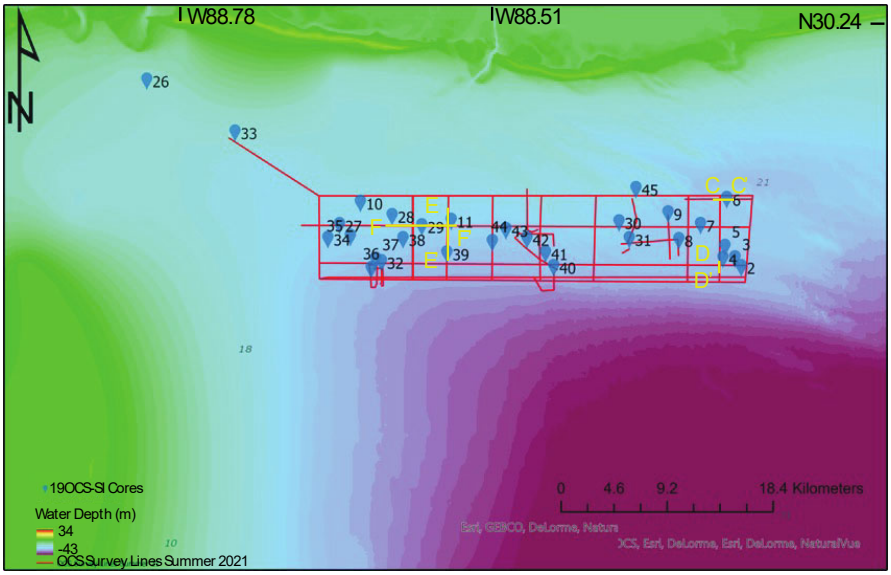

Figure 9. Geophysical example locations and new data collected.
A) Study area map showing locations of legacy geophysical examples (from Hollis et al. 2019). See Figure 5 for lease blocks. B) Newly acquired boomer data (red grid) and vibracores (blue dots) for this MS Co-Op1. Yellow lines are shown in Figure 18 (E-E' and F-F') and Figure 19 (C-C' and D-D').

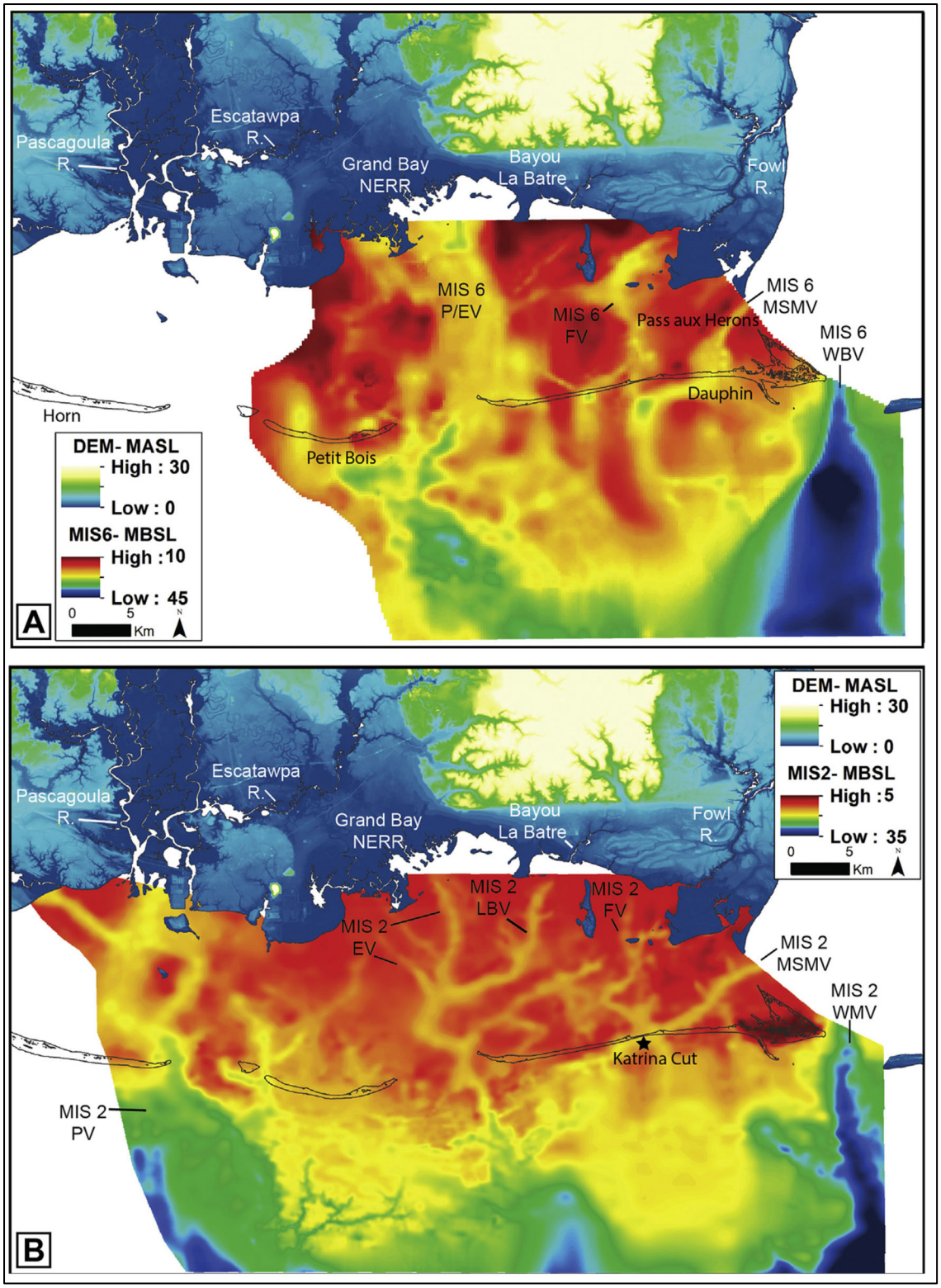

Figure 10. Incised valley maps produced in the study area.
From Hollis et al. 2019.
A) MIS 6 and B) MIS 2 incised valleys near Dauphin and Petit Bois Islands.

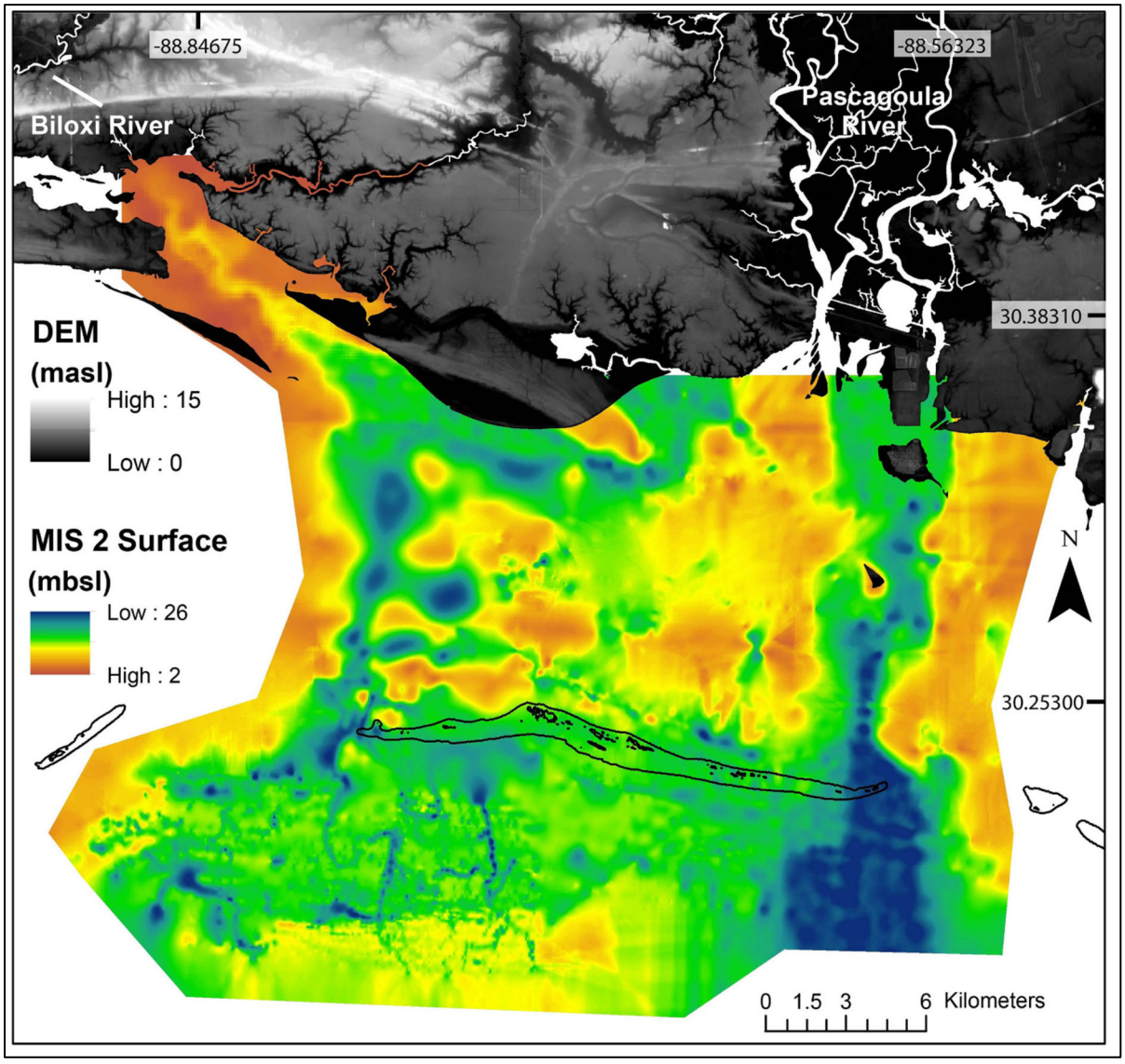

Figure 11. MIS 2 incised valleys near Horn Island.
From Gal et al. 2021.

7.1.3.5 Unconformity 5: Sand Ridge Ravinement Surface (sRs)

Beneath inner shelf sand ridge deposits, an erosional boundary separates the base from variable underlying stratigraphy (Figure 15B). Previous studies have identified basal scour from large-scale bedform migration (e.g., Goff 2014), and we similarly interpret this surface as the sand ridge ravinement surface (sRs).

7.2 Seismic-lithofacies

7.2.1 Unit 1: Undifferentiated Pleistocene

In sediment cores, Unit 1 is characterized by stiff, oxidized, mottled yellowish orange, brown gray, and greenish gray clays, sandy clays and clayey sands (Figure 12 through Figure 19). Plant roots and sand and mud-filled burrows are also present near the top (Figure 21 through Figure 24). Shell and plant material range are often abundant throughout the entire unit, although some cores are devoid of this material. Due to these factors, Unit 1 is interpreted as a paleosol, indicating it formed through subaerial exposure.

In geophysics, Unit 1 has variable reflector geometries and is found below the MIS 2 SB in the study area (Figure 12 through Figure 19). This unit contains various Pleistocene coastal plain deposits (marine, estuarine, and/or fluvial facies (Figure 12 through Figure 19) (Hummel and Parker 1995, Kramer 1990, Otvos 1985 and 1981)). These environments have been correlated to updip formations, where they have been dated to Pleistocene (Otvos 2001, 1986, and 1985). Because a complete delineation of these formations on the inner shelf is beyond the scope of this study, we refer to this lower unit as undifferentiated Pleistocene deposits.

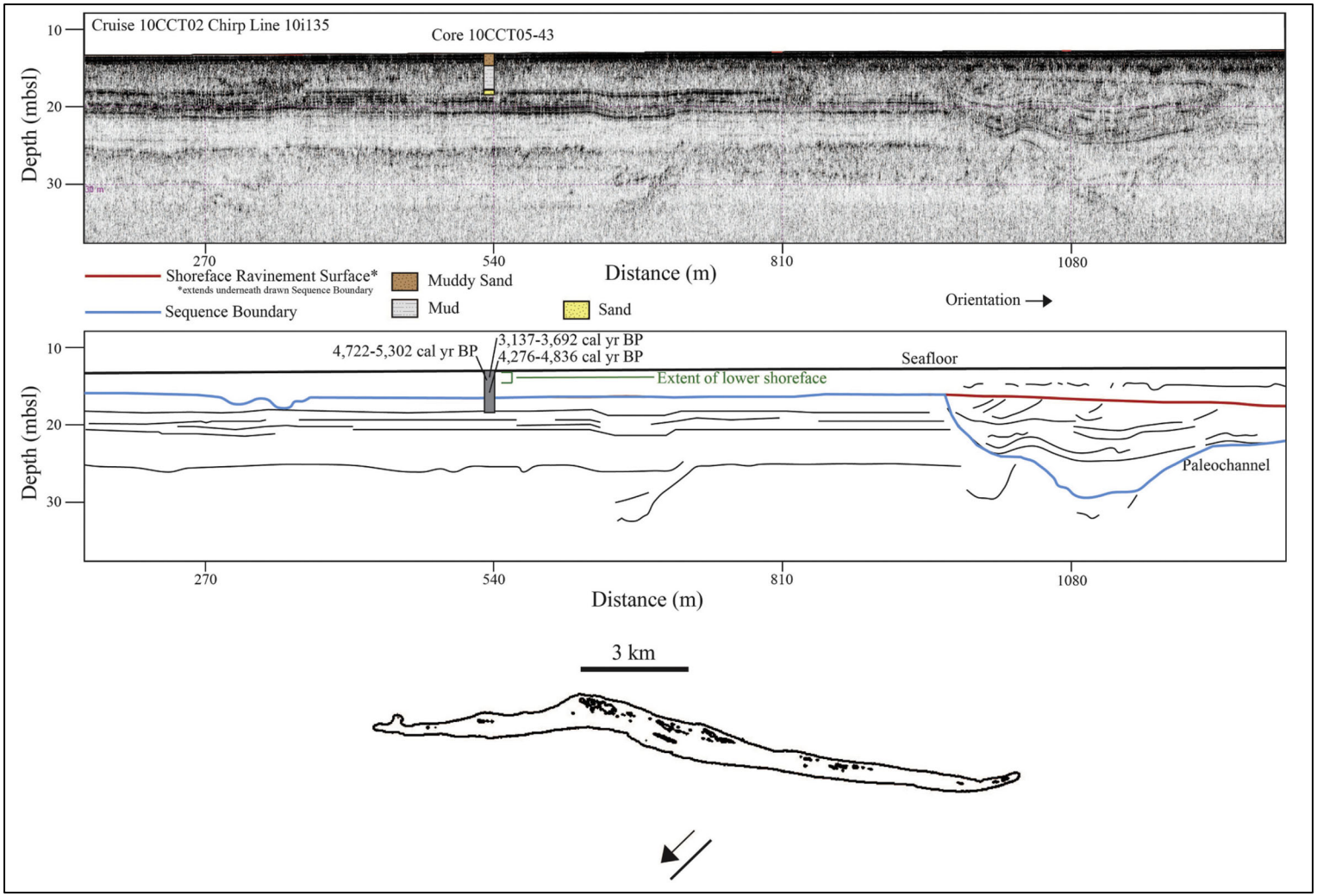

Figure 12. Example legacy CHIRP profile 10il35 offshore Horn Island.
From Gal et al. 2021.
Top image is uninterpreted; bottom image is interpreted. Note the geophysical surfaces and sedimentology of core 10CCT05-43 with radiocarbon ages (Table 4).

7.2.2 Unit 2: Fluvial Channel Sands

In sediment cores, Unit 2 consists of tan to white, moderately to poorly sorted fine to gravelly sands, with unidirectional and high angle cross stratification (Parker et al. 1993). Heavy minerals were also present, and shell material was notably absent. From updip, onland engineering borings along the Interstate-10 bridge, the reports describe 7–16m thick, clean sands which overly dense clays (Burns Cooley Dennis Inc 2016). These descriptions and depths are consistent with fluvial channel sand interpretations found in the offshore seismic profiles.

In geophysics, Unit 2 is characterized by channel fill geometry consisting of medium to high amplitude low frequency, chaotic to transparent reflectors. This is similar to previously interpreted channel facies identified from previous studies in Florida and Texas (Goff, 2014, Thomas and Anderson, 1994). Due to its depth and homogenous characteristics, this unit was often difficult to geophysically image. In some locations it was resolved well (Figure 12 through Figure 19), and here Unit 2 was bound by a sequence boundary and the TS. Based on these characteristics, this unit is interpreted as lowstand fluvial channel sands.

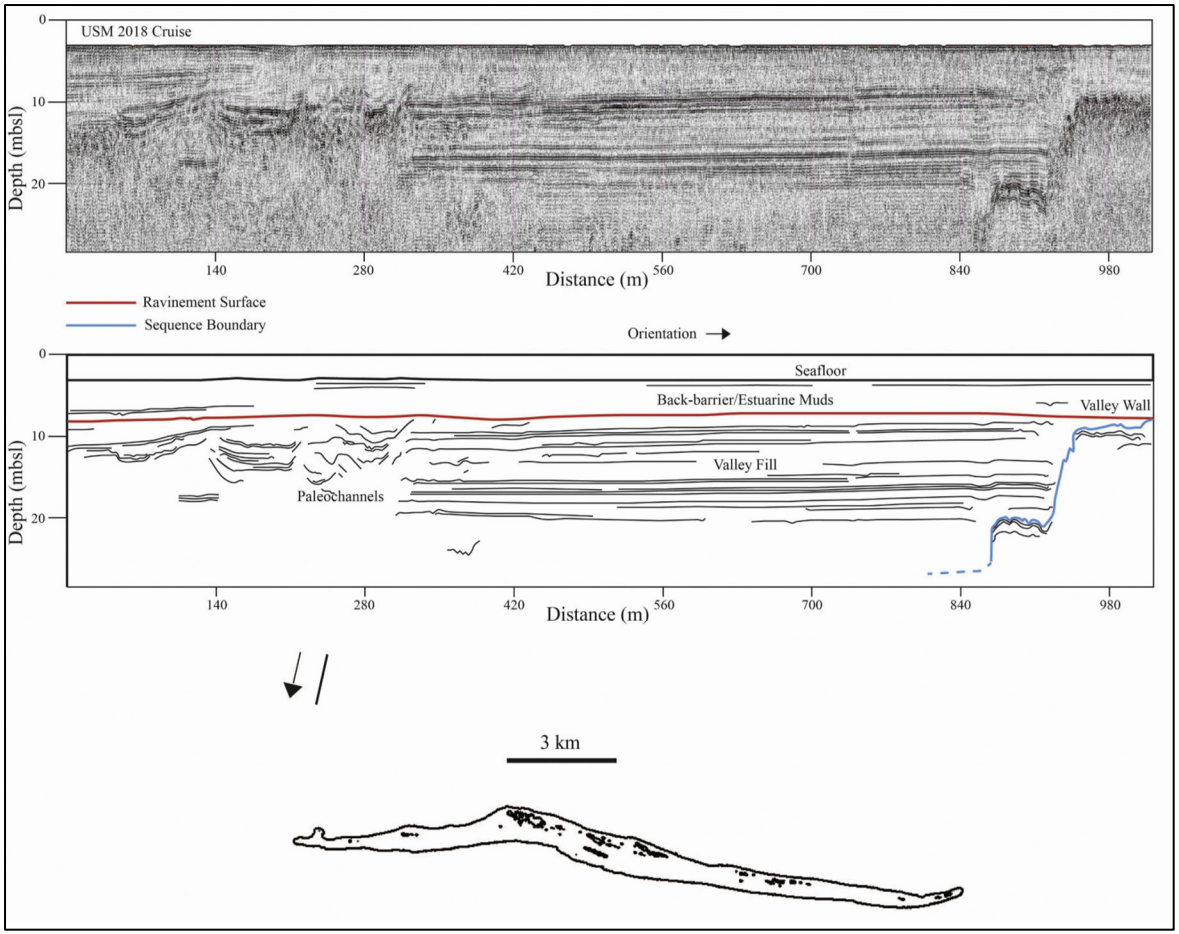

Figure 13. Example USM 2018 boomer profile in Mississippi Sound behind Horn Island.
From Gal et al. 2021.
Top image is uninterpreted, bottom image is interpreted. Note the clear MIS 2 incised valley wall.

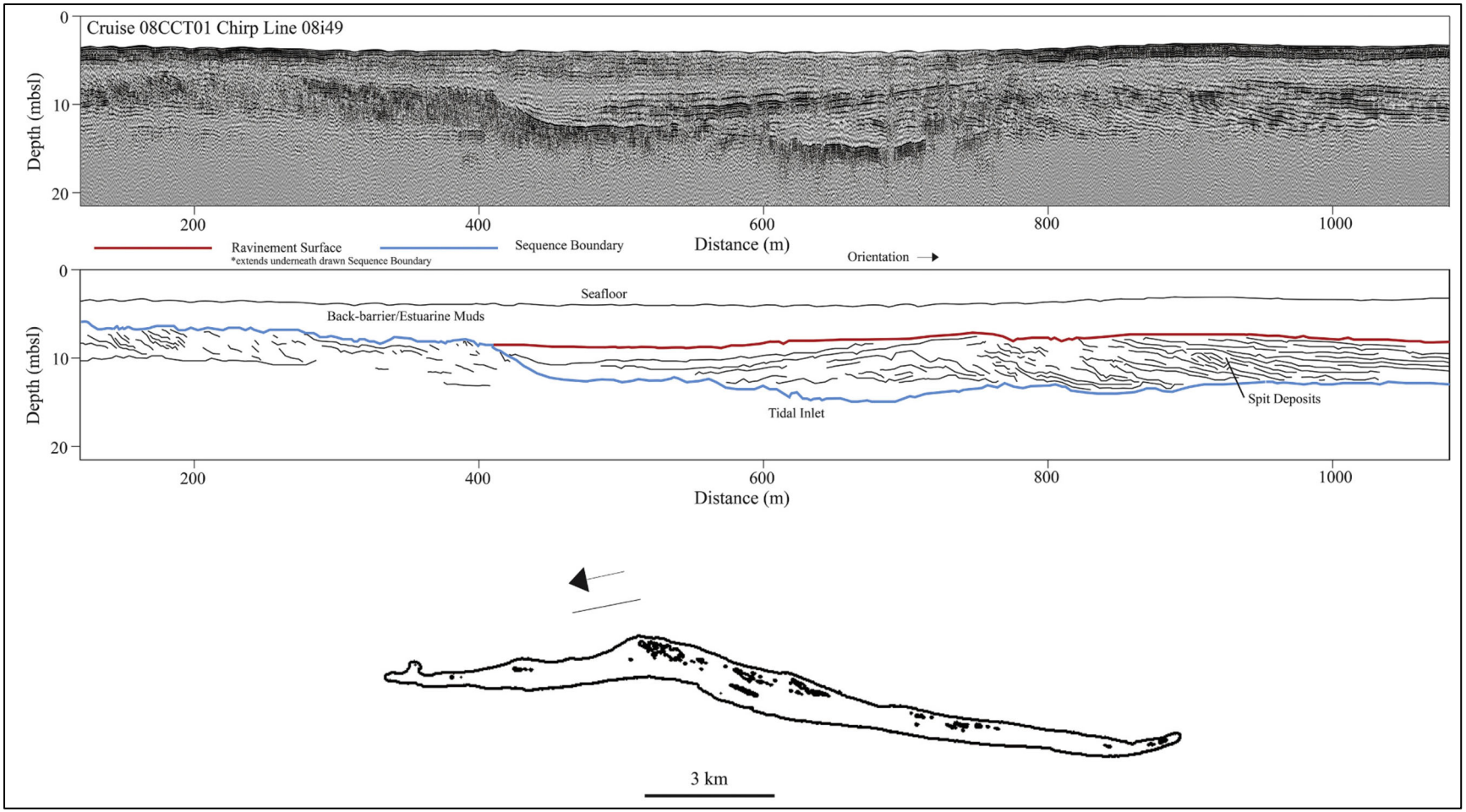

Figure 14. Example legacy CHIRP profile08i49 behind Horn Island.
From Gal et al. 2021.
Top image is uninterpreted, bottom image is interpreted.

7.2.3 Unit 3: Fluvial Point Bar

From sparse samples in sediment cores, Unit 3 was sampled only in the very upper intervals. The sediment consisted of well sorted, medium to fine sands that were interbedded with grayish brown, medium to fine sands and olive-gray muds (Figure 17, core 10CCT05-03). Shell content was minimal to absent throughout the unit (Kelso and Flocks 2015). Sand and mud filled burrows and wood fragments are common.

In geophysics, Unit 3 is characterized by low to medium amplitude, steeply dipping oblique and/or progradational reflectors (Figures 15A, B, 17). This implies the presence of higher sand content environments, such as fluvial bars or portions of bayhead deltas. In some geophysical lines, there is clear mounded feature with reflectors dipping in opposite directions or top lapping, low amplitude horizontal reflectors in the top sections (e.g., Bartek et al. 2004, Flocks et al. 2015, Greene et al. 2007, Thomas and Anderson 1994). This unit also consists of channel fill geometries and is interpreted as laterally accreted point bar deposits based on similarities to other systems (Durkin et al. 2015, Ghinassi et al. 2016, Reijenstein et al. 2011). Due to the sparse, shallow sediment core sampling, this unit is difficult to differentiate from possible fluvial bar facies.

7.2.4 Unit 4: Marsh

In sediment cores, Unit 4 consists of brown to dark gray peat (plant organic material) or root material in a poorly sorted sediment matrix. Shells are absent, and the sediment is mottled with burrows (Hummel and Parker 1995).

In geophysics, Unit 4 was thin (0.2–0.6m) and usually associated with subsurface gas, which caused geophysical data to be washed out (e.g. Zaremba et al. 2016). This unit is interpreted as marsh deposits and generally overlies Pleistocene deposits in the subsurface (Figure 22, core MS-9). Along back-barriers and bay margins, where it overlies washover sands (Figure 22, see core GSA-DI9). This unit was also found within the eastern Mississippi Sound and is dated between ~7500–6300 BP (Table 3) and is interpreted as saltmarsh. Other freshwater marsh deposits were found within fluvial incised valleys but were not used for generalized shoreline interpretations (Table 3).

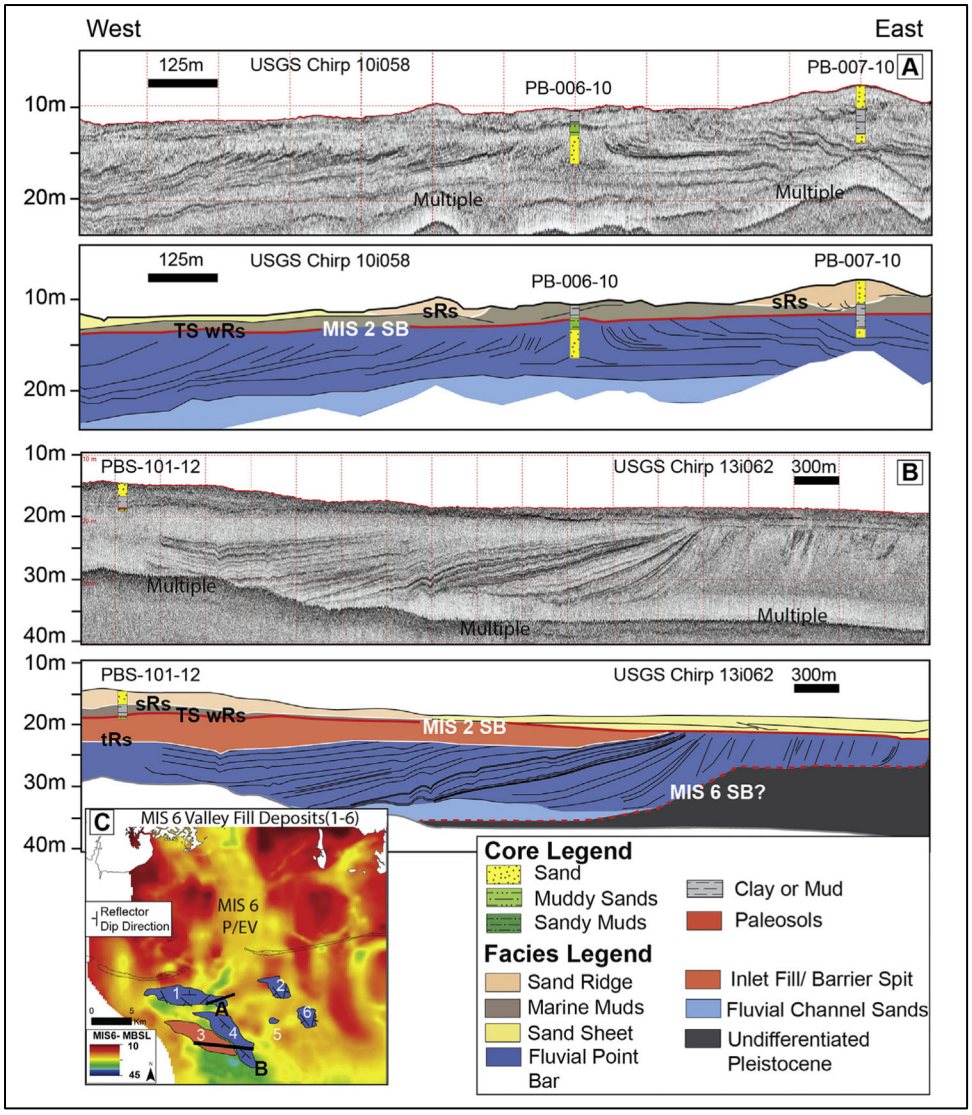

Figure 15. Example legacy CHIRP profiles 10i058 (A) and 13i062 (B).
From Hollis et al. 2019.
See Figure 9 for location. Top image pairs are uninterpreted and/or interpreted profiles. Note the geophysical surfaces and sedimentology of cores PB-006-10 and PBS-101-12.

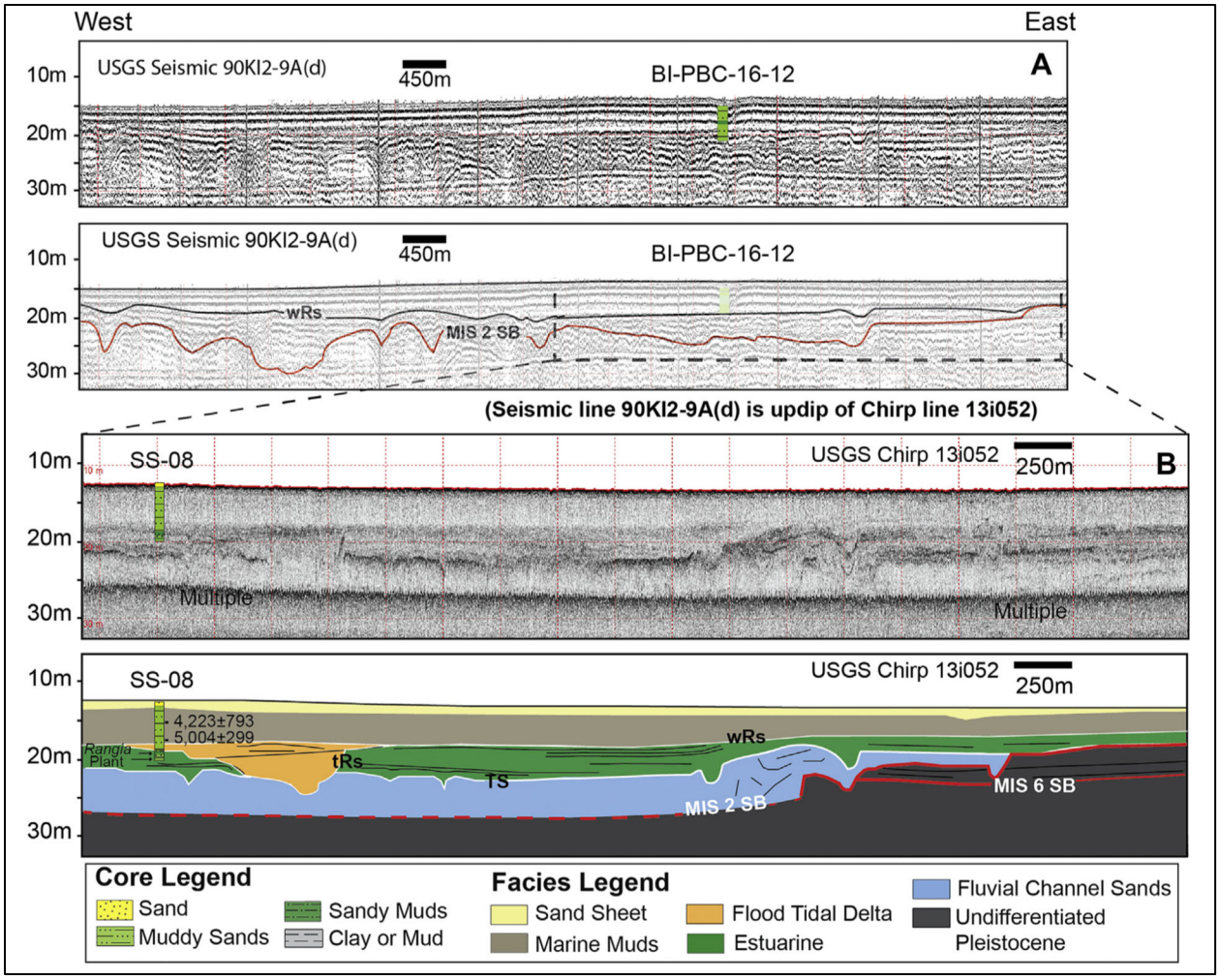

Figure 16. Example legacy boomer profiles 90KI2-9A(d) (A) and CHIRP profile 13i052 (B).
From Hollis et al. 2019.
See Figure 9 for location. Top image pairs are uninterpreted and/or interpreted profiles. Note the geophysical surfaces and sedimentology of cores PB-PBC-16-12 and SS-08 with radiocarbon ages (Table 2).

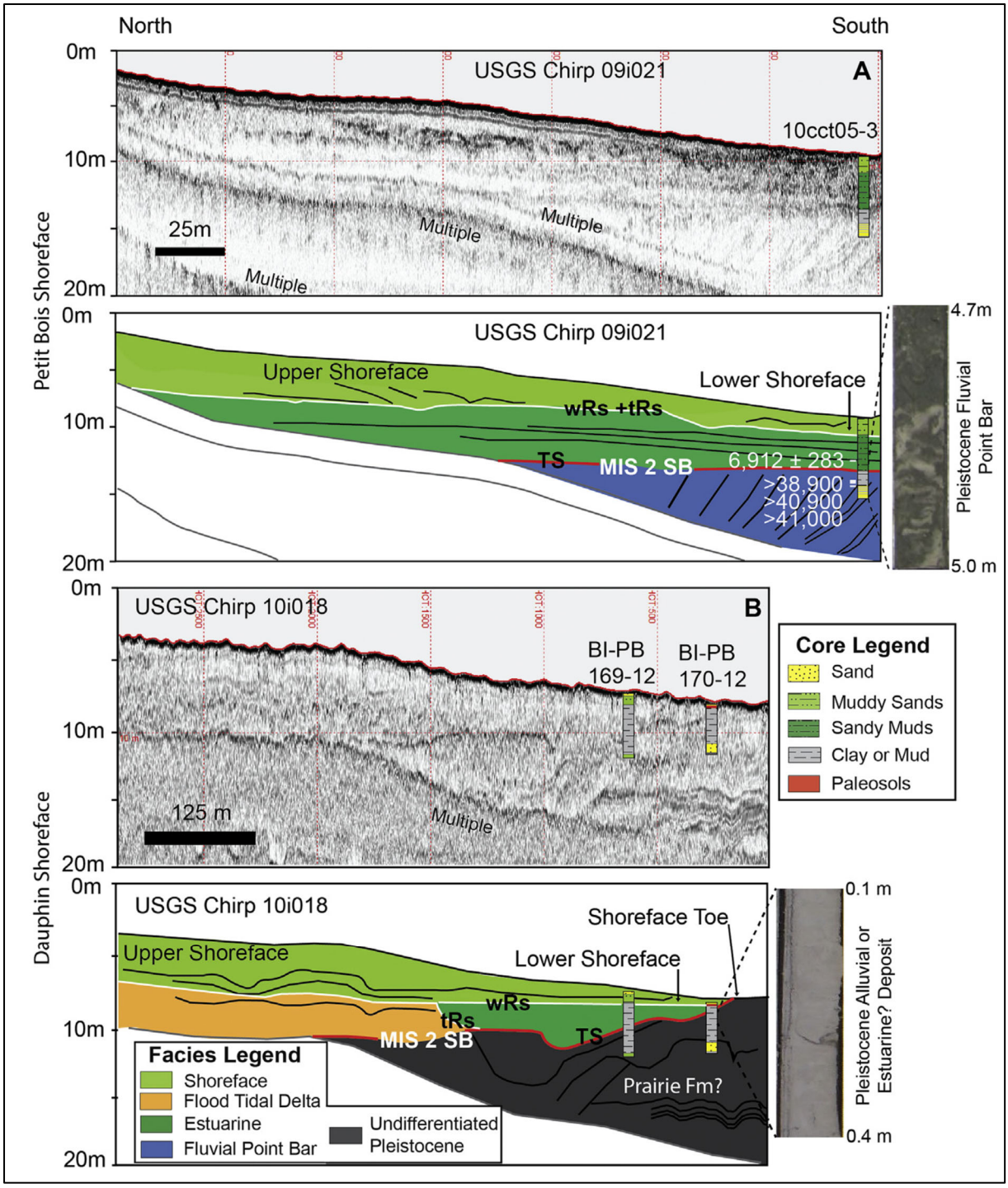

Figure 17. Example legacy CHIRP profiles 09i021 (A) and 10i018 (B).
From Hollis et al. 2019.
See Figure 9 for location. Top image pairs are uninterpreted and/or interpreted profiles. Note the geophysical surfaces and sedimentology of cores 10cct05-3 and BI-PB 169-12/ BI-PB 170-12 with radiocarbon ages (Table 2).

7.2.5 Unit 5: Oyster Biostrome

In sediment cores, Unit 5 contains non cemented, articulated and unarticulated oyster shell beds in a matrix of muddy sand and sand. This unit is thin (0.2–0.8 m) and is composed dominantly of *Crassostrea virginica* (10–30 psu range, prefer water depths of ~2.5 m) with sparse *Ostrea equestris* (>30 psu) (Parker 1960). The deposit was previously sampled and described within the eastern Mississippi Sound (Hummel and Parker 1995).

In geophysics, Unit 5 contained high amplitude, mounded and transparent reflectors, with parabolic to chaotic signal masking below (e.g. Goff et al. 2015, Corpus Christi Bay, Texas). This unit was imaged only in the eastern Mississippi Sound. This unit was interpreted to be an oyster biostrome (e.g. Hummel and Parker 1995) which formed ~3900 BP (Table 3).

7.2.6 Unit 6: Estuarine

In sediment cores, Unit 6 contains light to dark gray-brown, highly mottled, laminated and heavily bioturbated organic muds (Figures 20 through 24). Centimeter-scale, lenticular, silty sand and sandy silt beds, sand and/or mud pockets and burrows are also present (Flocks et al. 2015, Greene et al. 2007, Hummel and Parker 1995, McBride et al. 1991) (Figure 21 core 10cct05- 03; Figure 22, cores MS-9 and MS-3). Articulated mollusk and gastropod shells and shell-wood-plant fragments are common (Figure 21, core 10cct05-3, Figure 22 cores MS-9 and MS4-1). This 0.5–7 m thick unit was present throughout the Mississippi Sound.

In geophysics, Unit 6 contains low to high amplitude, wavy to parallel reflectors that were also observed to be transparent (Figure 16, core SS-08). This unit displays sheet drape and/or channel fill, onlapping external geometries previously described in the area (Flocks et al. 2015, Greene et al. 2007). Based on mollusk assemblages, this unit was interpreted as general estuarine deposits across a wide range of salinities (enclosed bay, upper bay, open bay and open bay facies: Parker (1960). Estuarine deposition began 9800 BP (Table 3), demonstrating variability in early Holocene valley flooding occurring on the inner shelf relative to late Holocene to modern deposition within the Mississippi Sound (Figures 25 through 27).

7.2.7 Unit 7: Inlet Fill and/or Barrier Spit

In sediment cores, Unit 7 contains grayish brown muddy sand, lenticular clays, which grades to massive fine shelly sand (Figure 20). This unit is a similar facies as described in Louisiana, North Carolina-South Carolina, and Texas (Miner et al. 2009, Moslow and Tye 1985, Simms et al. 2006). It ranges between 1.5 and 4 m thick and is observed near the modern barriers (Figure 21, core P-4, Fig. 22, core GI-3, DI-6, DI-3, GSA-4536) and/or within incised valleys (Figure 12).

In geophysics, Unit 7 is characterized by low to medium amplitude, laminated to transparent reflectors with laterally prograding geometry with a chaotic base (Miner et al. 2009). Based on this, it was interpreted as tidal inlet fill and/or prograding barrier spit, first dated to ~7200 BP (Table 3). Laterally prograding barrier islands are also observed from historical charts, supporting this interpretation (Buster and Morton 2011, Morton 2008).

7.2.8 Unit 8: Flood Tidal Delta

In sediment cores, Unit 8 consists of brownish gray, laminated massive silty to fine sand (Figure 20) including cross stratification and/or dipping beds (Figure 21, cores 10cct05-6 and 10cct05- 8) (McBride et

al. 1991, Siringan and Anderson 1993). The unit contained abundant shell fragments and sand-filled borrows. The unit ranged in thickness between 1 and 4 m and was found near modern tidal inlets (Main Pass of Mobile Bay, Petit Bois Pass, Horn Island Pass). Unit 8 is also preserved in certain cores within offshore valleys (Figure 16).

In geophysics, Unit 8 is characterized by low to medium amplitude and/or angle, medium frequency, landward dipping reflectors exhibiting lobate external geometry (e.g. Miner et al. 2009, Siringan and Anderson 1993). It is interpreted as flood tidal delta deposit, and is present from ~1850 CE to modern based on historical charts (Buster and Morton 2011). Radiocarbon dates from these facies near Petit Bois are 2300 BP (Table 2) (Figure 21, core 10cct05-6) and near Dauphin are 4100 BP (Table 2) (Figure 22, core MS-1).

7.2.9 Unit 9: Ebb Tidal Delta (Modern)

In sediment cores, Unit 9 is similar to Unit 8 except it is generally coarser grained and contains more sand dominated dark gray, well sorted fine to medium, cross stratified sands with abundant large shells (Figure 21, cores 10cct05-4 and 10cct05-17) (McBride et al. 1991, Miner et al. 2009, Siringan and Anderson 1993).

In geophysics, Unit 9 consists of seaward dipping reflectors (opposite of Unit 8) in a lobate geometry (Miner et al. 2009, Siringan and Anderson 1993). It is interpreted as ebb tidal delta deposits found only seaward of modern inlets. Historical charts show a history of wave modification, and tidal inlet throat avulsions and lateral migrations (Buster and Morton 2011, Byrnes et al. 2013, Morton, 2008).

7.2.10 Unit 10: Shoreface

In sediment cores, Unit 10 consists of light to dark gray or tan poorly sorted, interbedded sands and muds (Figure 20). The upper section has is generally sandier (Figure 21, core 10cct05-1 and 10cct05-17) and *Donax* sp. Shells are present (e.g., Rodriguez et al. 2001). The lower section generally consists of more mud with few, thin sand beds (Figure 21) and is similar to that described by Rodriguez et al. (2001) along the Texas coast. Some distal cores have an increase in mottling, likely due to bioturbation. Unit 10 contains wood-shell fragments, clay rip ups, peat balls, and sand and/or mud filled burrows (e.g. Rodriguez et al. 2001). This unit ranged in thickness between 0.5 and 3 m and was found seaward of the modern barriers.

In geophysics, Unit 10 consists of low-medium amplitude, medium frequency semi-laminated and/or transparent reflectors (e.g. Rodriguez et al. 2001) (Figure 21). Where it is thin, it is often difficult to distinguish from the seafloor in geophysical data. This unit is interpreted as the shoreface (upper and lower) whose ages range from 7000 to 1800 BP (Table 2; Figure 21, cores 10cct05-02 and PBO17-2). Shoreface units are present in modern environments.

7.2.11 Unit 11: Barrier and/or Backbarrier

In sediment cores, Unit 11 is characterized by two sub-units (Figure 20). Sub-unit A consists of light gray-white-massive to planar and cross-laminated bedding of fine to medium quartz sand. This sub-unit contains shell hash, organics, peat rip-up clasts, wood pieces, roots and sand and/or mud filled burrows (e.g. Moslow and Tye 1985, Otvos 1981). The thicknesses range between 3 and 14 m of sands comprising the islands. Sub-unit A is interpreted as barrier sand lithosomes composed of dune and foreshore facies (Figure 21 and Figure 22).

In sediment cores, sub-unit B consists of light gray, massive to slightly dipping planar laminated muddy sands (Figure 22, core MS-9). This thin layer (0.5–2 m thick) has numerous fining upward sequences and found along the back barrier. From geophysics of the subaqueous portion of sub-unit B, medium amplitude and frequency, semi-parallel, and chaotic reflectors characterize the deposit. Sub-unit B is interpreted as back barrier over wash deposits.

7.2.12 Unit 12: Sand Sheet

From sediment cores, Unit 12 is characterized by tan, massive to somewhat laminated, fine muddy, shelly quartz sand with some sand-mud filled burrows with a sharp basal lag (McBride et al. 1991, Parker et al. 1993). It ranges in thickness between 0.5 and 1.5 m.

From geophysics, this unit consists of low-medium amplitude, low frequency, parallel reflectors with a sheet-like geometry (Figures 15A, B, and 16B) previously described by Flocks et al. (2015). Due to the thin nature and homogeneity, it is challenging to resolve in geophysical data. This surficial unit is found from the inner shelf of the study area and is interpreted as the MAFLA marine sand sheet. Shelf currents have played an active role in reworking the deposit.

7.2.13 Unit 13: Sand Ridge

From sediment cores, Unit 13 contains tan to dark gray, massive/planar laminated, medium to coarse sand, with graded shelly material at the top and base (Flocks et al. 2015, Goff 2014, McBride et al. 1991, Parker et al. 1993). This unit ranges in thickness between 1 and 6 m, and is found offshore of Petit Bois, Petit Bois Pass, and seaward of Main Pass and the eastern portions of the study area (Figure 1 for location).

In geophysics, Unit 13 consists of low to medium amplitude, low frequency, generally parallel reflectors, with an erosional basal reflector (Figure 21A and B) (Flocks et al. 2015, Goff, 2014). Due to homogeneity of the deposit and the high sand content, it is difficult to image in geophysics. Unit 13 is interpreted as a shoreface attached and detached sand ridges, actively being reworked by shelf currents.

7.2.14 Unit 14: Marine Muds

From sediment cores, Unit 14 contains greenish-gray bioturbated clean to sandy muds with low organics (Figure 15C, core 10cct05-02 and PBO-17; Figure 20) (Thomas and Anderson 1994, Otvos, 1981). Marine fossil assemblages can be used to identify this deposit (Otvos 1981). In geophysics it consists of wavy and/or horizontal parallel reflectors or is acoustically transparent (Figure 12 through Figure 19). This makes it challenging to differentiate from Unit 6 using geophysical data alone (Thomas and Anderson 1994). This relatively thin unit (0.1–2 m) is interpreted as inner shelf marine muds.

7.3 Antecedent Topography and Paleofluvial Systems

7.3.1 MIS 6 Sequence Boundary

7.3.1.1 Fowl and La Batre systems

The Fowl River incised valley is 0.5–1 km wide and 20–25 mbsl. It is a bifurcating system with a series of smaller tributaries draining into it (Figure 10A). These features can be mapped through the Mississippi Sound and underneath the shoreface of western Dauphin Island and connect with the Pascagoula-Escatawpa valley to the southwest. A narrow section of the Western Mobile Valley system incises the

Pass aux Herons inlet to the Mississippi Sound, north of Dauphin Island (Figure 10A) (Greene et al. 2007, Hummel and Parker 1995). MIS 6 and MIS SB is separated by a thin, alluvial, deposit between ~2 and 5m thick on the interfluves within the Mississippi Sound.

Valley fill within the Fowl system previously reported consists of lower fluvial deposits with upper bayhead delta deposits (Greene et al. 2007). Within the La Batre system, only bayhead delta valley fill comprise the system within the Mississippi Sound area, constrained to MIS3-6 evidenced by two wood radiocarbon dead ages (>48,000 BP) within this deposit (Greene et al. 2007). Fossil assemblages (Rindsberg 1992) from Mississippi Sound document a Pleistocene delta lobe below the MIS 2 SB (Hummel and Parker 1995), consistent with the MIS 3-6 fluvial deltaic valley fill deposits reported by Greene et al. (2007).

7.3.1.2 Pascagoula-Escatawpa

The combined Pascagoula-Escatawpa River valley is a 5–10km wide and 25–38 mbsl, terraced system (Figure 10A). It widens in a seaward direction and tracks under eastern Petit Bois, and is the "MIS 2" valley previously mapped in the subsurface (Flocks et al. 2015). A shallower terrace is mapped by Twichell et al. (2011) offshore of Petit Bois Pass. Lidar data show a separate valley east of the modern Pascagoula river delta near Grand Bay (Figure 4), correlatating down-dip to the MIS 6 offshore valley. The Citronelle fault scarp orientation (Figure 4) (Otvos 1985) coincides with this location. The incised valley fill is capped by MIS 5 Pleistocene Prairie Formation alluvial deposits (Figure 4).

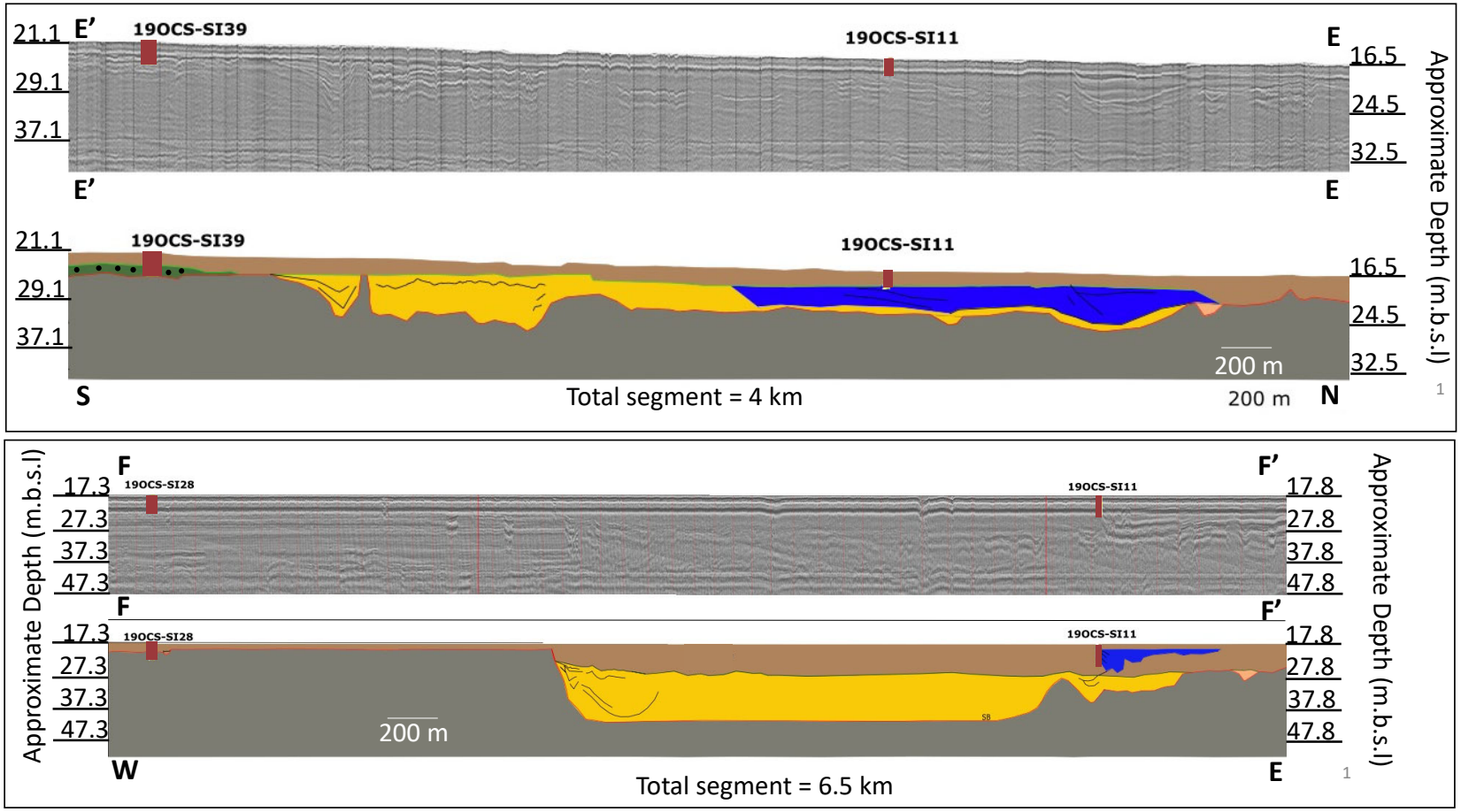

Figure 18. Boomer data and cores acquired for this study.
Modified from Miller et al. 2022.
Western study area profile locations are shown in Figure 9. E-E') Boomer line in a dip orientation crossing over cores 19OCS-SI39 and 19OCS-SI11. The line and cores show MIS 2 incised valley fluvial fill and associated floodplain deposits, and Holocene tidal inlet and/or coastal deposits within the incised valley. F-F') Boomer line in a strike orientation crossing over cores 19OCS-SI28 and 19OCS-SI11. The line and cores show an MIS 2 incised valley fluvial fill and prominent valley edge, as well as Holocene tidal inlet/coastal deposits within the incised valley. In both panels, red = MIS 2 SB, brown = Holocene marine, green dotted = Holocene floodplain, yellow = MIS 2 incised valley fluvial fill, pink = MIS 2 fluvial fill, blue = Holocene tidal inlet/coastal, and gray = undifferentiated Pleistocene.

The combined Pascagoula-Escatawpa valley fill consists of transparent to chaotic reflectors near the base of the valley (Figure 10, channel sands) but was not directly sampled via cores offshore. However, these reflectors can be traced onshore, where I-10 bridge (Figure 1) borings sample a correlative 9 m thick sand deposit occurring at similar elevations (Burns Cooley Dennis Inc 2016). In roughly 15–16 m current water depths, several, relatively large sandy deposits were mapped within the MIS 6 incised valley (Figure 10). These features contained reflectors dipping in opposite orientations, and they radiate in numerous directions from more central, mounded feature. Moving away from the central mounded feature, initially steeply dipping reflectors eventually become more gradual. The few cores that sample the upper part of this feature show generally clean sands, with interbedded sands and/or muds close to the mounded sections, and higher mud content in distal sections (Figure 15). Based on these characteristics, and the fact that they are only found within MIS 6 incised valleys, these identified features are interpreted as fluvial point bars. Seaward of the barrier islands, the upper sections of these fluvial point bars are truncated by two interpreted erosional surfaces: the transgressive (TS) and wave ravinement surface (wRS) (Figure 15). Within Mississippi Sound, laminated, semi-wavy and/or parallel reflectors overlie these fluvial deposits and are interpreted as estuarine and/or alluvial in origin. Greene et al. (2007) did not previously discuss a large MIS 6 Pascagoula-Escatawpa system. This is likely the result of a limited western survey extent in addition to the shallow data penetration of the 216s chirp relative to the boomer geophysical data used for this report (Figures 6 and 7).

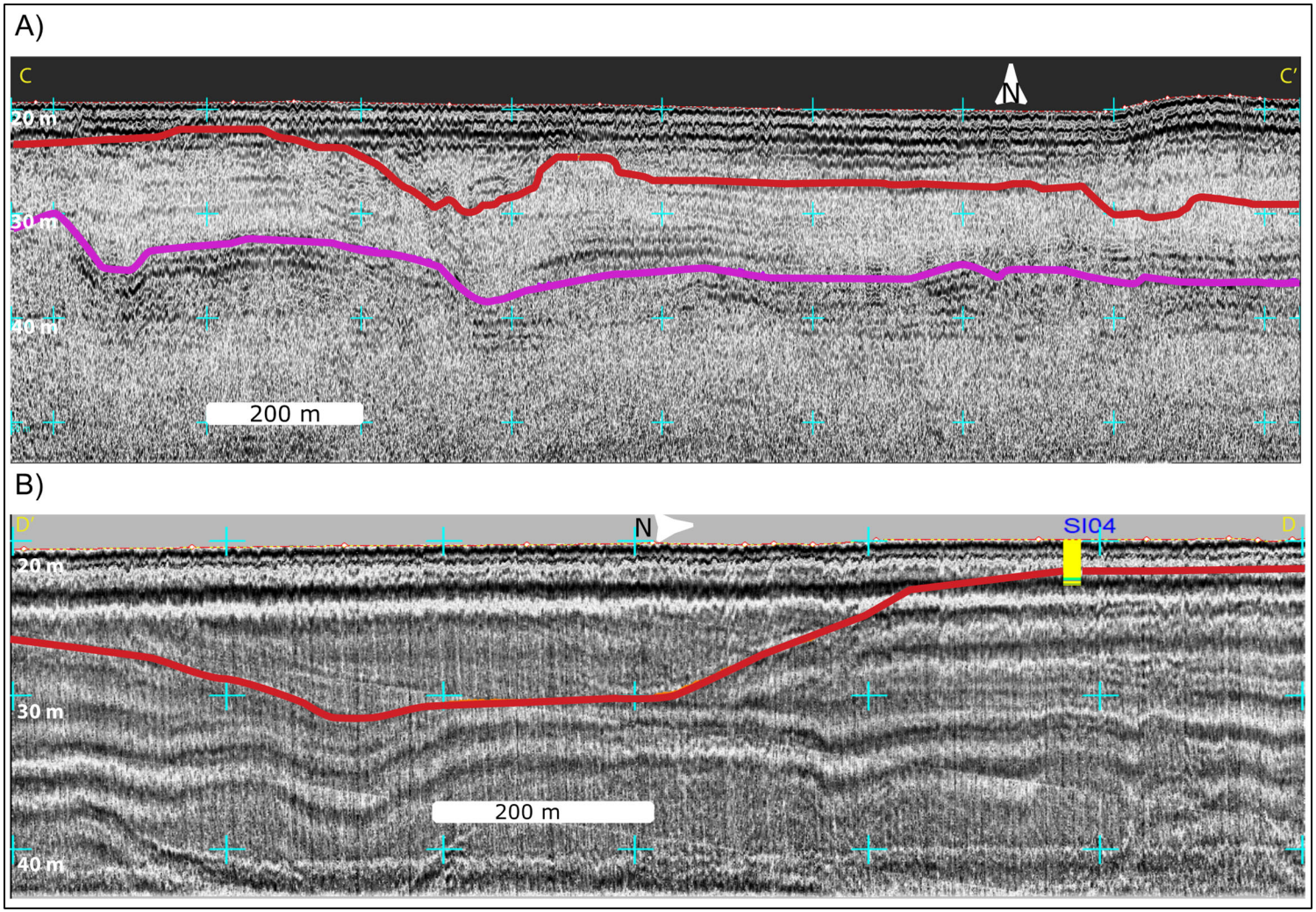

Figure 19. New boomer data and cores with interpretation from this study.
Modified from Culver-Miller et al. 2022.
A) Boomer line in a strike orientation (C-C') showing fluvial and marine reflectors. B) Boomer line in a dip orientation (D-D') over core SI04 showing fluvial and marine reflectors. MIS 2 SB shown in red line, and MIS 6 SB shown in purple line. Eastern study area profile locations are shown in Figure 9.

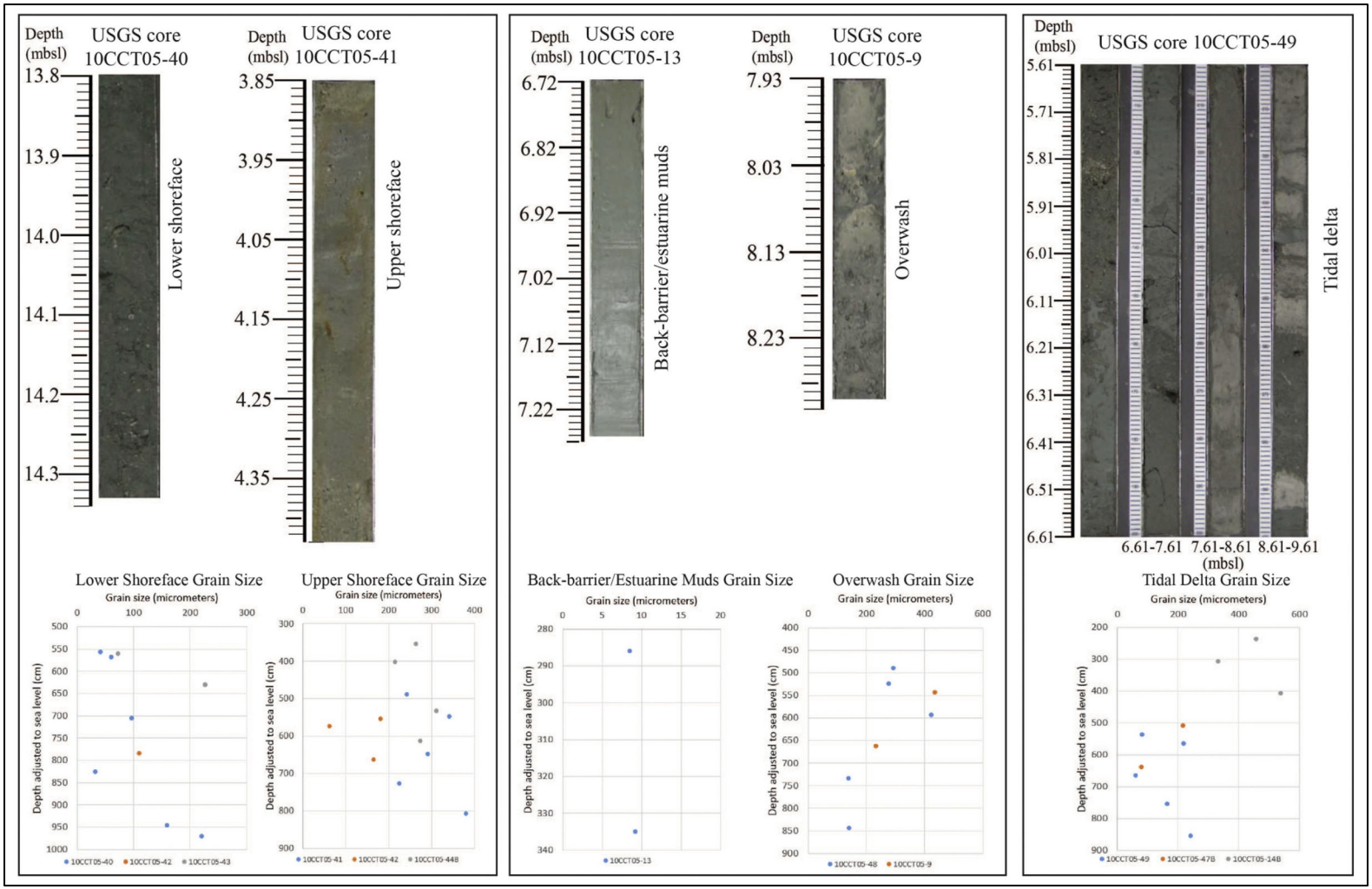

Figure 20. Lithofacies for this study.
From Gal et al. 2021.
Lower shoreface, upper shoreface, back-barrier, overwash, and tidal delta facies core photos and grain size compared with depth are shown.

7.3.2 MIS 2 Sequence Boundary

7.3.2.1 Fowl, La Batre, Escatawpa systems

The Fowl and La Batre MIS 2 incised valley systems are <1 km wide and incise to 10–14 mbsl (Figure 10B). Greene et al. (2007) report a number of narrow tributaries incising to 16–17 mbsl that were not mapped due to data resolution. In our study, we mapped a series of anastomosing tributary and/or distributary channels using additional geophysical data. These systems lie underneath the western portion of Dauphin Island near the location of Katrina Cut (Figure 10B). These incised channels have geophysically transparent to wavy parallel reflectors that are filled entirely with clay and/or clayey sand, interpreted as estuarine deposits. Hummel and Parker (1995) describe thin peat deposits directly overlying the MIS 2 SB within eastern Mississippi Sound. Radiocarbon ages constrain these deposits between 7500 and 6300 BP (Figure 22, MS-9, Table 3), consistent with the initial flooding from SLR during this period (Milliken et al. 2008).

The Escatawpa MIS 2 incised system consists of small, narrow tributary channels between 0.2 and 0.8 km wide to a depth of 4–10 mbsl within Mississippi Sound. Previous work documented 2–6 m deep "v" shaped MIS 2 incisions in our study area (Mullennex 2013, Locker et al. 2016). However, the Escatawpa systems lacks a major single MIS 2 valley (Kramer 1990, Mullennex, 2013), and can be correlated to the smaller, onshore modern fluvial systems from Lidar (Figure 10B). Kramer (1990) describe relatively thin (1–2 m), Holocene fluvial or deltaic sands interpreted as distributary mouth bars located in Grand Bay.

7.3.2.2 Pascagoula system

The Pascagoula incised system is 1–5 km wide and 15–25 mbsl, and underlies the eastern portion of Horn Island and Horn Island Pass (Figure 10B). Several complex interfluvial tributaries flow into the main incised valley in Mississippi Sound. Seaward of Petit Bois Island, and interfluvial MIS 2 area contains a number of ~200m wide, 25 mbsl tributaries draining towards the southwest which coalesce into the main Pascagoula incised MIS 2 valley (Figure 10B). These geometries are consistent with drainage networks onshore, for example from the Citronelle and Prairie Formations. Along the western portion of Petit Bois Island, a larger tributary drainage network exists. A shallow (relative to the seafloor), subaerial exposure surface is observed in sediment cores from the inner shelf, interfluve areas and upper sections of the MIS 6 valley. Flocks et al. (2015) document that this eastern valley upper reflector is truncated in the west by the higher elevation MIS 2 Pascagoula valley (Figure 16B).

Chirp data capture reflectors associated with fluvial channel sands in the bottom followed by estuarine, and tidal deposits which grade into upper 8 m thick marine deposits. These environments are separated by a number of ravinement surfaces (Figure 16B). The geophysical data resolve the base of these fluvial deposits (Figure 16A) nearshore, and cores penetrate the upper part of this layer further offshore (Figure 19). Estuarine and marine muds can be differentiated using the basal presence of plant material and *Rangia* sp. Shells with overlying sediments dated using marine mollusks (Figure 16B). Seaward of Horn Island, estuarine fill has been radiocarbon dated to between ~9800-5200 BP (Otvos 1986) (Table 3).

In Mississippi Sound, the base of the Pascagoula valley is challenging to resolve. R/V *Erda* 92-4 seismic data (Figure 7) rarely penetrates below 20–25 mbsl. On land, two I-10 bridge borings (Burns Cooley Dennis Inc 2016) describe 7–16 m thick, medium to coarse sands, which occur between 8 and 12m below stiff and/or dense clays, interpreted as MIS 2 Pascagoula valley basal fluvial channel sands. Up to 5 m of laminated, wavy parallel reflectors drape the entirety of Mississippi Sound. This deposit consists of sandy mud and/or mud and is interpreted as Holocene estuarine deposition. Tidal or fluvial deltaic fill was not identified within the Mississippi Sound section of this incised valley.

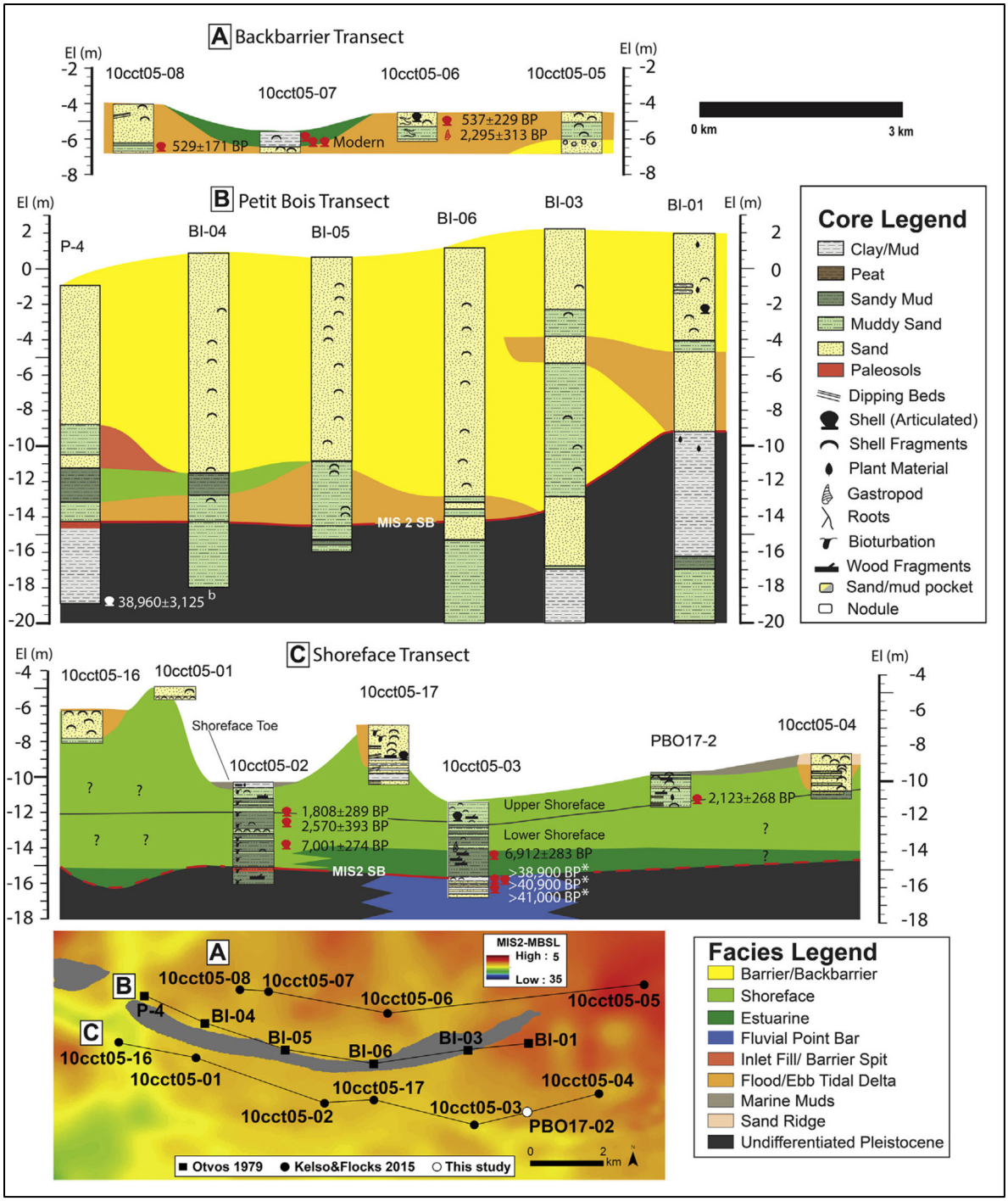

Figure 21. Example core transects, lithofacies, and radiocarbon ages near Petit Bois Island.
From Hollis et al. 2019.

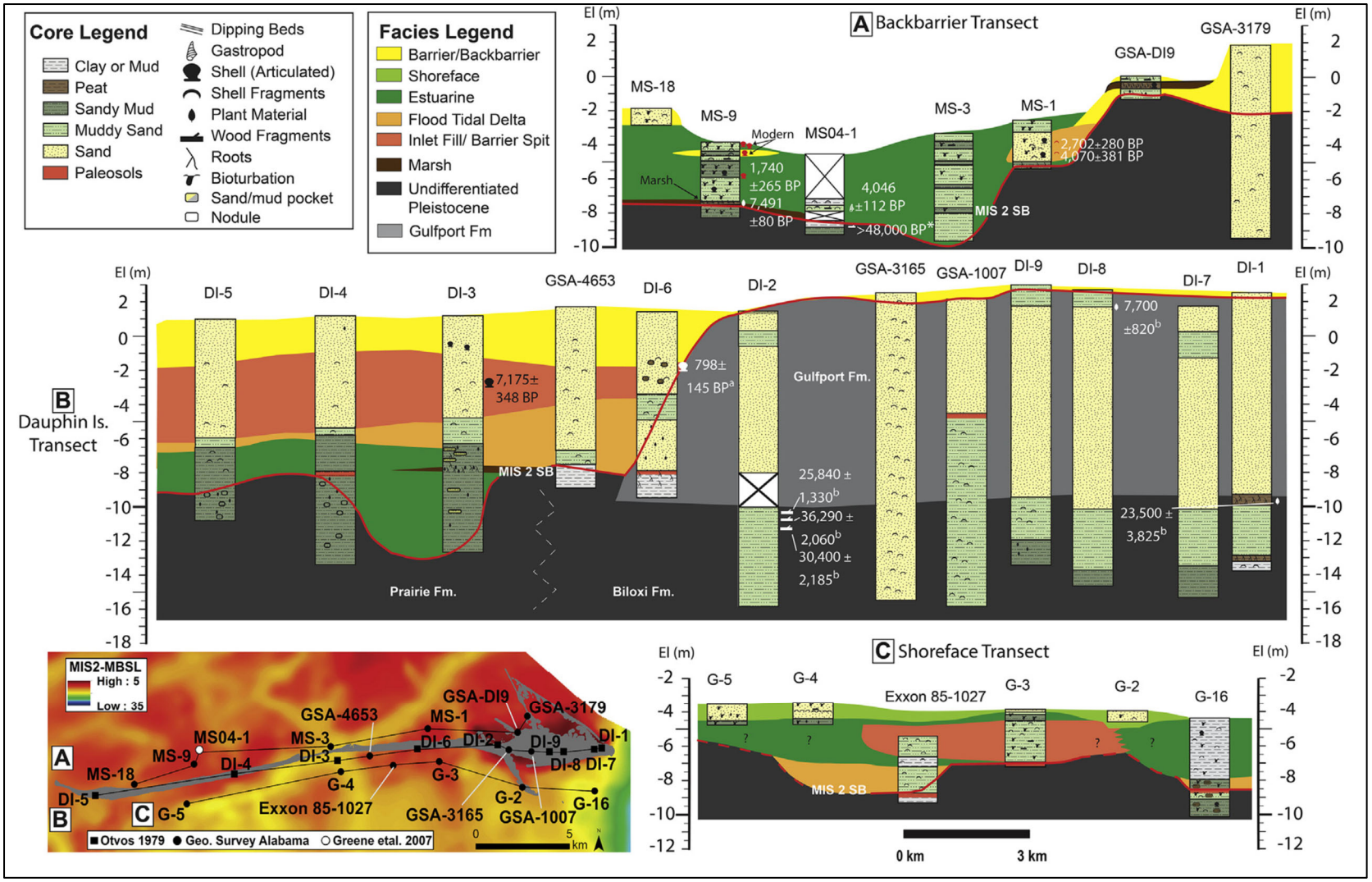

Figure 22. Example core transects, lithofacies, and radiocarbon ages near Dauphin Island.
From Hollis et al. 2019.

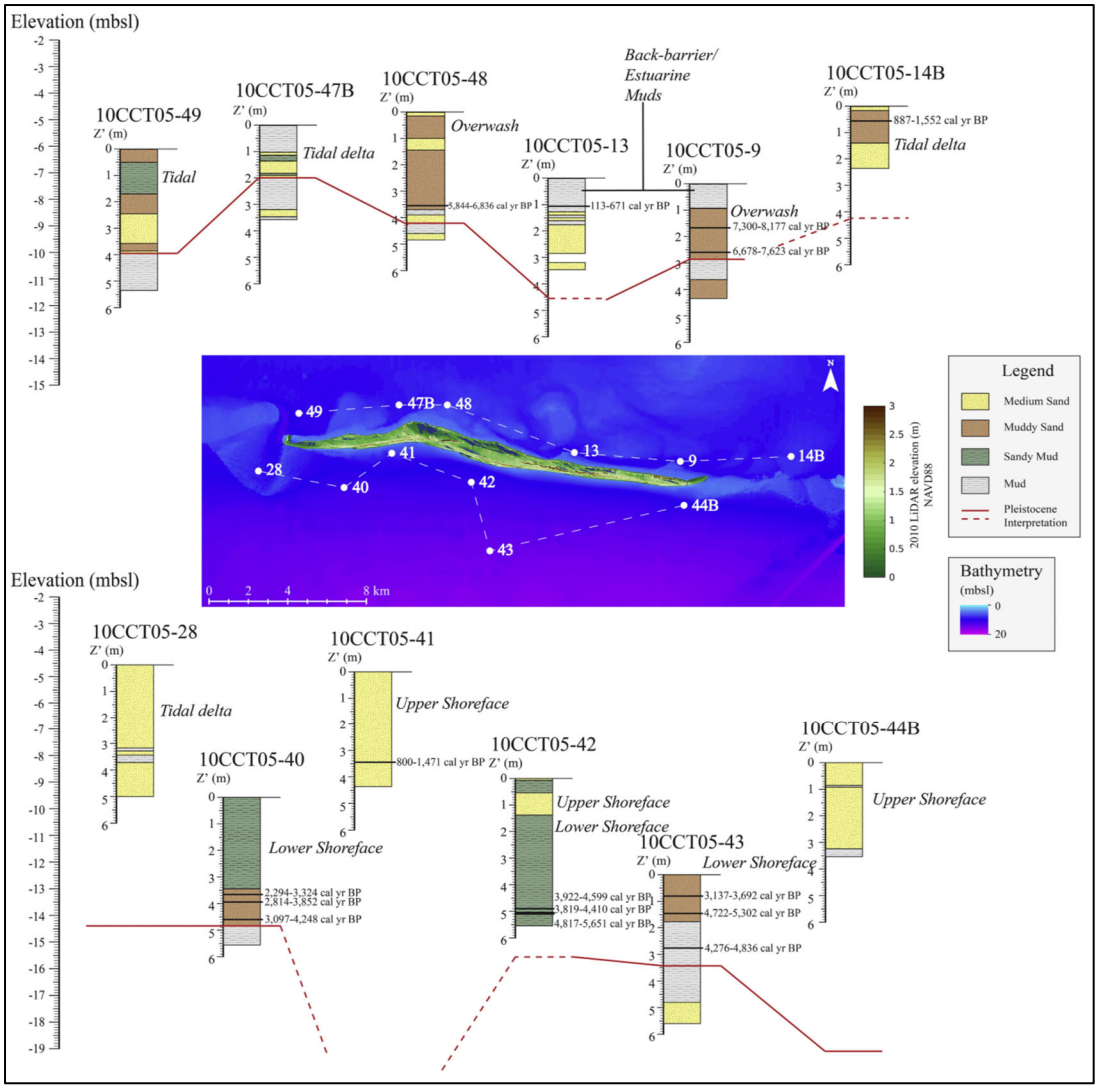

Figure 23. Example core transects, lithofacies, and radiocarbon ages around Horn Island.
From Gal et al. 2021.

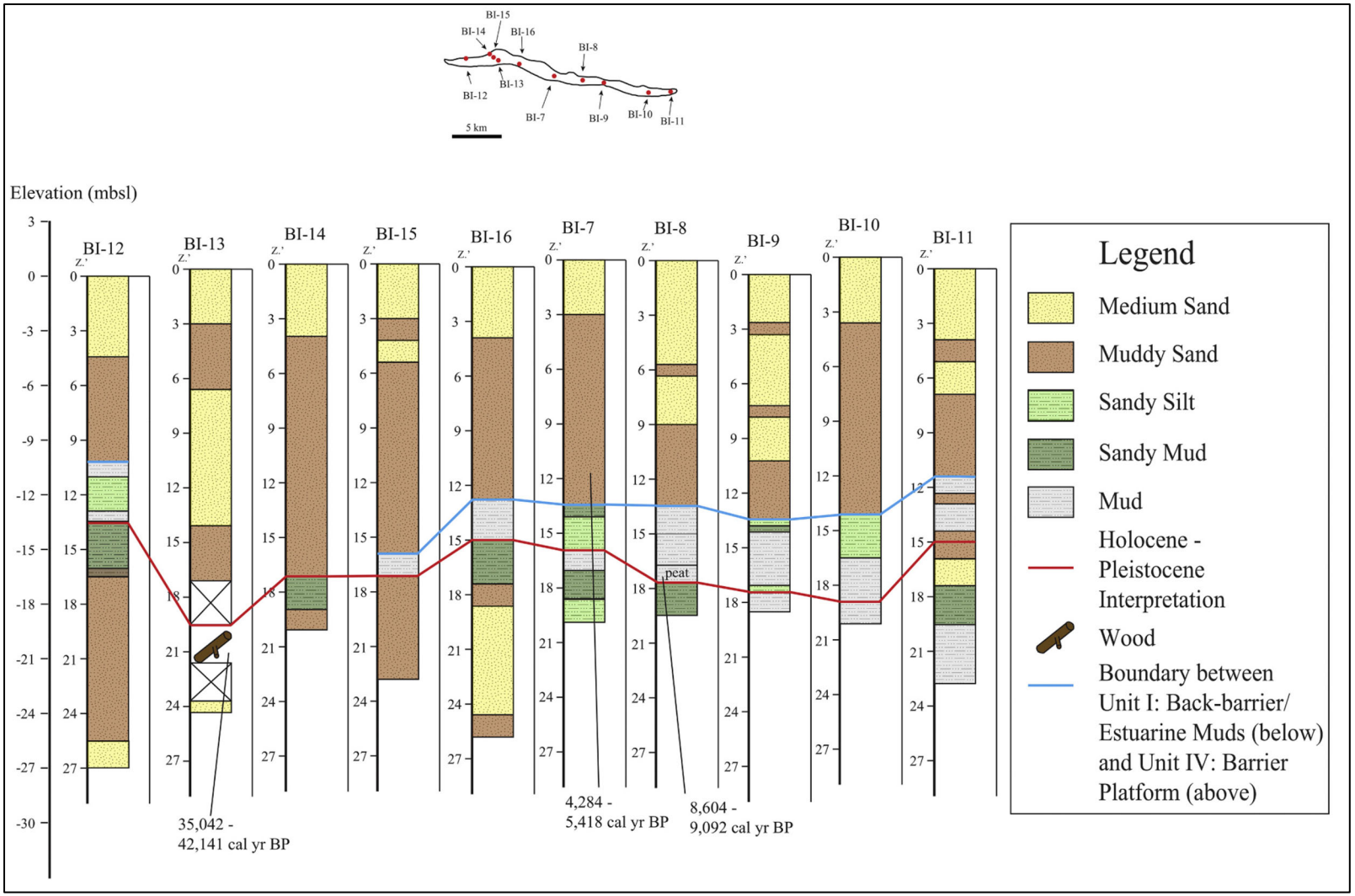

Figure 24. Example core transects, lithofacies, and radiocarbon ages through Horn Island.
From Gal et al. 2021.

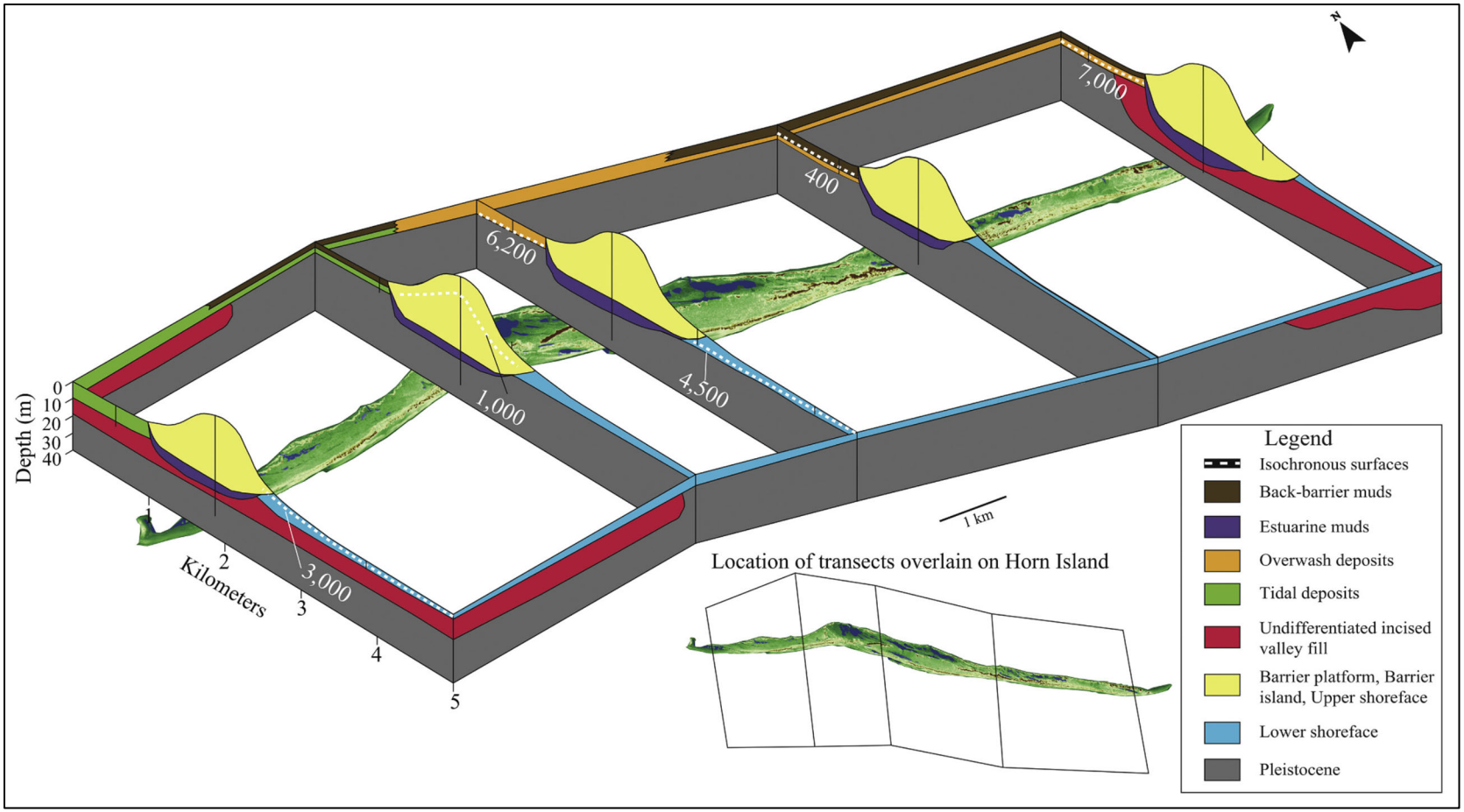

Figure 25. Example core transects, lithofacies, and radiocarbon ages from Horn Island.
From Gal et al. 2021.

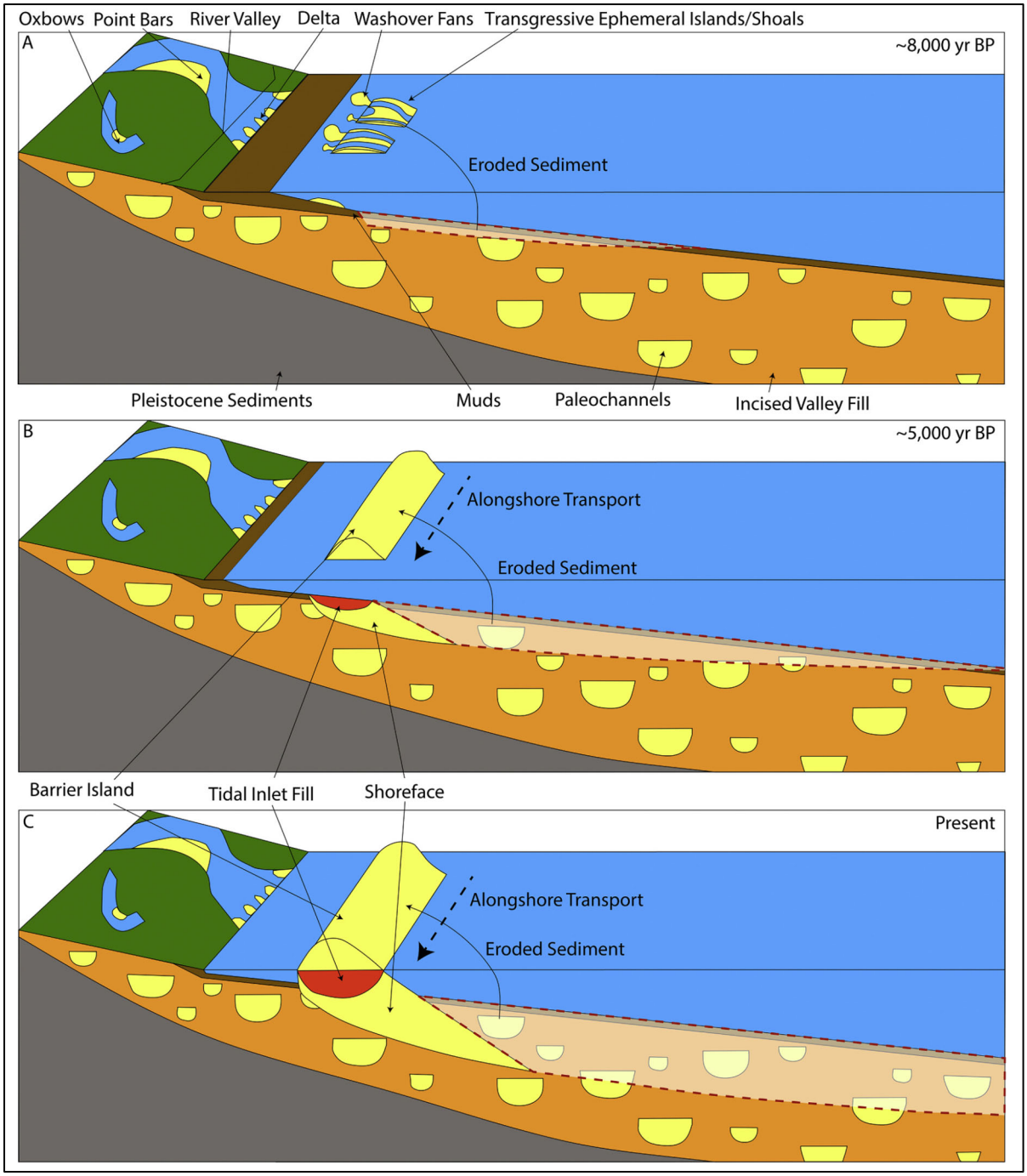

Figure 26. Processes leading to the evolution of Horn Island.
From Gal et al. 2021.

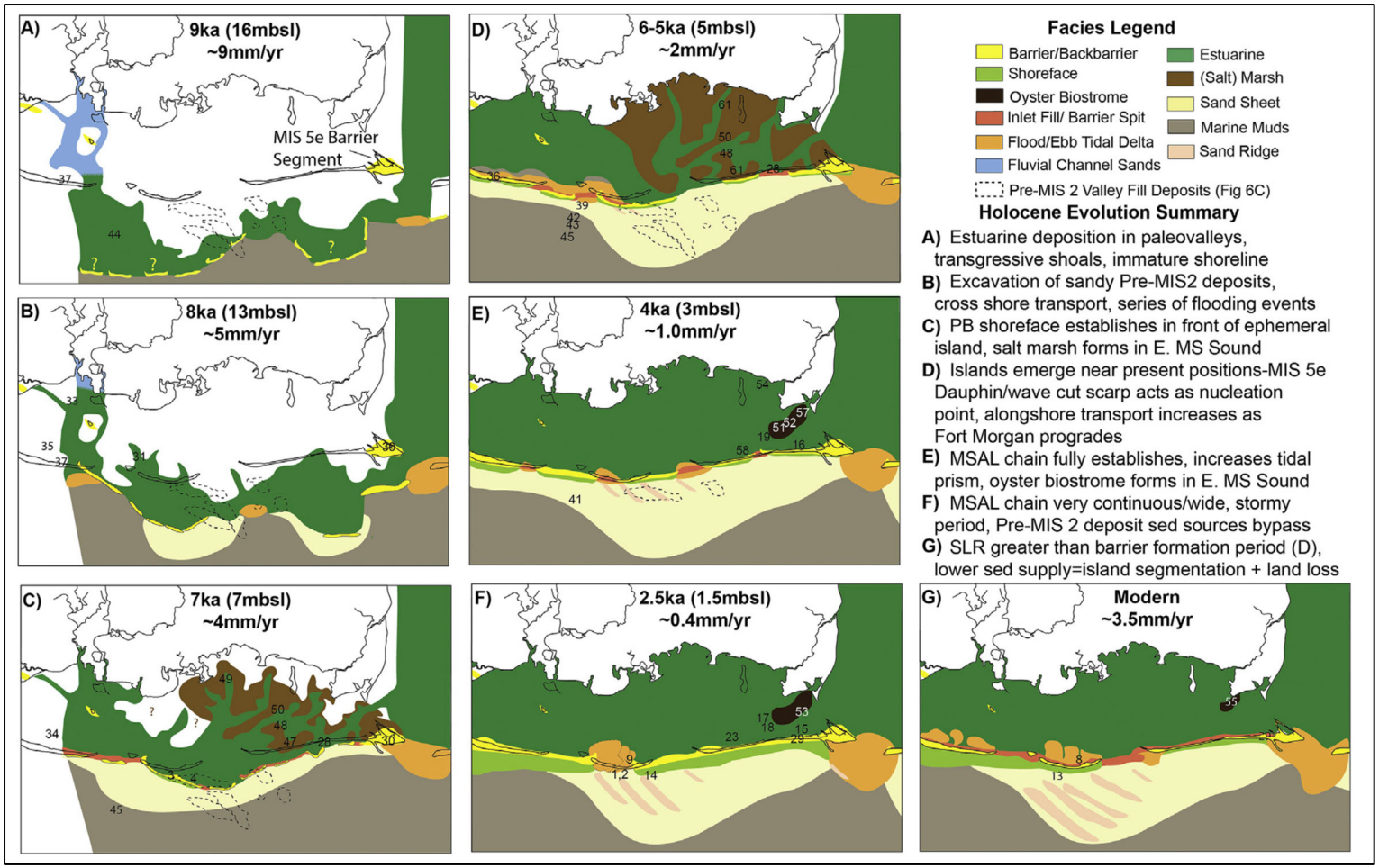

Figure 27. Paleoenvironmental interpretation around Petit Bois and Dauphin islands.
From Hollis et al. 2019.

7.4 Sand Volume Estimates

Before the MsCIP project, modern surficial sand ridges and inter ridge areas accounted for combined sand volume estimates of 8.7 x 10^6 m^3 (total deposit estimate 10.7 x 10^6 m^3) (Figure 28B) (Hollis et al. 2019, Flocks et al. 2015). Inter ridge areas accounted for combined sand-rich volumes of 9.4 x 10^6 m^3 (Figure 28B) (Hollis et al. 2019, Flocks et al. 2015). After completion of the MsCIP project, 9.78 x 10^6 m^3 were removed from these areas (USACE, 2021). This represents a removal of ~54% of the available estimated sand-rich components of the ridge and inter ridge area.

Based on data density, several locations in the study area allowed for additional volumes of potential sediment resource deposits to be quantified. Within Mississippi Sound, sediment volumes for a series of paleochannel features were quantified (Figure 28A). They ranged in volume from 0.405 to 4.278 x 10^6 m^3 of estimated sand-rich sediment. The estimated overburden ranged from 0.5 m to more than 20 m (Figure 28A).

Within the offshore MIS 6 Pascagoula-Escatawpa valley (below the locations of the surficial sand ridges), six relatively large sandy fluvial point bars and/or tidal inlet deposits were mapped using the core and geophysical data (Figure 28C, valley fill deposits 1–6). The estimated maximum combined sand-rich volume associated with these features is 183.4 x 10^6 m^3 (Hollis et al. 2019, Flocks et al. 2015). For context, the active barrier system is estimated at 455 x 10^6 m^3 (Figure 28B).

A

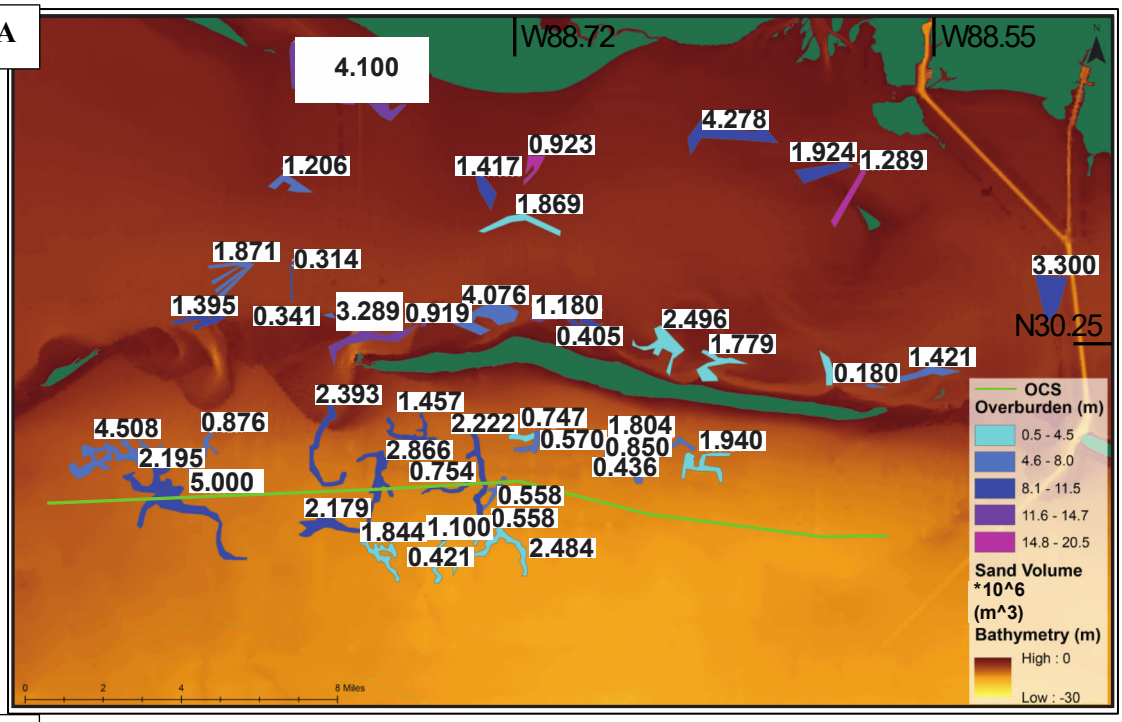

B

Modern Sink Unit	Volume ($\times 10^6$ m^3)	Ancient Source Unit
Sand Ridges	8.7	FPB (1)
Inter Ridge area	9.4	FPB(2)
Active Barrier System	455.0	Reworked Inlet Fill/Spit (3)
		FPB (4)
		FPB (5)
		FPB (6)
Total Sand Volume	473.1	Total Reworked Sand Volume

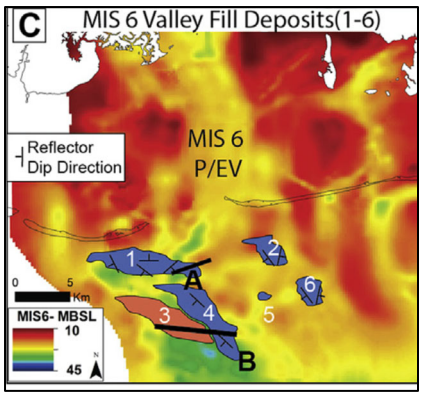

Figure 28. Estimated sand volumes in the study area.
A) Estimated sand volumes from paleochannels within incised valleys near Horn Island (Figure 6) (modified from Gal et al. 2021). Note that colors represent muddy overburden of varying thicknesses. B) Volumes for Holocene sink and reworked MIS 6 valley fill source units (Figure 6). Note that volumes for Sand Ridges and Inter Ridge areas were largely mined during MsCIP. Numbers in parentheses correspond to deposits in (C). Sand content estimated from cores. FPB=Fluvial Point Bar. Modified from Hollis et al. 2019.

7.5 Metadata Standards

Data for this project (new and legacy) are provided in formats appropriate for incorporation into the BOEM MMIS. Tabular (sedimentologic), geophysical (seismic, CHIRP) and ArcGIS (topographic, bathymetric, digitized data) data are archived in accordance with metadata standards established by the Federal Geographic Data Committee[1]. Data files include accompanying documentation files that completely describe the data.

[1] See https://www.fgdc.gov/metadata/geospatial-metadata-tools.

8 Summary

In summary, MS Co-Op1 compiled all available legacy geophysical and core data for the study area (Figure 5), performed QA/QC, and collected new data where appropriate. Importantly, the MIS 2 digital elevation model, which depicts the location of incised valleys, was mapped from the mainland rivers updip and traced seaward to the outer limit of legacy high quality data on the OCS (Figure 6). Significant Holocene sediment resources were identified, almost all of which being located within incised valleys (Figure 3). This included a quantification of the sediment type available (i.e., sand, mud, or mixed), volumes associated with each sediment type, as well as color, depth of deposit relative to sea level, and overburden thickness-sediment type (i.e., Figure 7). Using the geological fundamentals outlined above, the MS Co-Op1 was quite successful over a significant area (Figure 6). Importantly, the high-resolution framework of the MIS 2 surface represents a critical geologic framework upon which a more complete assessment of the study area can be developed. This assessment is useful for BOEM and its stakeholders and partners to begin to quantify available sediment resources for future projects, as well as to allow BOEM to better protect and manage those resources. In the eastern portion of the study area (Figure 10), this project estimated the surficial sand ridges and areas between these sand ridges contained an estimated 18.1 million cubic meters of sand-rich deposits (Figure 28) in most cases near the seabed before the MsCIP project. Of this, 9.78×10^6 m^3 was subsequently removed from these areas for the MsCIP project (USACE, 2021). However, significant sediment resources still remain. Stratigraphically below the former locations of the surficial ridge and inter ridge areas, MIS 6 Pascagoula-Escatawpa valley fill deposits still contain a combined estimated 183.4×10^6 m^3 sand-rich deposit volume (Figure 28C). In the western portion of the study area (Figure 11), an additional ~10 million cubic meters of sand-rich deposit contained within buried paleochannels with overburdens less than 4.5 meters (Figure 28).

9 Future Directions

MS Co-Op1 focused on providing a better understanding of the geologic evolution of Late Quaternary deposits offshore Mississippi and delineating and developing reserve estimates (volumes) of restoration quality sediment resources from the nearshore to the OCS. The paleo-Biloxi, Pascagoula, and Escatawpa river valleys are mapped with confidence to the northern portion of OCS Blocks (Protraction number NH16-04) 897-908, 942-952, and 987-996. However, the incised valleys mapped thus far end at these OCS Blocks because only a few sparse, low quality geophysical lines exist here. They currently cannot be mapped in high-resolution outside of the isolated 2-dimensional seismic lines, as they are 10 kilometers seaward of the MS Co-Op1 MIS 2 surface and contain no sediment cores for ground truthing the geology (Figure 6). These data gaps (identified in MS Co-Op1) will be used to inform new data collection, which will target the paleo- Biloxi, Pascagoula, and Escatawpa incised valleys (OCS Blocks (Protraction number NH16-04) 898-908, 942-952, and 987-996) in a recently funded Cooperative Agreement, "Continuing Mississippi Offshore Sediment Resources Inventory: Linking Quaternary Stratigraphic Evolution of the Mid Shelf (MS Co-Op2; M21AC00018). These new data and/or products to be collected include 1200 to 1500-line km of boomer seismic data, 80 to 100 sediment cores, 2000 grain size samples, modern sedimentation rates for ~10 cores using short-lived isotopes, paleo environmental interpretations, ArcGIS sand-rich polygons, and conceptual stratigraphic models. All data will then be synthesized, compared, interpreted, and presented in a geospatial context building on the work from MS Co-Op1.

10 Recommendations for Management

In the case of the NGOM, MS Co-Op1 indicates that incipient barrier islands were fed by sediment sourced from relict paleochannels and valley fill deposits on the OCS that had eroded during Holocene sea-level rise (Gal et al. 2021, Hollis et al. 2019). The eroded environments consisted of the same grain size, shape, density, and mineralogy as the existing Mississippi-Alabama barrier islands. This has also been demonstrated at other locations around the Gulf, specifically along the Texas coast (Anderson et al. 2016, Wallace et al. 2010). This connection and targeting these genetically related offshore sandy systems near specific islands would provide sediment of similar characteristics to that from which the barriers naturally formed and evolved.

In summary, the continued examination and assessment of geologically connected sediment resources in the OCS is critical because: 1) they consist of similar and/or identical sediment characteristics often sought for specific barrier systems; 2) they contain a record of past responses to physical forcing mechanisms (sea-level rise, storms, sediment supply variations) that is information helpful for future planning of sediment needs; and 3) they often represent a possible cost-effective opportunity for large-scale restoration projects due to their sediment quality and general proximities.

Barrier islands across the Gulf are regarded by many as the most vulnerable in the US. The need for sediment for future coastal restoration projects will be incredibly high, and all appropriate sources need to be located and carefully examined. However, because sediment, particularly sand, will be at a premium moving forward, we must use these resources carefully and with the best management approach, particularly because they are not renewable. This a priori knowledge of how modern-day systems are connected with their paleo-ancestors represents an important geologic framework we will need to take into account to restore and preserve these barrier islands. Locating suitable sediment close to the restoration site can reduce project costs by reducing transportation distance. Through our understanding of where the sediment came from, nature has provided us an answer that will help us build more cost-effective restoration projects.

References

Allen GP, Posamentier HW. 1993. Sequence stratigraphy and facies model of an incised valley fill: the Gironde Estuary, France. J Sediment Petrol. 63: 378–391.

Anderson JB, Rodriguez A, Abdulah KC, Fillon RH, Banfield LA, McKeown HA, Wellner JS. 2004. Late Quaternary stratigraphic evolution of the northern Gulf of Mexico: a synthesis. In: Anderson JB, Fillon RH, editors. Late Quaternary stratigraphic evolution of the Northern Gulf of Mexico Margin. Society for Sedimentary Geology, Special Publication 79. Tulsa (OK): SEPM. p. 1–23.

Anderson J, Milliken K, Wallace D, Rodriguez A, Simms A. 2010. Coastal impact underestimated from rapid sea level rise. Eos. 91(23): 205-206.

Anderson JB, Wallace DJ, Simms AR, Rodriguez AB, Milliken KT, 2014. Variable response of coastal environments of the northwestern Gulf of Mexico to sea-level rise and climate change: implications for future change. Mar Geol. 352: 348–366. [accessed 2022 December 11]; https://doi.org/10.1016/j.margeo.2013.12.008.

Anderson JB, Wallace DJ, Simms AR, Rodriguez AB, Weight RW, Taha ZP. 2016. Recycling sediments between source and sink during a eustatic cycle: systems of Late Quaternary Northwestern Gulf of Mexico Basin. Earth Sci Rev. 153: 111–138. [accessed 2022 December 11]; https://doi.org/10.1016/j.earscirev.2015.10.014.

Bartek LR, Cabote BS, Young T, Schroeder W. 2004. Sequence stratigraphy of a continental margin subjected to low-energy and low-sediment supply environmental boundary conditions: late Pleistocene-Holocene deposition offshore Alabama, U.S.A. In: Anderson JB, Fillon RH, editors. Late Quaternary stratigraphic evolution of the Northern Gulf of Mexico margin. Society for Sedimentary Geology, Special Publication 79. Tulsa (OK): SEPM. p. 85–109.

Blum MD, Roberts HH. 2009. Drowning of the Mississippi Delta due to insufficient sediment supply and global sea-level rise. Nat Geo. 2(7), p. 488-491.

BOEM, 2019. Final Environmental Assessment, Sand Survey Activities for BOEM's Marine Minerals Program, Atlantic and Gulf of Mexico. [accessed 2022 December 11]; https://www.boem.gov/sites/default/files/non-energy-minerals/MMP-Sand-EA-FONSI.pdf.

Bosse ST, Flocks JG, Forde, AS. 2017a. Digitized analog boomer seismic- reflection data collected during U.S. In: Geological Survey Cruises Erda 90-1_ HC, Erda 90-1_PBP, and Erda 91-3 in Mississippi Sound, June 1990, and September 1991. Data Series 1047. US Geological Survey Data Series. [accessed 2023 January 5]; https://doi.org/10.3133/ds1047.

Bosse ST, Flocks JG, Forde AS. 2017b. Archive of digitized analog boomer seismic reflection data collected during U.S. In: Geological Survey Cruise Acadiana 87-2 in the Northern Gulf of Mexico, June 1987. Data release. St. Petersburg (FL): US Geological Survey. [accessed 2023 January 5]; https://doi.org/10.5066/F7F47MC2.

Bosse ST, Flocks JG, Forde, AS. 2018a. Archive of digitized analog boomer seismic-reflection data collected during U.S. Geological Survey cruises Erda 92-2 and Erda 92-4 in Mississippi Sound, June and August 1992. Data release. St. Petersburg (FL): US Geological Survey. [accessed 2023 January 5]; https://doi.org/10.5066/F7RV0N0X.

Bosse ST, Flocks JG, Forde, AS. 2018b. Archive of digitized analog boomer minisparker seismic reflection data collected from the Northern Gulf of Mexico: 1981, 1990, and 1991: U.S. Geological Survey data release. [accessed 2022 December 11]; https://doi.org/10.5066/F7CN730G.

Bosse, ST, Flocks JG, Forde, AS. 2018c. Archive of digitized analog boomer seismic reflection data collected during USGS cruise USFHC in Mississippi Sound and Bay St. Louis, September 1989. St. Peterburg (FL): US Geological Survey. [accessed 2023 January 5]; https://doi.org/10.5066/F7J67G5B.

Brooks GR, Kindinger JL, Penland S, Jeffress Williams S. 1995. East Louisiana Continental Shelf sediments: a product of delta reworking. J Coast Res. 11(4): 1026–1036.

Burns, Cooley, Dennis, Inc. 2009. Engineering Boring Reports for Mississippi Department of Transportation. Project No.: ER/BR-0003-01(098)104555/101000, 25 p.

Buster NA, Kelso KW, Miselis JL, Kindinger JL. 2014. Sediment data collected in 2010 from Cat Island, Mississippi. Reston (VA): US Geological Survey. Data Series 834. [accessed 2023 January 5]; https://dx.doi.org/10.3133/ds834.

Buster NA, Morton RA. 2011. Historical bathymetry and bathymetric change in the Mississippi-Alabama coastal region, 1847–2009. US Geological Survey Scientific Investigations Map. 3154. Reston (VA): US Geological Survey. 13 p. [accessed 2023 January 5]; http://pubs.usgs.gov/sim/3154.

Byrnes MR, Rosati JD, Griffee SF, Berlinghoff JL. 2013. Historical sediment transport pathways and quantities for determining an operational sediment budget: Mississippi Sound barrier islands. J Coast Res. 63: 166–183.

Cattaneo A, Steel RJ. 2003. Transgressive deposits: a review of their variability. Earth Sci Rev. 62: 187–228.

Chesapeake Technologies. 2018. SonarWiz 6 software. Mountain View (CA): Chesapeake Technology, Inc. [accessed 2023 January 5]; https://chesapeaketech.com/.

Culver-Miller EA, Miller C, Wallace DJ, Minzoni RT, Elliott EA, Monica S, Gremillion SL, Dike C. 2021. Response of Coastal Systems within the Escatawpa MIS 2 Incised Valley to Holocene Sea-level Rise in the Northern Gulf of Mexico. AGU Fall Meeting 2021, New Orleans, LA, 13-17 December 2021.

Culver-Miller EA, Miller C, Wallace DJ, Totten RT, Elliott EA, Monica SB, Gremillion SL, Dike C. 2022. Timing and Response of Coastal Systems within the Northern Gulf of Mexico to changes in Sea Level during the Late Pleistocene-Early Holocene. AGU Fall Meeting 2022, Chicago, IL, 12-16 December 2022.

DeWitt NT, Flocks JG, Pendleton EA, Hansen ME, Reynolds BJ, Kelso KW, Wiese DS, Worley CR. 2012. Archive of single beam and swath bathymetry data collected nearshore of the Gulf Islands National Seashore, Mississippi, from West Ship Island, Mississippi, to Dauphin Island, Alabama: Methods and data report for USGS Cruises 08CCT01 and 08CCT02, July 2008, and 09CCT03 and 09CCT04, June 2009. US Geological Survey Data Series 675. Reston (VA): US Geological Survey. 1 CD. [2023 January 5]; https://dx.doi.org/10.3133/ds675.

Dike C. 2022. Coastal geomorphic response to sea-level rise, storms, and antecedent geology: Examples from the northern Gulf of Mexico [dissertation]. Hattiesburg (MS): University of Southern Mississippi. [accessed 2023 January 5]; https://aquila.usm.edu/dissertations/2005.

Dreher CA, Flocks JG, Kulp MA, Ferina NF. 2010. Archive of sediment data collected around the Chandeleur Islands and Breton Island in 2007 and 1987 (vibracore surveys: 07SSC04, 07SCC05, and 87039). Data Series 542. Reston (VA): US Geological Survey. [accessed 2023 January 5]; https://dx.doi.org/10.3133/ds542

Durkin PR, Hubbard SM, Boyd RL, Leckie DA. 2015. Stratigraphic expression of intra-point bar erosion and rotation. J Sediment Res. 85: 1238-1257.

Elko N, Briggs TR, Benedet L, Robertson Q, Thomson G, Webb BM, Garvey K. 2021. A century of US beach nourishment. Ocean Coastal Manage. 199: 105406.

Elsner JB, Kossin JP, Jagger TH. 2008. The increasing intensity of the strongest tropical cyclones. Nature. 455: 92–95.

Emanuel K. 2005. Increasing destructiveness of tropical cyclones over the past 30 years. Nature. 436: 686–688.

Emanuel K. 2021. Response of global tropical cyclone activity to increasing CO2: Results from downscaling CMIP6 models. J Clim. 34: 57–70.

Flocks J, Ferina N, Kindinger J. 2011. Recent geologic framework and geomorphology of the Mississippi-Alabama shelf, northern Gulf of Mexico. In: Buster N, Holmes C, editors. Gulf of Mexico: origins, waters and biota. Volume III: geology. College Station (TX): Texas A&M University Press. p. 157–173.

Flocks JG, Kindinger JL, Kelso KK. 2015. Geologic control on the evolution of the inner shelf morphology offshore of the Mississippi barrier islands, northern Gulf of Mexico, USA: Cont Shelf Res. 101: 59–70. [accessed 2022 December 11]; https://dx.doi.org/10.1016/j.csr.2015.04.008.

Flocks JG, Kindinger JL, Kelso KK, Bernier J, DeWitt, N, FitzHarris, M. 2014. Near-surface stratigraphy and morphology, Mississippi inner shelf, northern Gulf of Mexico. Reston (VA): US Geological Survey. Report No.: Open-File Report 2015–1014.26 p. [accessed 2023 January 5]; https://dx.doi.org/10.3133/ofr20151014

Forde AS, Dadisman SV, Flocks JG, Wiese DS. 2011a. Archive of digital chirp sub bottom profile data collected during USGS cruises 09CCT03 and 09CCT04, Mississippi and Alabama Gulf Islands, June and July 2009. Data Series 590. Reston (VA): US Geological Survey. 6 DVDs. [accessed 2023 January 5]; https://pubs.usgs.gov/ds/590/

Forde AS, Dadisman SV, Flocks JG, Wiese DS, DeWitt NT, Pfeiffer WR, Kelso KW, Thompson, PR, 2011b. Archive of digital chirp sub bottom profile data collected during USGS cruises 10CCT01, 10CCT02, and 10CCT03, Mississippi and Alabama Gulf Islands, March and April 2010. Data Series 611. Reston (VA): US Geological Survey. [accessed 2023 January 5]; https://doi.org/10.3133/ds611Forde AS, Dadisman SV, Kindinger JL, Miselis JL, Wiese DS, Buster NA, 2012. Archive of digital chirp subbottom profile data collected during USGS cruise 10BIM04 offshore Cat Island, Mississippi, September 2010. Data Series 724. Reston (VA): US Geological Survey. 2 DVDs. [accessed 2023 January 5]; https://doi.org/10.3133/ds724

Forde AS, Flocks JG, Kindinger JL, Bernier JC, Kelso KW, Wiese DS. 2015. Archive of digital chirp sub bottom profile data collected during USGS Cruise 13CCT04 offshore of Petit Bois Island, Mississippi, August 2013. Data Series 924. Reston (VA): US Geological Survey. 3 DVDs. [accessed 2023 January 5]; https://dx.doi.org/10.3133/ds924.

Frazier DE. 1967. Recent deltaic deposits of the Mississippi River: their development and chronology. Trans Gulf Coast Assoc Geol Soc. 17: 287– 315.

Frazier DE. 1974. Depositional-episodes: their relationship to the Quaternary stratigraphic framework in the northwestern portion of the Gulf Basin. Geological Circular 74-1. Austin (TX): Bureau of Economic Geology, University of Texas at Austin. 28 p.

Gal NS, Wallace DJ, Miner MD, Hollis RJ, Dike C, Flocks JG. 2021. Influence of antecedent geology on the Holocene formation and evolution of Horn Island, Mississippi, USA. Mar Geol. 43: 106375. [accessed 2022 December 11]; https://doi.org/10.1016/j.margeo.2020.106375.

Ghinassi M, Ielpi A, Aldinucci M, Milovan F. 2016. Downstream-migrating fluvial point bars in the rock record. Sediment Geol. 334: 55–96.

Goff J. 2014. Seismic and core investigation off Panama City, Florida, reveals sand ridge influence on formation of the shoreface ravinement. Cont Shelf Res. 88: 34–46.

Goff J, Lurgin L, Gulick SP, Thirumulai K, Okumura Y. 2015. Oyster reef die-offs in stratigraphic record of Corpus Christi Bay, Texas, possibly caused by drought- driven extreme salinity changes. Holocene. 26: 511–519. [accessed 2022 December 11]; https://doi.org/10.1177/0959683615612587.

Gonzalez S, Bentley Sr., SJ, DeLong KL, Xu K, Obelcz J, Truong J, Harley GL, Reese CA, Caporaso A. 2017. Facies reconstruction of a late Pleistocene cypress forest discovered on the northern Gulf of Mexico continental shelf. Trans Gulf Coast Assoc Geol Soc. 67: 133–146.

Greene DL, Rodriguez AB, Anderson JB. 2007. Seaward-branching coastal-plain and piedmont incised-valley systems through multiple sea-level cycles: late Quaternary examples from Mobile Bay and Mississippi Sound, U.S.A. J Sediment Res. 77: 139–158.

Gulf Coast Research Lab. 2004. Mississippi Office of Geology Historic Cores. [accessed 2023 February 2]; https://geology.deq.ms.gov/coastal/Core_historic_cores.htm

Gulf Coast Research Lab. 2021. Mississippi Office of Geology Recent Cores. [accessed 2023 February 2]; https://geology.deq.ms.gov/coastal/Core_recent_cores.htm

Hein CJ, FitzGerald DM, Milne GA, Bard K, Fattovich R. 2011. Evolution of a Pharaonic harbor on the Red Sea: implications for coastal response to changes in sea level and climate. Geology. 39(7): 687-690.

Hollis RJ, Wallace DJ, Miner MD, Gal NS, Dike C, Flocks JG. 2019. Late Quaternary evolution and stratigraphic framework influence on coastal systems along the North-Central Gulf of Mexico, USA. Quat Sci Rev. 223. 105910. [accessed 2023 January 4]; https://doi.org/10.1016/j.quascirev.2019.105910.

Hrvacevic Z. 2020. MsCIP completes the restoration of Ship Island. DredgingToday.com. [accessed 2023 January 4]; https://www.dredgingtoday.com/2020/12/21/mscip-completes-the-restoration-of-ship-island/

Hummel RL, Parker SJ. 1995. Holocene geologic history of Mississippi Sound, Alabama. Tuscaloosa (AL): Geological Survey of Alabama. Circular Issue 185. 91 p.

Kelso KW, Flocks JG. 2015. Archive of sediment data from vibracores collected in 2010 offshore of the Mississippi barrier islands. Data Series 903. St. Petersburg (FL):US Geological Survey. [accessed 2023 January 4]; https://dx.doi.org/10.3133/ds903.

Kindinger JL. 1988. Seismic stratigraphy of the Mississippi-Alabama shelf and upper continental slope. Mar Geol. 83: 79–94.

Kindinger JL, Balson PS, Flocks JG. 1994. Stratigraphy of the Mississippi-Alabama Shelf and the Mobile River Incised-Valley System. In: Dalrymple RW, Boyd R, Zaitlin BA, editors. Incised-valley systems: origin and sedimentary sequences. SEPM Special Publication 51. Tulsa (OK): SEPM (Society for Sedimentary Geology).

Kindinger JL, Miselis JL, Buster NA. 2014. The shallow stratigraphy and sand resources offshore from Cat Island, Mississippi. Reston (VA): US Geological Survey and US Army Corps of Engineers. Report No.: Open-file report 2014-1070. 83 p. [accessed 2023 January 4]; https://doi.org/10.3133/ofr20141070

Kindinger JL, Penland S, Williams SJ, Suter JR. 1989. Inner shelf deposits of the Louisiana-Mississippi-Alabama region, Gulf of Mexico. Trans Gulf Coast Assoc Geol Soc. 39: 413–420.

Kramer KA. 1990. Late Pleistocene to Holocene geologic evolution of the Grande Batture Headland Area, Jackson County, Mississippi [thesis]. Starkville (MS): Mississippi State University. 165 p.

Locker SD, Smith CG, DeWitt NT, Forde AS, Stalk CA, Fredericks JJ. 2016. Geologic Framework and Surficial Processes, Grand Bay, Mississippi-Alabama. Bays and Bayous Conference, Biloxi, MS, Nov. 30-Dec. 1: p. 90.

McBride RA, Moslow TF. 1991. Origin, evolution, and distribution of shoreface sand ridges, Atlantic inner shelf, U.S.A. Mar Geol. 97: 57-85.

McBride RA, Byrnes MR, Penland S, Pope DL, Kindinger JL. 1991. Geomorphic history, geologic framework, and hard mineral resources of the Petit Bois Pass area, Mississippi-Alabama. In: Shanley KW, Perkins BF. Coastal depositional systems in the Gulf of Mexico: quaternary framework and environmental issues: twelfth annual research conference, Gulf Coast Section, Society of Economic Paleontologists and Mineralogists Foundation. Houston, Texas, December 8–11, 1991. Tulsa (OK): Society for Sedimentary Geology: 116-127.

McCarthy JJ. 2009. Reflections on: our planet and its life, origins, and futures. Science. 326 (5960): 1646–1655.

McGowen JH, Garner LE, Wilkinson BH. 1977. The Gulf shorelines of Texas: processes, characteristics, and factors in use. Austin (TX): University of Texas at Austin. Bureau of Economic Geology Geological Circular 77-3. 30 p.

Milliken KT, Anderson JB, Rodriguez AB. 2008. A new composite Holocene sea- level curve for the northern Gulf of Mexico. In: Anderson JB, Rodriguez AB, editors. Response of Upper Gulf Coast estuaries to Holocene climate change and sea-level rise. Special Paper 443. Boulder (CO): Geological Society of America. p. 1–11.

Miller C, Culver-Miller EA, Wallace DJ, Minzoni RT, Elliott EA, Monica S, Gremillion SL, Dike C. 2021. Reconstructing the MIS 2 Pascagoula-Biloxi Paleovalley and Associated Valley-Fill in the Northern Gulf of Mexico. AGU Fall Meeting 2021. AGU Fall Meeting 2021, New Orleans, LA, 13-17 December 2021. [accessed 2023 February 2]; https://agu.confex.com/agu/fm21/meetingapp.cgi/Paper/890190

Miller CM, Culver-Miller EA, Wallace DJ, Totten RT, Elliott EA, Monica SB. 2022. Early Holocene/Late Pleistocene Paleoshoreline Reconstruction in the Northern Gulf of Mexico. AGU

Fall Meeting 2022. AGU Fall Meeting 2022, Chicago, IL, 12-16 December 2022. [accessed 2023 February 2]; https://agu.confex.com/agu/fm22/meetingapp.cgi/Paper/1118272

Miner MD, Kulp MA, FitzGerald DM, Georgiou IY. 2009. Hurricane-associated ebb-tidal delta sediment dynamics. Geology. 37: 851–854.

Miselis J L, Buster NA, Kindinger JL. 2014. Refining the link between the Holocene development of the Mississippi River Delta and the geologic evolution of Cat Island, MS: implications for delta-associated barrier islands. Mar Geol. 355: 274–290.

Mississippi Department of Environmental Quality. 2016. [accessed 2016 June 1]; https://geology.deq.ms.gov/coastal/Publications.htm.

Mitchum RM, Vail PR, Sangree JB. 1977. Seismic stratigraphy and global changes of sea level, Part 6: Stratigraphic interpretation of seismic reflection patterns in depositional sequences. In: Payton CE., editor. Seismic stratigraphy applications to hydrocarbon exploration, Memoir 26. Tulsa (OK): American Association of Petroleum Geologists. p. 117–133.

Morton, RA. 2008. Historical changes in the Mississippi-Alabama barrier islands and the roles of extreme storms, sea level and human activities. J Coast Res 24. 1587-1600.

Moslow TF, Tye RS. 1985. Recognition and characterization of Holocene tidal inlet sequences. Mar Geol 63. 129-151.

Mullennex A.J. 2013. Spatial correlation between framework geology and shoreline morphology in Grand Bay, Mississippi [thesis]. Starkville (MS): Mississippi State University. 192 p.

Nayegandhi A, Brock JC, Wright CW, Miner MD, Yates X, Bonisteel JM. 2016a. USGS Data Series 416. EAARL Coastal Topography–Pearl River Delta 2008: Bare Earth. [accessed 2022 December 29]; http://pubs.usgs.gov/ds/416/.

Nayegandhi A, Brock JC, Wright CW, Miner MD, Yates X, Bonisteel JM. 2016b. USGS Data Series 417. EAARL Coastal Topography–Pearl River Delta 2008: First Surface. [accessed 2022 December 29]; http://pubs.usgs.gov/ds/417/.

[NOAA] National Oceanic and Atmospheric Administration. 2007. Biloxi, Mississippi Coastal Digital Elevation Model. [accessed 2023 February 2]; https://www.ncei.noaa.gov/access/metadata/landing-page/bin/iso?id=gov.noaa.ngdc.mgg.dem:241.

[NOAA] National Oceanic and Atmospheric Administration. 2009. Mobile, Alabama 1/3 Arc-Second NAVD88 Coastal Digital Elevation Model. NOAA National Geophysical Data Center. [accessed 2023 February 2]; https://www.ncei.noaa.gov/access/metadata/landing-page/bin/iso?id=gov.noaa.ngdc.mgg.dem:671.

[NOAA] National Oceanic and Atmospheric Administration. 2019a. Sea Level Trends, Dauphin Island, AL Station 8735180. NOAA National Geophysical Data Center. [accessed 2019 June 8]; https://tidesandcurrents.noaa.gov/sltrends/sltrends_station.shtml?id=8735180.

[NOAA] National Oceanic and Atmospheric Administration. 2020. Sea Level Trends–Relative Sea Level Trend 8747437 Bay Waveland, Mississippi. [accessed 2023 January 4]; https://tidesandcurrents.noaa.gov/sltrends/sltrends_station.shtml?id=8747437

[NOAA] National Oceanic and Atmospheric Administration. 2021. Historical Hurricane Tracks. [accessed 2022 December 11]; https://coast.noaa.gov/hurricanes.

Nordfjord S, Goff JA, Austin JA, Gulick SPS. 2006. Seismic cacies of incised-valley fills, New Jersey Continental Shelf: implications for erosion and preservation processes acting during latest Pleistocene-Holocene transgression. J Sediment Res. 76: 1284-1303.

Oppenheimer M, Glavovic BC, Hinkel J, van de Wal R, Magnan AK, Abd-Elgawad A, Cai R, Cifuentes-Jara M, DeConto RM, Ghosh T, Hay J, Isla F, Marzeion B, Meyssignac B, Sebesvari Z. 2019. Sea level rise and implications for low-lying islands, coasts and communities. In: Pörtner HO, Roberts DC, Masson-Delmotte V, Zhai P, Tignor M, Poloczanska E, Mintenbeck K, Alegría A, Nicolai M, Okem A, Petzold J, Rama B, Weyer NM, editors. IPCC special report on the ocean and cryosphere in a changing climate. Geneva (CH): Intergovernmental Panel on Climate Change. [accessed 2023 February 3]; https://www.ipcc.ch/srocc/

Otvos EG. 1978. New Orleans– south Hancock Holocene barrier trends and origin of Lake Pontchartrain. Trans Gulf Coast Assoc Geol Soc. 28: 337– 355.

Otvos EG. 1979. Barrier island evolution and history of migration, north central Gulf Coast. In: Leatherman SP, editor. Barrier islands. New York (NY): Academic Press. p. 291–319.

Otvos EG. 1981. Barrier island formation through nearshore aggradation stratigraphic field evidence. Mar Geol. 43: 195–243.

Otvos EG. 1985. A New stratigraphic system, geologic evolution and potential economic resources in the Mississippi Sound Area, Mississippi-Alabama. Mississippi Mineral Resources Institute, Open File Report 85-6F: 71 p.

Otvos EG. 1986. Stratigraphy and potential economic sand resources of the Mississippi-Alabama Barrier Island System and adjacent offshore areas. Mississippi Mineral Resources Institute, Open-File Report 86-1F: 67 p.

Otvos EG. 2001. Chapter H: Mississippi Coast: stratigraphy and quaternary evolution in the Northern Gulf Coastal Plain framework. In: Gohn GS, editor. Stratigraphic and Paleontologic Studies of the Neogene and Quaternary Sediments in Southern Jackson County, Mississippi. Report No.: U.S. Geological Survey Open-File Report 01-415-H. 59 p. [accessed 2022 December 29]; https://pubs.usgs.gov/of/2001/of01-415/

Otvos EG, Giardino MJ. 2004. Interlinked barrier chain and delta lobe development, northern Gulf of Mexico. Sediment Geol. 169: 47–73.

Parker RH. 1960. Ecology and distributional patterns of macro-invertebrates, Northern Gulf of Mexico. In: Shepard FP, Phleger FB, van Andel TH, editors. Recent sediments, northwest Gulf of Mexico: a symposium summarizing the results of work carried on in Project 51 of the American Petroleum Institute, 1951-1958. Tulsa (OK): American Association of Petroleum Geologists. p. 302–337.

Parker SJ, Davies DJ, Smith WE (Geological Survey of Alabama, Tuscaloosa, AL). 1993. Geological, economic, environmental characterization of selected near-term leasable offshore sand deposits and competing onshore sources for beach nourishment. Geological Survey of Alabama Final Report. New Orleans (LA): US Department of the Interior, Minerals Management Service. Obligation No.: 14-35-

0001-30630. [accessed 2022 December 29]; https://www.boem.gov/sites/default/files/mm-research/2021-05/AL_1993_Parker.pdf

Pendleton EA, Barras JA, Williams SJ, Twichell DC. 2010. Coastal vulnerability assessment of the Northern Gulf of Mexico to sea-level rise and coastal change. Report No.: USGS Open-File Report 2010-1146. [accessed 2022 December 29]; http://pubs.usgs.gov/of/2010/1146/.

Pendleton EA, Baldwin WE, Danforth WW, Dewitt NT, Forde AS, Foster DS, Kelso KW, Pfeiffer WR, Turecek AM, Flocks JG, Twichell DC. 2011. Geophysical data from offshore of the Gulf Islands National Seashore, Cat Island to Western Horn Island, Mississippi. Report No.: USGS Open-File Report 2010-1178. [accessed 2022 December 29]; https://pubs.usgs.gov/of/2010/1178/.

Pfeiffer WR, Flocks JG, DeWitt NT, Forde AS, Kelso K, Thompson PR, Wiese DS (US Geological Survey and Jacobs Technology Inc., St. Petersburg, FL). 2011. Archive of side scan sonar and swath bathymetry data collected during USGS cruise 10CCT02 offshore of Petit Bois Island including Petit Bois Pass, Gulf Islands National Seashore, Mississippi, March 2010. Report No.: US Geological Survey Data Series 577.

Reese CA, Harley GL, Delong KL, Bentley SJ, Xu K, Gonzalez S, Truong JT, Obelcz J, Caporaso A. 2018. Stratigraphic pollen analysis performed on a late Pleistocene cypress forest preserved on the northern Gulf of Mexico continental shelf. J Quat Sci. 33: 865–870.

Reijenstein HM, Posamentier HW, Bhattacharya JP. 2011. Seismic geomorphology and high-resolution seismic stratigraphy of inner-shelf fluvial estuarine, deltaic, and marine sequences, Gulf of Thailand. AAPG Bull 95(11): 1959–1990.

Reimer PJ, Bard E, Bayliss A, Beck JW, Blackwell PG, Ramsey CB, Buck CE, Cheng H, Edwards RL, Friedrich M., Grootes PM, Guilderson TP, Haflidason H, Hajdas I, Hatte C, Heaton TJ, Hoffmann DL, Hogg AG, Hughen KA, Kaiser KF, Kromer B, Manning SW, Niu M, Reimer RW, Richards DA, Scott EM, Southon JR, Staff RA, Turney CSM, van der Plicht J. 2013. IntCal13 and Marine13 radiocarbon age calibration curves 0 to 50,000 years BP. Radiocarbon. 55: 1869–1887.

Rindsberg AK. 1992. Holocene ichnology of eastern Mississippi Sound, Alabama. Tuscaloosa (AL): Geological Survey of Alabama. Circular 167. 75 p.

Roberts HH, Fillon RH, Kohl B, Robalin JM, Sydow JC. 2004. Depositional architecture of the Lagniappe Delta: sediment characteristics, timing of depositional events, and temporal relationship with adjacent shelf-edge deltas. In: Anderson JB, Fillon RH, editors. Late Quaternary stratigraphic evolution of the Northern Gulf of Mexico margin. Special Publication No. 79. Tulsa (OK): SEPM (Society for Sedimentary Geology). p. 143–188.

Rodriguez AB, Fassell ML, Anderson JB. 2001. Variations in shoreface progradation and ravinement along the Texas coast, Gulf of Mexico. Sedimentol. 48: 837-853.

Sanford JM, Harrison AS, Wiese DS, Flocks JG (US Geological Survey and Jacobs Technology Inc., St. Petersburg, FL). 2016a. Archive of digitized analog boomer seismic reflection data collected from Lake Pontchartrain, Louisiana to Mobile Bay, Alabama, during cruises onboard the R/V ERDA-1, June and August, 1992. Report No.: US Geological Survey Data Series 370. [accessed 2022 December 29]; https://pubs.usgs.gov/ds/370/

Sanford JM, Harrison AS, Wiese DS, Flocks JG (US Geological Survey and Jacobs Technology Inc., St. Petersburg, FL). 2016b. Archive of digitized analog boomer seismic reflection data collected from the Mississippi- Alabama-Florida shelf during cruises onboard the R/V Kit Jones, June 1990 and July

1991. Report No.: US Geological Survey Data Series429. [accessed 2022 December 29]; https://pubs.usgs.gov/ds/429/

Sanford JM, Harrison AS, Wiese DS, Flocks JG (US Geological Survey, St. Petersburg, FL). 2016c. Archive of digitized analog boomer and minisparker seismic reflection data collected from the Alabama-Mississippi-Louisiana Shelf during cruises onboard the R/V Carancahua and R/V Gyre, April and July, 1981. Report No.: US Geological Survey Data Series 428. [accessed 2022 December 29]; https://doi.org/10.3133/ds428

Saucier RT. 1968. Recent geomorphic history of the Pontchartrain Basin [dissertation]. Baton Rouge (LA): Louisiana State University. 189 p. [accessed 2022 December 29]; https://digitalcommons.lsu.edu/cgi/viewcontent.cgi?article=2417&context=gradschool_disstheses

Simms AR, Anderson JB, Blum M. 2006. Barrier-island aggradation via inlet migration: Mustang Island, Texas. Sediment Geol 187: 105-125.

Siringan FP, Anderson JB. 1993. Seismic facies, architecture, and evolution of the Bolivar Roads tidal inlet/delta complex, East Texas Gulf Coast. J Sediment Petrol. 63: 794–808.

Smith KEL, Nayegandhi A, Wright CW, Bonisteel JM, Brock JC. 2016a. USGS Data Series 400. EAARL Coastal Topography–Northern Gulf of Mexico, 2007: Bare Earth. [accessed 2022 December 29]; http://pubs.usgs.gov/ds/400/.

Smith KEL, Nayegandhi A, Wright CW, Bonisteel JM, Brock JC. 2016b. USGS Data Series 399. EAARL Coastal Topography–Northern Gulf of Mexico, 2007: First Surface. [accessed 2022 December 29]; http://pubs.usgs.gov/ds/399/.

Thomas MA, Anderson JB. 1994. Sea-level controls on the facies architecture of the Trinity/Sabine Incised-Valley System, Texas Continental Shelf. In: Dalrymple R, Boyd R, Zaitlin BA, editors. Incised valley systems: origin and sedimentary sequences. SEPM Special Publication No. 51. Tulsa (OK): SEPM (Society for Sedimentary Geology). p. 63–82.

Twichell DC, Pendleton E, Baldwin W, Foster D, Flocks J, Kelso K, DeWitt N, Pfeiffer W, Forde A, Krick J, Baehr J (US Geological Survey, Woods Hole, MA and St Petersburg, FL; US Army Corps of Engineers, Mobile, AL). 2011. The shallow stratigraphy and sand resources offshore of the Mississippi barrier islands. USGS Open-File Report 2011-1173, version 1.1. 65 p.

[USACE] US Army Corps of Engineers. 2021. Regarding the use of outer continental shelf sand resources for the Mississippi coastal improvements program comprehensive barrier island restoration project, Gulf Islands National Seashore, Mississippi. Final project completion report summary BOEM negotiated agreement no. OCS-G 35929, 314 p.

Wallace DJ, Anderson JB, Fernandez R. 2010. Transgressive ravinement versus depth of closure: a geological perspective from the upper Texas Coast. J Coast Res. 26: 1057–1067.

Wallace DJ, Anderson JB, Rodriguez AB. 2009. Natural versus anthropogenic mechanisms of erosion along the upper Texas Coast. In: Kelley JT, Pilkey OH, Cooper JAG, editors. America's most vulnerable coastal communities: The Geological Society of America special paper 460. Boulder (CO): Geological Society of America. p. 137–147. [accessed 2022 December 29]; http://dx.doi.org/10.1130/2009.2460(10)

Webster PJ, Holland GJ, Curry JA, Chang HR. 2005. Changes in tropical cyclone number, duration, and intensity in a warming environment. Science. 309: 1844-1846.

Wentworth, CK. 1922. A scale of grade and class terms for clastic sediments. J Geol. 30:377–392.

Zaitlin BA, Dalrymple RW, Boyd R. 1994. The stratigraphic organization of incised-valley systems associated with relative sea-level change. In: Dalrymple RW, Boyd R, Zaitlin BA, editors. Incised-valley systems: origin and sedimentary sequences. Society for Sedimentary Geology Special Publication 51. Tulsa (OK): SEPM. p. 45–60.

Zaremba N, Mallinson D, Leorri E, Culver S, Riggs S, Mulligan R, Horsman E, Mitra S. 2016. Controls on the Stratigraphic framework and paleoenvironmental change within a Holocene estuarine system: Pamlico Sound, North Carolina, USA. Mar Geol. 379: 109–123.

Department of the Interior (DOI)

The Department of the Interior protects and manages the Nation's natural resources and cultural heritage; provides scientific and other information about those resources; and honors the Nation’s trust responsibilities or special commitments to American Indians, Alaska Natives, and affiliated island communities.

Bureau of Ocean Energy Management (BOEM)

The mission of the Bureau of Ocean Energy Management is to manage development of U.S. Outer Continental Shelf energy and mineral resources in an environmentally and economically responsible way.

BOEM Environmental Studies Program

The mission of the Environmental Studies Program is to provide the information needed to predict, assess, and manage impacts from offshore energy and marine mineral exploration, development, and production activities on human, marine, and coastal environments. The proposal, selection, research, review, collaboration, production, and dissemination of each of BOEM’s Environmental Studies follows the DOI Code of Scientific and Scholarly Conduct, in support of a culture of scientific and professional integrity, as set out in the DOI Departmental Manual (305 DM 3).